UNIVERSITEIT VAN PRETORIA
UNIVERSITY OF PRETORIA
YUNIBESITHI YA PRETORIA

Some contributions to joint monitoring of mean and variance of normal populations

by

Mandla Doctor Diko

Submitted in partial fulfillment of the requirements for the degree

Magister Scientiae

In the Department of Statistics

In the Faculty of Natural and Agricultural Sciences

University of Pretoria

April 2014

Declaration

I, Mandla Doctor Diko, declare that this dissertation, which I hereby submit for the degree Magister Scientiae in Applied Statistics at the University of Pretoria, is my own work and has not previously been submitted by me for a degree at this or any other tertiary institution.

Signature: _____   Date: _____

Acknowledgements

I would like to sincerely thank my supervisor, Prof. S. Chakraborti, and my co-supervisor, Dr. M.A. Graham, for their extraordinary efforts throughout my studies in the Department of Statistics at the University of Pretoria. Their professional knowledge, insightful observations and guidance were crucial during the entire process of doing my research.

Summary

In **Chapter 1,** we give a brief introduction to statistical process control (SPC) and provide definitions as well as background information regarding the research conducted in this mini-dissertation. This will aid in familiarizing the reader with concepts and terminology that are helpful to the following chapters. The Phase II Shewhart $(\overline{X}, R)$ charting scheme for jointly monitoring the process mean and standard deviation is usually implemented using 3-sigma limits for the individual component charts. There are three major issues with this: (i) It is assumed that the charting statistics are normally distributed; (ii) Multiple testing (or the multiplicity issue), since two charts are used at the same time to make decisions about the in-control (IC) state of the process, thus the false alarm rate (*FAR*) is inflated; (iii) The effect of parameter estimation, which is known to degrade chart performance. Hence, in **Chapter 2** and **Chapter 3**, we illustrate the severity of these three issues on the IC properties of the $(\overline{X}, R)$ charting scheme when parameters are known (i.e. Case K) and when parameters are unknown (i.e. Case U), respectively. For both Case K and Case U, a method is presented for deriving the new charting constants taking proper account of the three issues listed above. Furthermore tables of the new charting constants are provided for both Case K and Case U, for some specified nominal IC average run-length (*ARL*) and sample sizes to aid in implementing the $(\overline{X}, R)$ chart in practice.

Previous applications of the $(\overline{X}, R)$ chart to survey data ignore the non-normality of the survey scales, ignore the multiplicity issue, ignore the effects of parameter estimation and do not take advantage of the correlation structure inherent in survey scales (see applications in Marks and O'Connell (2003), Maguad (2005, 2007)), as a result the *FAR* is inflated. In **Chapter 5**, we provide a case study where we apply the $(\overline{X}, R)$ charting scheme to student evaluation of teaching (SET) survey data. In our case study, factor analysis is used to reduce the dimension of the data and to take account of correlation. Then the data is transformed to near normality using the square root transformation. The transformed data is then subjected to Phase I and Phase II analysis using $(\overline{X}, R)$ charting scheme. Our Phase II analysis uses the new charting constants in Chapter 3, which we derived to mitigate the effects of multiplicity, the standard use of 3-sigma limits, and parameter estimation. As a result, we strongly believe that our method in this case study keeps the *FAR* at the nominally expected level compared to the methods used in previous applications.

Furthermore, as a prelude to our case study in Chapter 5; in **Chapter 4** we review the non-standard applications of SPC charts reported in literature from 2000 to 2012, inclusive. We classify them into six groups according to the application domain. For each domain, the nature of the application is described and analysed with respect to the control chart technique used, the purpose to which the control chart has been applied, the performance measures used, the units of analysis and the data sources. We summarise some findings of our preliminary analysis. In particular, we uncovered two additional application domains that were missing in the review of MacCarthy and Wasusri (2001). The two additional application domains are animal production and personal everyday situations.

Finally, **Chapter 6** wraps up this mini-dissertation with a summary of the research carried out and offers concluding remarks concerning unanswered questions and / or future research ideas.

Table of Contents

Chapter 1

Introduction

In this chapter, we establish the importance of Statistical Process Control (SPC). We provide some notation and definitions. Specifically, we distinguish between (i) common cause and assignable cause variation (ii) various types of data (iii) Phase I and Phase II analysis (iv) various types of control charts. Finally in Section 1.11, Section 1.12 and Section 1.13, we present our research focus and objectives.

1.1.   Notation

The table below lists some of the abbreviations and notation that will be used throughout the dissertation.

Table 1.1. Abbreviations and notation

SPC	Statistical process control
QC	Quality control
pmf	Probability mass function
cdf	Cumulative distribution function
n	Sample size / rational subgroup size
$X_1, X_2, \ldots, X_n$	Random variables in a sample
$x_1, x_2, \ldots, x_n$	Observations in a sample
IC	In-control
OOC	Out-of-control
ARL	Average run-length
ARL_0	Nominal average run-length
$ICARL$	In-control average run-length
$AICARL$	Attained in-control average run-length
$SDRL$	Standard deviation of the run-length
MRL	Median run-length
FAR	False alarm rate
FAR_0	Nominal false alarm rate
$AFAR$	Attained false alarm rate
FAP	False alarm probability
UCL	Upper control limit
CL	Center line
LCL	Lower control limit
SET	Student evaluation of teaching
$CUSUM$	Cumulative sum
$EWMA$	Exponentially weighted moving average

1.2   Statistical process control

All work done in order to turn an input into an output for a customer is a process (Stapenhurst (2005)). Process outputs may be manufactured goods such as automobiles, computers, clothing, as well as services such as the generation and distribution of electrical energy, public transportation, banking, retailing and healthcare. It is always important to keep the customer happy and satisfied; and this can be done by controlling and improving the quality of manufactured goods and services. Quality improvement is the reduction of the variability in processes and products (outputs) (Montgomery (2013), Chapter 1, page 7). Quality control (QC) refers to the control of quality by any means. Statistical process / quality control (SPC/SQC) refers to the use of statistically based tools and techniques principally for the improvement of quality and productivity (Stapenhurst (2005)). SPC techniques have been applied primarily in manufacturing processes. However, with the availability of commercial software, SPC applications have moved far beyond manufacturing into biology, medicine, athletics, finance, legal services and other areas.

1.3   Common and assignable cause variation

Every process, whether manufacturing or non-manufacturing, shows some variation in its output. There are two types of variation, namely:

  i.   common cause (chance cause) variation and
 ii.   special cause (assignable cause) variation.

Common cause variation is the natural or inherent variation that occurs in any process, whereas assignable cause variation is not inherent to the process. Assignable cause variation can be a result of factors (assignable causes of variation) which can be identified and eliminated, such as operator fatigue or defective raw materials. The assignable cause variation needs to be reduced so that the quality of the output of a process may be improved (see Montgomery (2013), Chapter 5, page 189).

2

1.4   Types of data

In this section we distinguish between the various types and classes of data prevalent in SPC.

1.4.1   Attributes and variables data

To understand variability and thus improve quality, a suitable process or product quality characteristic must be measured. In other words data must be collected from the process. In a process, data can be continuous or discrete (see Montgomery (2013), Chapters 6 & 7).

Variables data usually result from measurements where you can choose the precision, such as cost, weight, length, time, volume, porosity and chemical concentration, which are expressed in a numerical measurement. In view of that, variables data is used to refer to continuous measurements. Attributes data are so-called because they are based on whether an item has an attribute or not. Attribute data are usually counts, for example, the number of flaws or errors on a piece of paper. In view of that, attributes data is used to refer to discrete measurements.

1.4.2   Independent and autocorrelated data

The majority of research on SPC control charting techniques has considered the case where the process data is independently distributed, i.e. uncorrelated. In the presence of autocorrelated data the control charting technique becomes more involved. A standard approach to dealing with autocorrelated data is to use residual control charts. The residual control charts were first introduced in Alwan and Roberts (1988). To implement residual charts, an appropriate time series model is fitted to the autocorrelated observations and the residuals are then used in the construction of the chart. Although autoregressive moving average (ARMA) models are popular in SPC techniques, any suitable time series model can be used such as an autoregressive (AR) model, a moving average (MA) model or an autoregressive integrated moving average (ARIMA) model. An interested reader is referred to Psarakis and Papaleonida (2007) for a detailed discussion on SPC procedures for monitoring autocorrelated processes.

3

1.5   In-control and out-of-control

A process is said to be in-control (IC) when only natural variation (i.e. common causes variation) is present and a process is declared to be out-of-control (OOC) when unusual variation (i.e. special causes variation) is present. A timely identification of the sources of special cause variation is very important to maintain the quality of the output.

1.6   Control chart

Control charts are an effective tool in SPC for detecting changes in processes that may affect the quality of the products. Three horizontal lines plus the charting statistic constitute a control chart. The three lines are a center line (*CL*), an upper control limit (*UCL*) and a lower control limit (*LCL*). One of the control limits may be omitted if there is no interest in it, which would be the case when an upward (or downward) shift is less (or more) likely than a downward (upward) shift. The *CL* is typically taken to be the average of the statistic being plotted and the control limits are typically at distances of 3 standard deviations (of the plotting / charting statistic) above and below the *CL*. The use of control limits other than 3-sigma limits have been advocated in the literature; see, for example, Nelson (2003). The charting statistics which are calculated from individual or subgroups of observations are plotted in the time order in which they are sampled from the process so that the time behavior of the process can be observed visually. If a charting statistic plots within the control limits, then there is no signal and the process is deemed stable or IC. On the contrary, if a charting statistics plots on or above the *UCL*; or, on or below the *LCL* then there is a signal and a search for assignable or special causes can be initiated. Once the special cause is detected it must be rectified. A typical two-sided Shewhart-type control chart is illustrated in Figure 1.1.

4
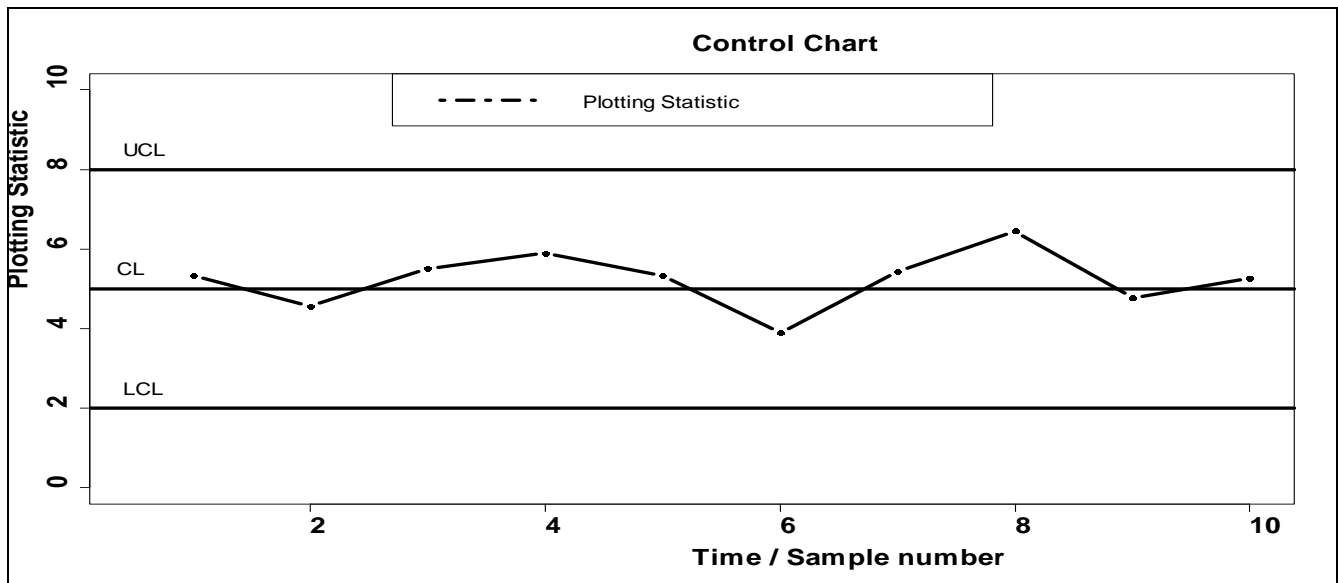
Figure 1.1. A typical two-sided Shewhart-type control chart

1.7   Rational subgrouping

In SPC applications subgroups should be selected such that if there is an assignable cause leading to an OOC signal, the chance of differences between the subgroups should be greater than the chance of differences within the subgroups. Stated differently, the variation among the readings within a subgroup should be due to the natural process variation only and there should be no opportunity for assignable causes to add to this variation (Montgomery (2013), Chapter 5). An example of rational subgrouping would be to sample from each machine if several machines are being used to produce an output. In other words, the output from each machine should be monitored separately instead of sampling from the items after the outputs of the machines have been pooled together. If the outputs of the machines have been combined before sampling, such subgroups will not be able to detect machine-to-machine differences. This is referred to as a masking effect, since the machine-to-machine differences will effectively be masked. In some cases it is not possible to form rational subgroups and in these cases it is appropriate to take individual observations ($n = 1$).

5

1.8 Phase I and Phase II

Unlike when the parameters are known (denoted by Case K), when process parameters are unknown (denoted by Case U), control charts can be applied in a two phase procedure: Phase I (the retrospective phase) and Phase II (the prospective phase). Phase I is an exploratory phase and some of the main aims include:

   i.   doing some preliminary (statistical) analyses, planning, administration, design of the study, data collection and other exploratory work such as goodness of fit analysis, factor analysis etc.,
   ii. assessing the stability of the process,
   iii. understanding the process variability, and
   iv. providing estimates of any unknown process parameters once all the observations associated with assignable causes have been removed from the Phase I sample.

The reader is referred to the detailed literature review by Chakraborti et al. (2009) for the technical details regarding performance measures and other issues related to Phase I control charting. Once an IC reference sample is established, Phase II analysis can start. In Phase II, future samples are monitored for departures from the IC state.

It is well-known that the use of estimated parameters significantly affects the statistical performance of Phase II charts (see Jensen et al. (2006)), making Phase I analysis, a phase of great importance. Even though this is the case, the majority of research on SPC control charting techniques has considered the development of Phase II charts only. In this dissertation, our focus is primarily on Phase II charts which are used for future process monitoring, however, Phase I will be briefly considered in Chapters 5.

It should be noted that some authors have advocated the use of self-starting charts (see, for example, Hawkins (1987)) in order to avoid the need for Phase I. However studies on self-starting charts have shown that they do not perform well if the process is initially unstable. This being said, it is important to note that self-starting charts can be useful in some cases such as low-volume, short-run processes and in start-up situations.

1.9   Control chart performance measures

Performance measures are used to study and compare the performance of various control charts. The run-length (denoted by *N*) of a control chart is a random variable that represents the number of plotted statistics until the control chart signals an OOC event for the first time. The average run-length (*ARL*) is the expected number of subgroups to be plotted until the chart signals for the first time (see Human and Graham (2007)). In Phase II effective charts should have a small out-of-control average run-length (*OOCARL*) while maintaining a large in-control average run-length (*ICARL*). Phase II charts are usually designed to have a pre-specified or nominal *ICARL* value $ICARL_0 = 370$.

The false alarm rate (*FAR*) is the probability that a single charting statistic plots on or outside the control limits when the process is actually IC. When the IC run-length distribution is geometric, then the *FAR* can be expressed as

$$FAR = \frac{1}{ICARL} \tag{1.1}$$

Hence, if the nominal *FAR* value is $FAR_0 = 0.0027$, then the nominal *ICARL* is equal to $ICARL_0 = 1/0.0027 = 370.4$, which is the case for the typical Shewhart $\overline{X}$ chart with 3-sigma limits with known parameters. This means that, even if the process remains IC, an OOC signal will be generated once every 370 samples, on average.

There are other measures of Phase II chart performance such as the standard deviation of the run-length (*SDRL*) and percentiles of the run-length such as the median run-length (*MRL*). The idea of looking at percentiles, in SPC, goes back to Barnard (1959) and more recently researchers such Khoo et al. (2011) have advocated the use of percentiles in SPC applications.

In Phase I, the run-length distribution and its properties are not the recommended design and evaluation measures, because in Phase I the signaling and non-signalling events are not independent. Furthermore, the plotting statistics are plotted and compared simultaneously with the same control limits (i.e. multiple testing). Hence, the false alarm probability (*FAP*), which is the probability that one or more

7

plotting statistics plot outside the control limits, is the recommended control chart design and evaluation metric in Phase I (see Chakraborti et al. (2009)).

1.10   Types of control charts

In this section we distinguish between the different types and classes of SPC charts. We give some of their relative advantages and mention situations where each could be used.

1.10.1 Shewhart, CUSUM and EWMA control charts

There are three main classes of control charts: the Shewhart chart, the cumulative sum (CUSUM) chart and the exponentially weighted moving average (EWMA) chart. Shewhart-type charts (see Shewhart (1926)) make the decision of whether the process is IC based on only the most recent information. In contrast CUSUM-type charts (see Page (1954)) and EWMA-type charts (see Roberts (1959)) are based (in different) ways on past information along with current information. Owing to this feature, these charts are more efficient to detect small and moderate shifts. In this dissertation, we will be focusing mostly on Shewhart-type charts. Since we focus mainly on Shewhart-type control charts, some background is given here.

Assume that $X_{i1}, X_{i2}, ..., X_{in}$ denote a random sample of size $n \geq 1$ from the process at time $i = 1,2,3,....$ Let T be a sample statistic that measures some quality characteristic of interest and suppose that the mean and standard deviation of T are given by u_T and σ_T, respectively. Then the control limits and CL are given by

$$UCL = \mu_T + k\sigma_T$$

$$CL = \mu_T \qquad\qquad (1.2)$$

$$LCL = \mu_T - k\sigma_T$$

where $k > 0$ is the charting constant which is a design parameter that represents the distance of the control limits from the CL, expressed in standard deviation units. As mentioned in Section 1.6, k is typically taken to be 3, however the use of control limits other than 3-sigma limits have been advocated in the literature; see, for example, Nelson (2003).

8

1.10.2 Parametric and nonparametric control charts

Parametric control charts are based on some particular distributional assumption for the underlying process distribution, such as normality. However, in many applications there is not enough information to justify such an assumption and control charts that do not depend on a particular distributional assumption are desirable. Nonparametric or distribution-free control charts can serve this broader purpose. For detailed overviews on nonparametric control chart literature, the reader is referred to Chakraborti et al. (2001), Chakraborti and Graham (2007) and Chakraborti et al. (2011).

1.10.3 Variables and attributes control charts

There are a variety of different types of control charts. Selecting the appropriate chart for any particular set of data is very important. Control charts used to analyze variables data can be based on the sample mean ($\overline{X}$) or the sample median ($\tilde{X}$) when monitoring location and the sample range (R), the sample standard deviation (S) or the sample variance (S^2) when monitoring spread.

Attributes charts include the *p* (fraction nonconforming) chart, the *np* (number nonconforming) chart, the *c* (number of nonconformities) chart and the *u* (average number of nonconformities per unit) chart and they are used for monitoring data that are counted. The *p* and *np* charts are used when the counts are assumed to have a binomial distribution. However, the *c* and *u* charts are used when the counts are assumed to have a Poisson distribution.

1.10.4 Univariate and multivariate control charts

The majority of research on SPC control charting techniques has considered the development of univariate charts where only one process characteristic is monitored at a time. Multivariate control charts are appropriate when two or more correlated process characteristics have been measured and there is a need to monitor them simultaneously, because monitoring these quality characteristics independently would be misleading. See Bersimis et al. (2007) for a detailed overview on multivariate control charts up to the year 2007.

9

1.11   Non-standard applications of SPC charts to customer satisfaction survey data

The primary application domain for SPC charts has been in process control and process improvement in manufacturing business. Recently, applications of control charts have been reported in domains outside of conventional production systems. These applications that cannot be considered as conventional applications in manufacturing processes or production systems, although there might be similarities in some cases, are defined as non-standard applications (MacCarthy and Wasusri (2001)).

MacCarthy and Wasusri (2001) reviewed non-standard applications of SPC charts reported in literature from the period 1989 to 2000, inclusive. In their review, they identified the types of non-standard problems to which SPC charts have been applied. They highlighted the issues that arise in non-standard application domains and provided some guidance to practitioners who want to implement SPC charts more generally. One important group of applications they mentioned is the application of SPC charts to monitor the level of customer satisfaction, typically from a service operation. The source of data for this application is typically from a survey. Thus, as expressed by MacCarthy and Wasusri (2001) "...*it may be difficult to use the raw data from surveys, which are likely to be ordinal, with SPC charts that are designed for ratio scale data. The nature of data obtained from surveys may not be normally distributed and the correlation between the questions potentially complicates the problem.*" Therefore, more advanced techniques and statistical expertise may need to be applied to prevent high false alarm rates.

Wardell and Candia (1996) showed that the effects of using the classical $\overline{X}$ chart based on sample ranges to ordinal survey data are to increase the false alarms rate. They also showed that an $\overline{X}$ chart with limits based on subgroup standard deviations is much more robust to the effects of the non-normality of survey data. However, they argued that the implementation of the $\overline{X}$ chart might be complicated by the large, variable subgroup sizes typical of survey data. They then proposed two alternative charts, the χ^2 control chart and the extension of the *p* chart (called the modified *p* chart). Both the χ^2 chart and the modified *p* chart can easily handle variable sample sizes, and are based on the actual distribution of survey data. However, as noted by Ding et al. (2006), these charts are complex and are not well established in literature. Another alternative method of dealing with moderate to severe non-normality, as noted by (Montgomery (2013), Chapter 5), is to "...*transform the original data (say by taking logarithms) to produce a new set of data whose distribution is closer to normal*".

10

To reiterate Wardell and Candia (1996) only isolated the effects of non-normality of survey data on the $\overline{X}$ chart. They ignored the correlation issue, the multiplicity issue (combined use of the $\overline{X}$ and R chart, see Section 1.12) and parameter estimation; which is known to degrade chart performance, see for example Jensen et al. (2006).

As mentioned before survey questions are usually correlated. Monitoring correlated quality characteristics independently can be very misleading (see Montgomery (2013), Chapter 11). This suggests the use of multivariate charts (see Section 1.10.4). However, it is known that as the number of variables grows, the traditional multivariate control charts lose efficiency with regard to shift detection (Montgomery (2013), Chapter 11). An accepted approach in these situations is to reduce the dimensionality of the data by using principal components or factor analysis. Montgomery (2013), Chapter 11, page 533 shows how this can be done. Jensen and Markland (1996) used factor analysis to reduce a 22 items of a service quality survey questionnaire to 4 factors. Using these 4 factors, they constructed a multivariate T^2 control chart to detect highly satisfactory and unsatisfactory perceptions of overall service for individual customers. For customers found to be out of control on the T^2 control chart, a set of control charts, relating to the 4 factors were constructed to find out the origin of the problem.

Next we briefly describe the issue of multiplicity.

1.12   Two chart joint monitoring of mean and variance of a normal population

Usually the $\overline{X}$ chart is used together with the R (or S) chart to monitor the process mean and standard deviation of a normally distributed process, respectively. The reason for this is that the control limits for an $\overline{X}$ chart are functions of the IC standard deviation, hence an increase in the variability may lead to a false signal on the $\overline{X}$ chart, and likewise, a decrease in variability may cause the $\overline{X}$ chart to fail to signal even though a shift in the mean has also occurred (Hawkins and Deng (2009)). In spite of this, in practice, the mean and variance charts are constructed and evaluated completely independently. As noted by Gan (1997), doing so is *"basically looking at a bivariate problem using two univariate procedures."*, and may give misleading results. Furthermore, as expressed by McCracken and Chakraborti (2013) *"schemes consisting of two independent charts can be affected by the classical 'multiple testing' problem, and if adjustments are not made to these charts control limits to account for*

11

this fact, the false alarm rate (FAR) is inflated, since the process is deemed to be OOC whenever a signal occurs on either chart. For example, if each chart is set at a nominal FAR of 0.0027 and the charts operate independently, the overall FAR (the probability of a false alarm on at least one chart) is $1 – (1 – 0.0027)^2 = 0.0054$, a 100% increase from the nominal 0.0027. This FAR inflation can ruin the efficacy of the resulting monitoring procedure. Therefore, practitioners using a two-chart scheme should select control limits for each chart such that the overall FAR is a specified value."

Note that Wardell and Candia (1996) evaluated only the $\overline{X}$ chart, thus they ignored the multiplicity issue. Fortunately, however, the modified *p* chart (just as with the classical *p* chart), which they proposed as a remedy to the issue of the non-normality of survey data does not need to be used together with a variability chart, since the variability chart is correlated to the mean chart (the modified *p* chart) and thus may not add important new information (Wardell and Candia (1996)).

To summarize, we have seen that there is a need to examine the *FAR* or the *ICARL* of the $\overline{X}$ and *R* charts when they are applied in tandem, as a combination of two charts (i.e. a combo scheme). There is a need for new control limits for the $\left(\overline{X}, R\right)$ charting scheme; which account for the effects of multiplicity and parameter estimation. Furthermore, we have seen that an application of the $\left(\overline{X}, R\right)$ charting scheme to customer satisfaction survey data may require some statistical expertise in data transformation and data reduction methods to deal with the non-normality and correlation issues, respectively.

1.13   Research objectives

In this dissertation, we focus on the combined use of the Phase II Shewhart $\overline{X}$ and *R* chart for monitoring the process mean and standard deviation of a normally distributed process, respectively. As noted by McCracken and Chakraborti (2013) *"such charts (for both Phase I and II) have not yet been studied in literature."* We show that the currently used control limits of the $\left(\overline{X}, R\right)$ charting scheme (as shown in Montgomery (2013, Chapter 6)) are incorrect because they cause more false alarms. Hence, we illustrate a technique for obtaining the correct control limits and then afterwards we provide a table of charting constants to aid implementation. We examine both the Case K and Case U in Chapters 2 and 3, respectively.

12

Woodall and Montgomery (1993) noted that there is a continuing need for publications of case studies showing the benefits of SQC in general. Thus, this motivated us to provide a case study in Chapter 5 that applies the $\left(\overline{X}, R\right)$ charting scheme (which we develop in Chapter 3) to students' evaluation of teaching (SET) survey data. We hope that our case study will provide some guidance to practitioners who want to use the $\left(\overline{X}, R\right)$ charting scheme to survey data in general and more in-particular to SET survey data.

There is also a continuing need for review papers that examine the nature and types of approaches used in different SPC charts applications (MacCarthy and Wasusri (2001)). In this regard and as a prelude to our case study, we give an overview of the literature on non-standard applications of SPC charts from 2000 to 2012, inclusive.

The rest of the dissertation is organized as follows: In Chapters 2 and 3 we address the problem of joint monitoring of the mean and the variance of a normally distributed process. Since it is easier to discuss the main ideas in the situation where the process mean and standard deviation are known (i.e. Case K) we first focus on this situation in Chapter 2. In practice, of course, there will be situations where the process parameters are unknown and need to be estimated from a set of Phase I or reference data, (i.e. Case U) and will be discussed in Chapter 3. In Chapter 4, we give an overview of the literature on non-standard applications of SPC. In Chapter 5, we present a case study that applies the $\left(\overline{X}, R\right)$ charting scheme to SET survey data. Finally, Chapter 6 provides a summary and offers some ideas for future research. Note that most of our results throughout this dissertation were evaluated using the software R version 3.0.1, the corresponding R codes are all given in the Appendix, at the end of each chapter.

Chapter 2

The $(\overline{X}, R)$ charting scheme when standards are known (Case K)

2.1 Introduction

While, a lot of work has been done in monitoring the mean and the standard deviation of a normally distributed process using Shewhart or Shewhart-type charts (Quesenberry (1993), Chen (1997, 1998), Chakraborti (2000, 2006)), few studies have considered the performance of these charts as they are applied in tandem (i.e. as a combination of two charts), which is how they are used in practice (see Montgomery (2013), Chapter 6). Multiple charts used in this manner are often called combination charting schemes (or combo schemes). For example, when the process mean is monitored with the Shewhart $\overline{X}$ chart, practitioners are advised to also monitor the standard deviation with an R (or an S) chart. Thus, two charts are used together in a combo scheme to make a decision about the IC or the OOC state of the process. The process is declared IC when both charts plot within their respective control limits and display random patterns. By contrast, the process is declared OOC when at least one of the charts shows an out-of-control situation, such as a non-random pattern or a point plotting outside the control limits. These two chart combo monitoring schemes can also consist of a pair of CUSUM, or EWMA charts. One for the mean and one for the variance, or even a combination of one CUSUM and one EWMA chart (see McCracken and Chakraborti (2013a, b), for a comprehensive review of all publications on joint monitoring of mean and variance up to the year 2012).

We use the $(\overline{X}, R)$ combo charting scheme in the discussion that follows even though there are recent books that suggest using a different spread chart, such as the S chart, see for instance Montgomery (2013, Chapter 6). We do this because the R chart is simple and continues to be used industry. It is easier to discuss the main ideas in case the process mean and standard deviation are known or specified (the so-called standards known case or Case K) and so we focus our attention to this case in this chapter. We begin with an example. We then show that the combination scheme, as applied now, results in highly inflated false alarm rates relative to what is nominally expected. Finally we present the

14

corrected or adjusted $(\overline{X}, R)$ charting scheme which involves finding the correct charting constants accounting for multiple (joint) charting.

Example 2.1

As an illustration, suppose that we interested in monitoring the mean of a normally distributed process. Suppose also that the IC mean and standard deviation of the process are known to be 8.53 and 3.36, respectively. Assuming that samples of size $n = 5$ are taken periodically from the process, the Shewhart control limits for the $\overline{X}$ chart (see Montgomery (2013), Chapter 6) are given by

$$UCL_{xbar} = \mu_0 + 3\frac{\sigma_0}{\sqrt{n}} = 8.53 + 3 \times \frac{3.36}{\sqrt{5}} = 13.04$$

$$LCL_{xbar} = \mu_0 - 3\frac{\sigma_0}{\sqrt{n}} = 8.53 - 3 \times \frac{3.36}{\sqrt{5}} = 4.02$$

Similarly, the Shewhart control limits for the R chart (see Montgomery (2013), Chapter 6) are given by

$$UCL_R = D_2\sigma_0 = (4.918) \times 3.36 = 16.53$$

$$LCL_R = D_1\sigma_0 = -0.27 \times 3.36 = -0.895$$

In Figures 2.1, 2.2, 2.3 and 2.4 (the corresponding R codes are given in Appendix 2), we show an application of these control limits to a set of simulated data. Note that it is standard practise to draw the $\overline{X}$ chart above the R chart (Stapenhurst (2005)). The recipe given in Montgomery (2013, Chapter 6) is to examine the R chart first. That is, if the R chart signals then the standard deviation must be brought under control, before considering the $\overline{X}$ chart, whether it signals or not (see Figure 2.1 and Figure 2.2). On the other hand, if the R chart does not signal but the $\overline{X}$ chart does (see Figure 2.3), then there is possibly a shift in the mean and a search for assignable causes may be undertaken. In Figure 2.4, both charts plot within their respective control limits and show a random pattern, so there is no signal and the process is said to be IC.

15
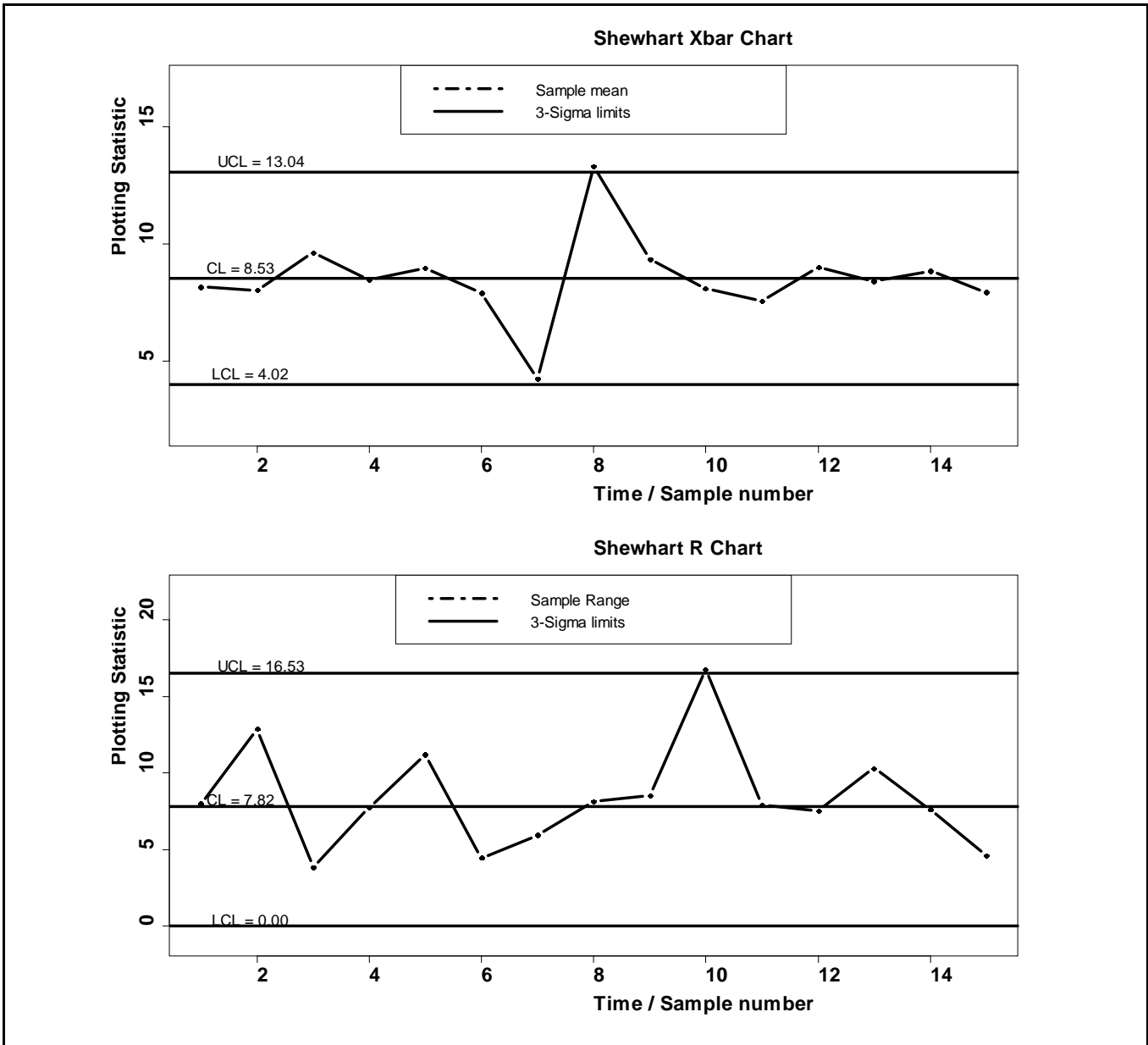
Figure 2.1. The Shewhart $\overline{X}$ and R charts with 3-sigma limits for $n = 5$ when both charts signal

16
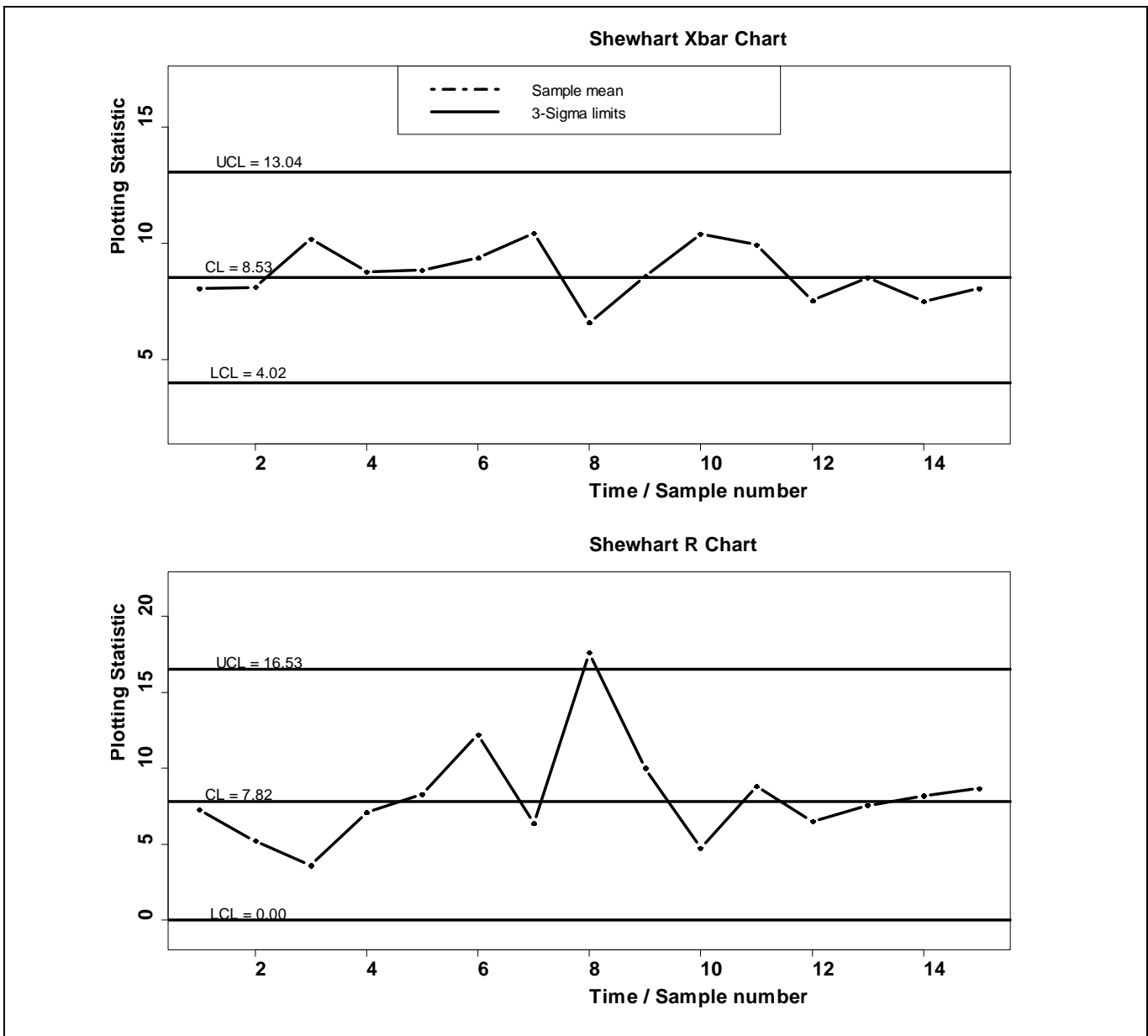
Figure 2.2. The Shewhart $\overline{X}$ and R charts with 3 sigma limits for $n = 5$ when only the R chart signals

17
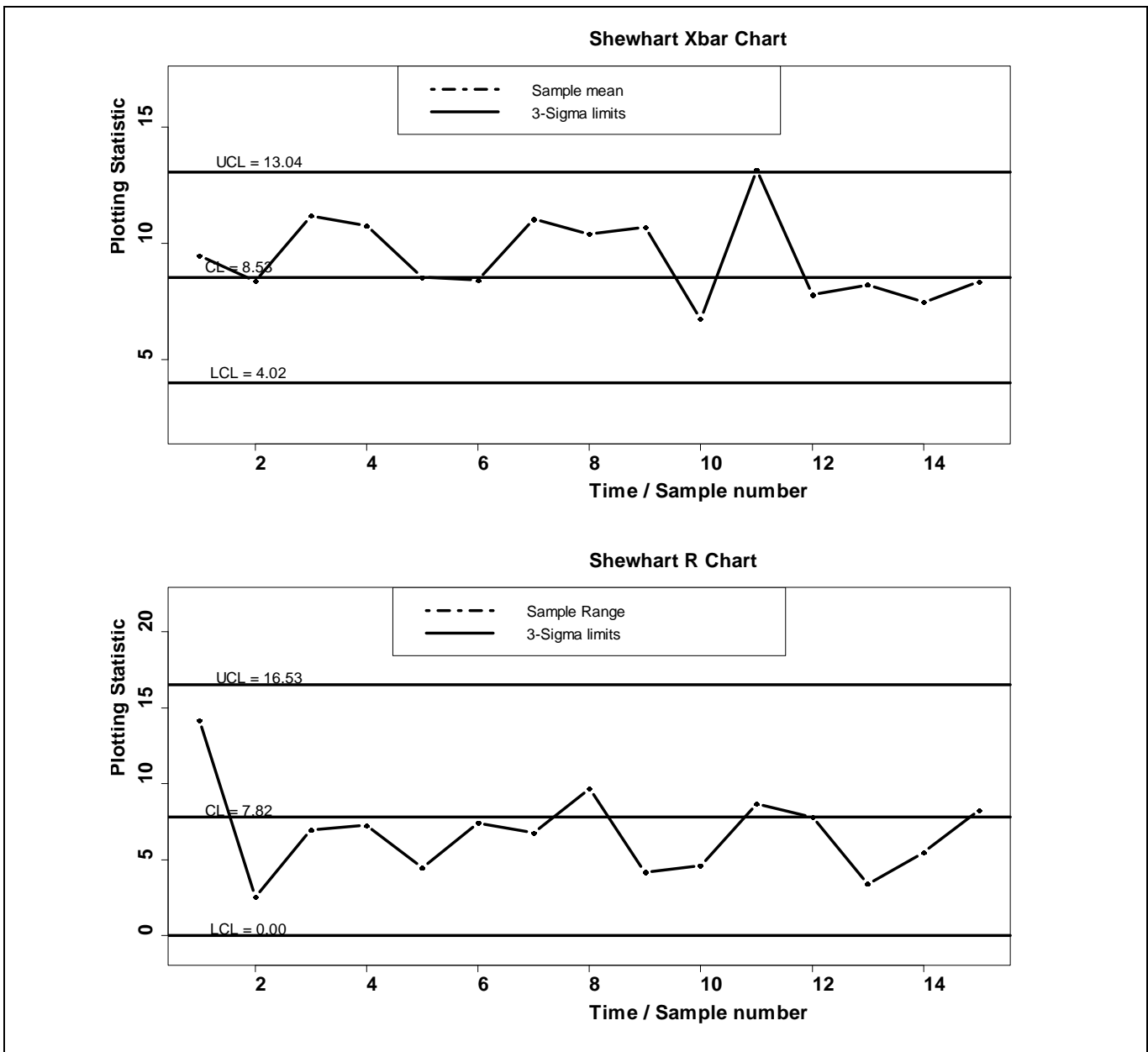
Figure 2.3. The Shewhart $\overline{X}$ and R charts with 3-sigma limits for $n = 5$ when only the $\overline{X}$ chart signals

18
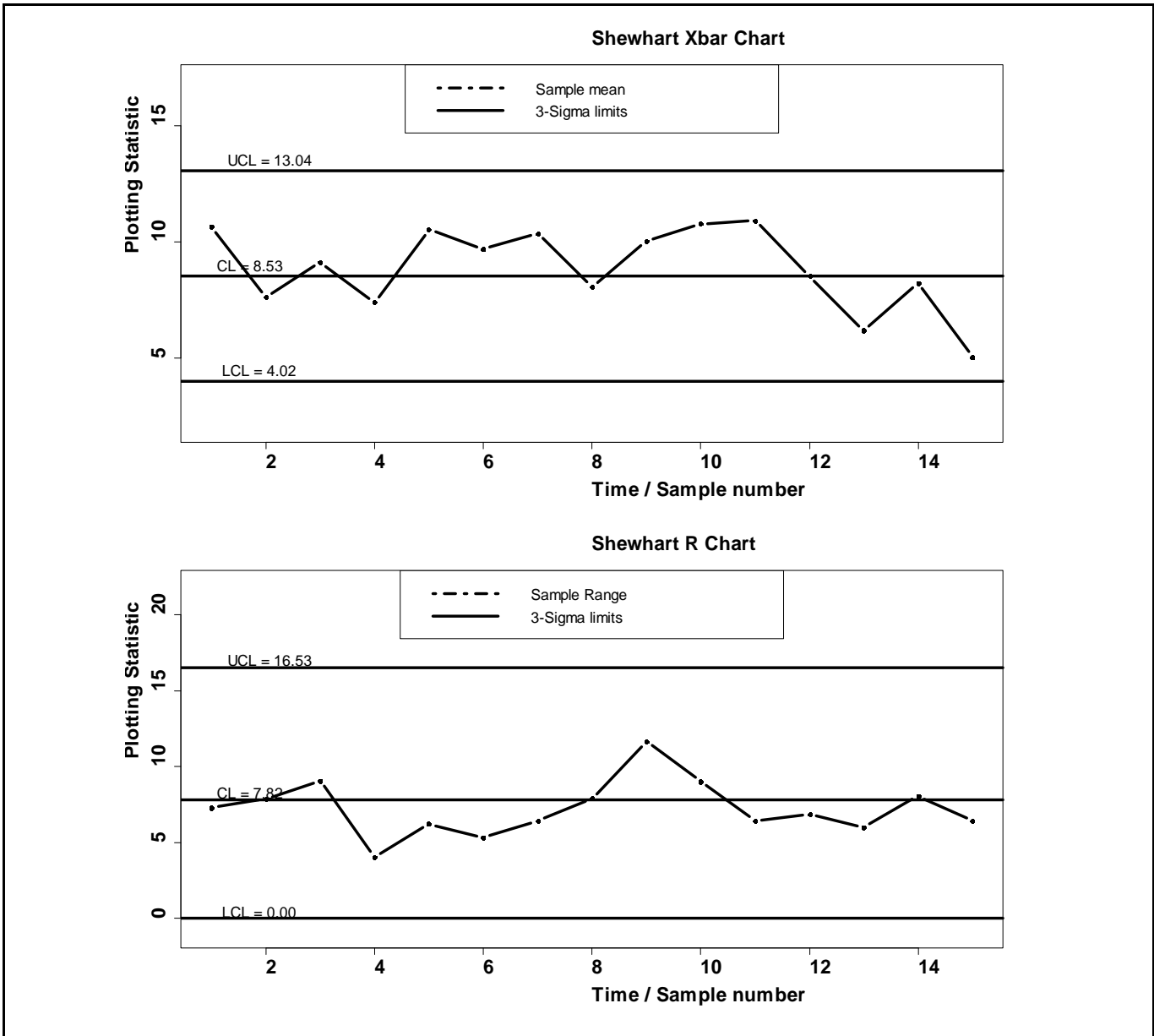
Figure 2.4. The Shewhart $\overline{X}$ and R charts with 3-sigma limits for $n = 5$ when neither chart signals

We demonstrate in the next section that there are major issues with this standard charting approach. The main problem with using this combo scheme is that the overall performance of the scheme is not what is nominally expected. In fact, the *attained false alarm rate* (*AFAR*) is much higher (or the *attained in-control average run-length* (*AICARL*) is much shorter) than the nominally expected false alarm rate (FAR_0) or the nominally expected in-control average run-length $(ICARL_0)$, see for example Table 2.1. This must be of real concern to all, since no matter which chart is used to monitor the mean and the standard deviation, the IC chart performance will degrade significantly and this can lead to a general loss of confidence in the control charting scheme.

19

The false alarm rate inflation happens due to *two* main reasons:

The first one is multiple testing, as two charts are used simultaneously in the decision making process, the combo chart or scheme does not deliver a $FAR_0 = 0.0027$. In fact, the *AFAR* of the combo scheme is far higher than 0.0027, as shown in Table 2.1. This means that a lot more false alarms are issued, leading to faulty decisions, possible work stoppages and reducing the value of the control charting scheme. Note that the fact that the two component charts are independent does not solve the problem of multiple testing but it does play a role in finding a correction.

The second one relates to the standard practice of using 3-sigma control limits in the individual charts. This is a common practice and is recommended in most textbooks, including Montgomery (2013, Chapter 6). However, note that even though the process is assumed to be normal, the plotting statistics $\overline{X}$ and R, each has a different sampling distribution, hence each component chart with a 3-sigma limit, has a different *AFAR* or *AICARL*. This, in turn, is shown in Table 2.1 to yield a completely different *AFAR* or *AICARL* for the combo chart. Likewise, each component chart has its own *AFAR* which can differ from the FAR_0 and $ICARL_0$ of the combo scheme, see for example Table 2.1.

2.2   Correcting the control limits

In order to correct these problems so that the overall (combo) scheme has the correct FAR_0, the control limits of the individual charts must be properly adjusted. To account for the multiplicity issue, the limits need to be adjusted so that the combo scheme has a specified $ICARL_0$. For the second issue, it will be seen that using 3-sigma limits on both charts does not work and one needs to use probability limits for each of the individual control charts.

We now review the conventional $(\overline{X}, R)$ scheme showing that the application of the scheme results in highly inflated *FAR* relative to what is nominally expected. However, since the properties of the combo scheme are a function of the properties of its component charts, we start by describing the individual component charts first.

20

2.2.1 The Shewhart $\overline{X}$ control chart

Let X_{ij}, $j = 1, 2, ..., n$ and $i = 1, 2, ...$ denote samples of size n from a normal distribution with a known IC mean $\mu = \mu_0$ and a standard deviation $\sigma = \sigma_0$, respectively. The plotting statistic of the Shewhart $\overline{X}$ chart for the ith sample is the sample mean $\overline{X}_i$. Recall that under the normality assumption, $\overline{X}_i$ follows a normal distribution with mean and variance of μ_0 and σ_0^2 / n, respectively. This result together with the *FAR₀* (or equivalently, the *ICARL₀*), are used to construct the Shewhart $\overline{X}$ chart. For example, for a nominal $FAR_0 = 0.0027$ (or equivalently, for a nominal $ICARL_0 = 370.40$) and IC values $\left(\mu = \mu_0, \sigma = \sigma_0 \right)$, the lower and upper control limits of the 3-sigma $\overline{X}$ chart are given in Montgomery (2013), Chapter 6, as

$$LCL_{xbar} = \mu_0 - 3\frac{\sigma_0}{\sqrt{n}} = \mu_0 - \Phi^{-1}\left(1 - 0.0027/2\right)\frac{\sigma_0}{\sqrt{n}}$$

$$\text{and} \tag{2.1}$$

$$UCL_{xbar} = \mu_0 + 3\frac{\sigma_0}{\sqrt{n}} = \mu_0 + \Phi^{-1}\left(1 - 0.0027/2\right)\frac{\sigma_0}{\sqrt{n}}$$

respectively, where Φ denotes the cdf of the standard normal distribution and Φ^{-1} denotes its quantile function. These control limits yield an *AFAR* of

$$\begin{aligned}
AFAR_{xbar} &= P(Signal|IC) \\
&= P(\overline{X}_i > UCL_{xbar} \mid IC) + P(\overline{X}_i < LCL_{xbar} \mid IC) \\
&= 1 - \Phi(3) + \Phi(-3) \\
&= 0.0027
\end{aligned}$$

and hence the *AICARL* of

$$AICARL_{xbar} = AFAR_{xbar}^{-1} = 0.0027^{-1} = 370.40 .$$

Table 2.1 (see the corresponding R code in Appendix 2) shows the IC performance of the $\overline{X}$ chart in terms of the *AFAR*, *AICARL* and the percentage difference (% diff) between the *AFAR* and FAR_0.

21

From Table 2.1, it can be seen that both the $AFAR_{xbar}$ and the $AICARL_{xbar}$ do not depend on the sample size and their values are equal to the nominal $FAR_0 = 0.0027$ and $ICARL_0 = 370.40$, respectively. However, this is not the case for the R and the $(\overline{X}, R)$ combo charts. We discuss these next.

2.2.2   The Shewhart R control chart

The 3-sigma Shewhart $\overline{X}$ control chart limits given in (2.1) depend on σ. Thus, one must ensure that σ is IC, that is $\sigma = \sigma_0$, and that it stays IC. This is why it is recommended to run a control chart, either the R chart or the S chart for the standard deviation, simultaneously, with the $\overline{X}$ chart.

The plotting statistic for the R chart is the sample range R_i and the IC distribution of R_i is approximated by the normal distribution: $R_i \sim N(\sigma_0 d_2, \sigma_0 d_3)$ where d_2, d_3 are constants defined later, this approximation and a given FAR_0 value are used to construct the R chart. Thus, for an $FAR_0 = 0.0027$ (or $ICARL_0 = 370.40$), the control limits of the Shewhart 3-sigma R chart are given in Montgomery (2013), Chapter 6, as

$$LCL_R = D_1 \sigma_0$$
$$UCL_R = D_2 \sigma_0 \tag{2.2}$$

where $D_1 = d_2 - 3d_3 = d_2 - \Phi^{-1}(1 - 0.0027/2)d_3$ and $D_2 = d_2 + 3d_3 = d_2 + \Phi^{-1}(1 - 0.0027/2)d_3$.

The constants d_2, d_3 depend on n and are tabulated in, for example, Montgomery (2013), page 720. The $AFAR$ for the 3-sigma R chart is

$$AFAR_R(n) = P(Signal \mid IC) = 1 - F_W(D_2) + F_W(D_1) \tag{2.3}$$

where $F_W(w)$ denotes the IC cdf of the relative range $W = R/\sigma_0$. Thus, the $AICARL$ is given by

$$AICARL_R(n) = [AFAR_R(n)]^{-1} \tag{2.4}$$

22

where $d_2 = E(W) = \int_{-\infty}^{\infty} (1 - F_W(w))dw = d_2(n)$ and $d_3 = \sqrt{Var(W)} = \sqrt{E(W^2) - d_2(n)^2}$ are the mean and the standard deviation of W, respectively, and

$$F_W(w) = n\int_{-\infty}^{\infty} [\Phi(x+w) - \Phi(x)]^{n-1} \phi(x)dx \qquad (2.5)$$

denotes the IC cdf of W, see Barbossa et al. (2011).

Table 2.1. The *AFAR* and *AICARL* values for the $(\overline{X}, R)$ combo chart and its component charts for different sample sizes

n	$\overline{X}$ chart		R chart			$(\overline{X}, R)$ combo scheme		
	AFAR	*AICARL*	*AFAR*	% diff	*AICARL*	*AFAR*	% diff	*AICARL*
3	0.00270	370	0.00584	116.41%	171	0.00853	215.81%	117
4	0.00270	370	0.00495	83.33%	202	0.00764	182.83%	131
5	0.00270	370	0.00460	70.48%	217	0.00729	170.02%	137
6	0.00270	370	0.00445	64.73%	225	0.00714	164.28%	140
7	0.00270	370	0.00438	62.11%	228	0.00706	161.66%	142
8	0.00270	370	0.00435	61.19%	230	0.00704	160.75%	142
9	0.00270	370	0.00435	61.22%	230	0.00704	160.78%	142
10	0.00270	370	0.00437	61.76%	229	0.00706	161.31%	142
15	0.00270	370	0.00449	66.44%	223	0.00718	165.98%	139
50	0.00270	370	0.00506	87.24%	198	0.00774	186.73%	129
100	0.00270	370	0.00538	99.19%	186	0.00806	198.65%	124

Figure 2.5 (see the R code in Appendix 2) compares the IC run-length cdf of the R chart for $n = 5$, 10, 100 with the cdf of the geometric distribution with parameter $FAR_0 = 0.0027$. It can be seen that the IC run-length cdf's of the R chart are much steeper compared to the nominally expected geometric cdf with parameter $FAR_0 = 0.0027$. This means that the 3-sigma limits R chart gives more false alarms on

23

average than what is expected nominally. Note that, when *n* is increased to 100, the IC run-length cdf is expected to approach that of the nominal geometric distribution. However, as seen in Figure 2.5, this is not true for the 3-sigma *R* chart. This undesirable phenomenon can be attributed to the fact that the sample range is a less efficient estimator of the population standard deviation and the efficiency of the sample range deteriorates for larger values of *n* (Stapenhurst (2005)).
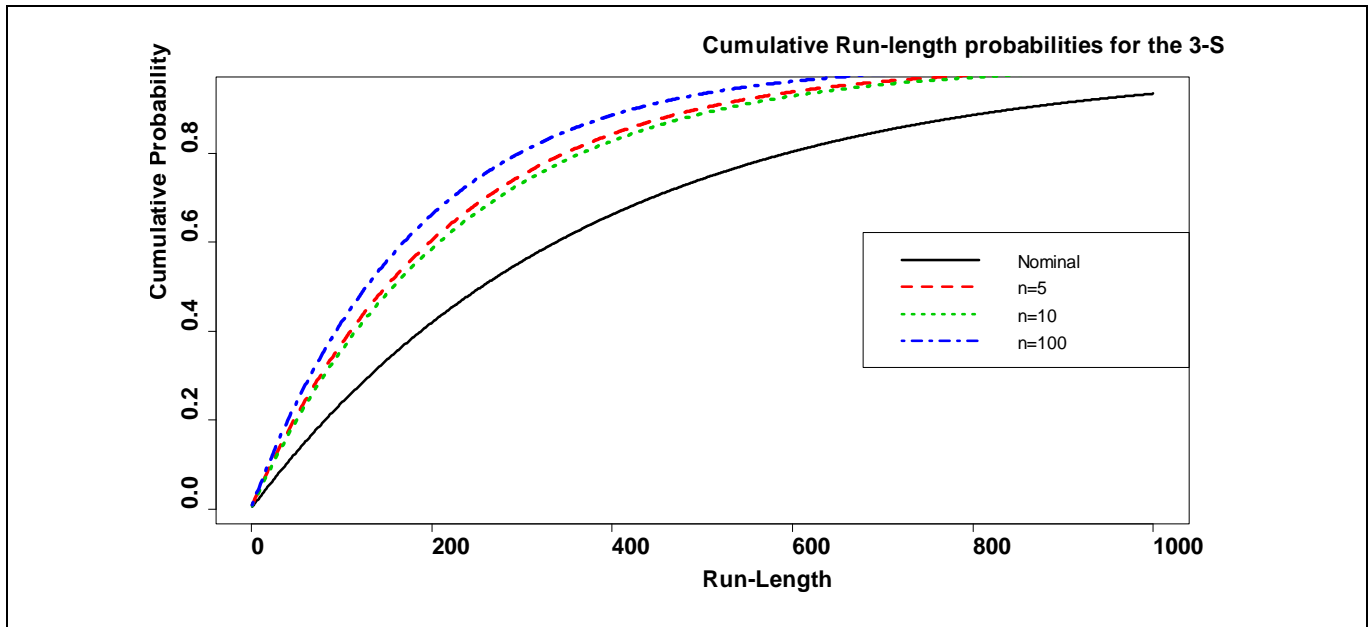
Figure 2.5. Comparison of the IC run-length cdf's of the Shewhart 3-sigma *R* chart for different sample sizes against the geometric cdf with parameter $FAR_0 = 0.0027$

Furthermore, from Table 2.1 it can be seen that for the *R* chart and sample sizes $4 \leq n \leq 100$ the percentage difference % diff ranges from 70.48% to 99.19% of the $FAR_0 = 0.0027$ (equivalently, the *AICARL* of this chart is reduced by 70.48% to 99.19% from its nominal value of 370.40). Therefore, using the 3-sigma limits on the *R* chart highly inflates the *FAR* (and reduces the *AICARL*) by up to two times their nominal values. This should be a cause for real concern.

These results are not surprising and somewhat known in the literature. For example, recently Barbosa et al. (2011) showed that the normal distribution is not a good approximation for the sample relative range (or the sample range) distribution. They pointed out that the upper quantiles of the distribution of *W*, which are required to calculate the *UCL* of the *R* chart are under approximated, causing frequent occurrences of false alarms. Furthermore the lower order quantiles of the distribution of *W,* which are needed for calculating the *LCL* in the *R* control chart, are not only quite different, but "*the normal*

24

approximation is totally inconsistent with the positive domain of the range statistic, causing obvious drawbacks, among others, the impossibility to detect a decrease in variability (eventually process improvement)." The latter can be seen in Example 2.1, where the $LCL_R = -0.895$. For this reason, it is standard practise to round up the LCL_R to 0.

In summary, using the normal approximation and the usual 3-sigma limits on the R chart is highly problematic, because the normal distribution is not a good approximation for W (or R) distribution. Next we discuss the effects of multiple testing.

2.2.3 Effects of multiple testing

As noted before, in practice, the Shewhart 3-sigma $\overline{X}$ chart and a spread chart such as the R chart are used together to make decisions about the status (IC or OOC) of a process. This combo charting scheme gives a signal when at least one of the two component charts, the $\overline{X}$ or the R chart, signals. The *AFAR* of this combo $(\overline{X}, R)$ charting scheme can be calculated as follows

$$
\begin{aligned}
AFAR_{combo}&(n)\\
&= P\left(\text{at least one chart signals}|IC\right)\\
&= 1 - P\left(\text{no signal on } \textit{either} \text{ chart}|IC\right)\\
&= 1 - P\left[\left(LCL_{xbar} < \overline{X}_i < UCL_{xbar},\ LCL_R < R_i < UCL_R\right)|IC\right]\\
&= 1 - \left(1 - AFAR_{xbar}\right)\left(1 - AFAR_R(n)\right)\\
&= 1 - \left(1 - ICARL_{xbar}^{-1}\right)\left(1 - ICARL_R^{-1}(n)\right)
\end{aligned}
\tag{2.6}
$$

where we utilize the independence of $\overline{X}_i$ and R_i for the normal distribution. Hence the *AICARL* of the $(\overline{X}, R)$ combo scheme in Case K is

$$
AICARL_{combo} = \left[1 - \left(1 - AICARL_{xbar}^{-1}\right)\left(1 - AICARL_R^{-1}\right)\right]^{-1}
\tag{2.7}
$$

and the IC run-length cdf of the $(\overline{X}, R)$ combo scheme is given by

$$P(N \leq t) = 1 - \left[(1 - AFAR_{xbar})(1 - AFAR_R(n)) \right]^t . \tag{2.8}$$

Using the IC run-length cdf, the performance of the 3-sigma limits combo $(\overline{X}, R)$ charting scheme is shown in Figure 2.6 (see the corresponding R code in Appendix 2) and compared to the nominal geometric cdf with parameter $FAR_0 = 0.0027$. It can be seen that the IC run-length cdf's for the combo scheme are much more steeper than the cdf of the geometric distribution with parameter $FAR_0 = 0.0027$. This means that the combo scheme issues more false alarms than what is nominally expected. Thus, the effect of using two charts, the $\overline{X}$ and the R chart together inflates the false alarm rate by a substantially high amount. This can be attributed to the simple reason that these charts were not designed to be used together and also that the approximate but not the exact sampling distribution of R_i was used to construct the R chart. Note that, increasing n to 10 somewhat improves the normal approximation to the distribution of R_i a little bit and hence reduce the effects of using 3-sigma limits on the R chart, however, it does nothing to reduce the more serious effects of multiple testing.
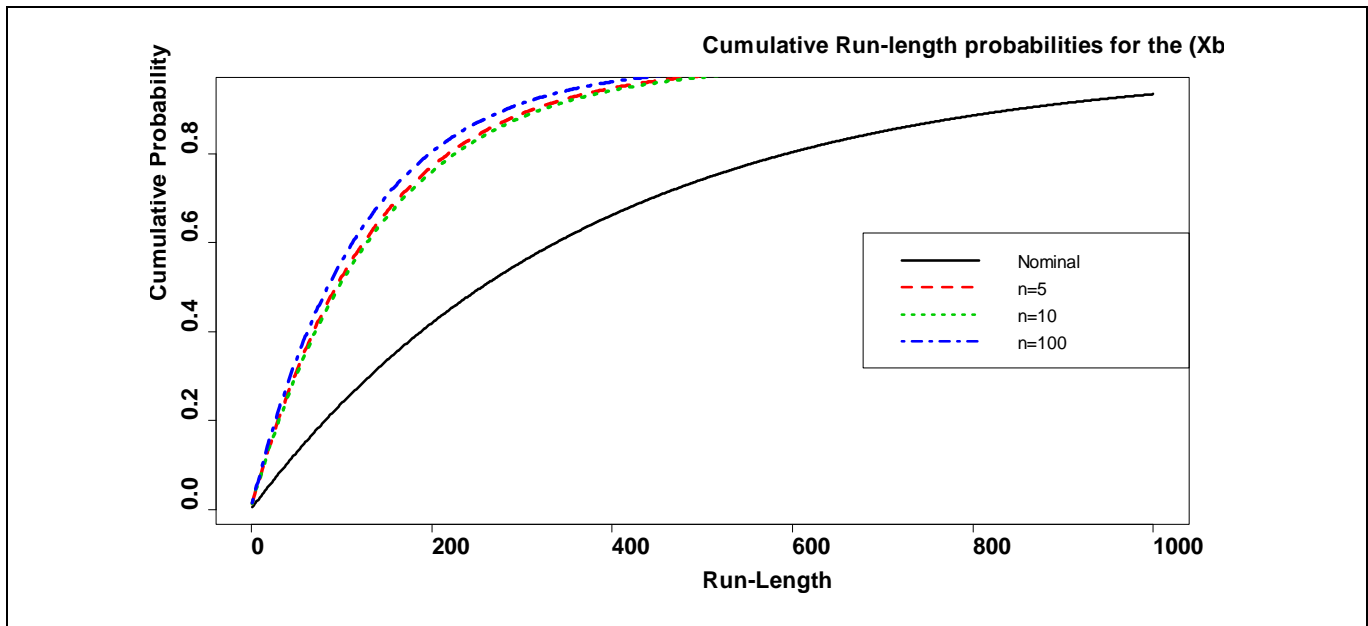
Figure 2.6. Comparison of the IC run-length cdf's of the combo $(\overline{X}, R)$ charting scheme for different sample sizes against the geometric cdf with parameter $FAR_0 = 0.0027$

Further, in Table 2.1, for $n = 3$, the *FAR* inflation is more than 200%, roughly three times higher than the $FAR_0 = 0.0027$. Even for a sample size of 100, the *AFAR* for the $(\overline{X}, R)$ combo chart is about 200% higher than the nominal value. Thus the current practice of using two charts together, roughly

26

doubles or triples the *FAR*. This needs to be seriously taken into consideration when designing the combo charting scheme.

2.2.4   New control limits adjusted for 3-sigma and multiplicity effects

We have shown in the above sections that if the 3-sigma and the multiplicity effects are not properly addressed when designing the $(\overline{X}, R)$ combo charting scheme, the whole control charting process runs the risk of becoming useless in practice. We now present a method for finding the charting constants and control limits of the $(\overline{X}, R)$ chart scheme taking *proper* account of both the multiplicity and 3-sigma limits effects.

We have seen that in Section 2.2.3, the *FAR* of the combo chart is given by

$$FAR_{combo}(n) = 1 - (1 - FAR_{xbar}(n))(1 - FAR_R(n)).$$

It seems reasonable to assume that each of the component charts should play an equal role in the combo charting scheme. From this point of view, if we let the *FAR* for each of the component charts to be the same, say $FAR_{xbar} = FAR_R(n) = D$, then the false alarm rate of the $(\overline{X}, R)$ combo scheme equals

$$FAR_{combo}(n) = 1 - (1 - D)^2.$$

Solving this expression for *D* we get

$$D = 1 - \sqrt{1 - FAR_{combo}(n)} = 1 - \sqrt{1 - ICARL_{combo}^{-1}(n)} \tag{2.9}$$

Thus, if we wish to have a nominal $ICARL_{combo}(n) = A$ or a $FAR_{combo}(n) = A^{-1}$, the *FAR*0 or the *ICARL*0 for the *individual component charts* would be

$$FAR_0 = D = 1 - \sqrt{1 - A^{-1}} \ \text{ or } \ ICARL_0 = (1 - \sqrt{1 - A^{-1}})^{-1}$$

27

respectively. Once D is found, it should be used to find the control limits (charting constants) in each of the component charts.

Thus, for the $\overline{X}$ chart, the correct charting constant should be the $100(1-D/2)^{\text{th}}$ quantile of the standard normal distribution and so the $\overline{X}$ chart limits corrected for multiple testing are given by

$$LCL_{xbar} = \mu_0 - \Phi^{-1}(1-D/2)\frac{\sigma_0}{\sqrt{n}}$$

and $\qquad\qquad$ (2.10)

$$UCL_{xbar} = \mu_0 + \Phi^{-1}(1-D/2)\frac{\sigma_0}{\sqrt{n}}$$

respectively. Similarly, for the R chart, the probability limits that are corrected for multiple testing are given by

$$LCL_R = D_1\sigma_0$$
$$UCL_R = D_2\sigma_0$$

$\qquad\qquad$ (2.11)

where

$$D_1 = d_2 - \Phi^{-1}(D/2)d_3$$
$$D_2 = d_2 + \Phi^{-1}(1-D/2)d_3.$$

One point to note here is that the R chart shown in (2.11) corrects for multiplicity but is based on the approximate normality (as reflected in the calculation of D_1 and D_2), which is problematic as discussed earlier in Section 2.2.2. Therefore, we recommend that the exact IC sampling distribution of R_i be used to find the charting constants and construct the exact probability limits for the Shewhart R chart. The exact charting constants in this case are thus given by the $100(D/2)^{\text{th}}$ and the $100(1-D/2)^{\text{th}}$ quantiles of the IC distribution of W,

$$LCL_R = F_W^{-1}(D/2)\sigma_0$$
$$UCL_R = F_W^{-1}(1-D/2)\sigma_0$$

$\qquad\qquad$ (2.12)

28

where F_W is the IC cdf of W.

One comment is in order here: A popular approach to correcting for multiple testing is using the so-called Bonferroni adjustment (Ryan (2000)). For k component tests, the Bonferroni adjusted charting constants are given by the $100(FAR_{combo}/2k)^{th}$ and the $100[1-(FAR_{combo}/2k)]^{th}$ percentiles of the marginal *IC* distribution of the standardised charting statistics of both the $\overline{X}$ and R charts. Using (2.10) and a Taylor's expansion, it can be shown that in this case D is approximately equal to $FAR_{combo}/2$. Thus, the multiple testing corrected limits are also approximately equal to the Bonferroni adjusted limits.

Table 2.2 presents the new charting constants corrected for multiplicity and the exact distribution issues for the $(\overline{X}, R)$ charting scheme for $n=3(1)10$ and an $ICARL_{combo}(n)=370$ and 500, see R code in Appendix.

Table 2.2. New charting constants for the Shewhart $(\overline{X}, R)$ combo charting scheme with $ICARL_0 = A$ = 370, 500 and $n = 3(1)10$

n	$ICARL_0$=A=370				$ICARL_0$=A=500			
	D	$\overline{X}$ **chart**	**R chart**		**D**	$\overline{X}$ **chart**	**R chart**	
3	0.00135	3.205	0.050	5.208	0.0010	3.290	0.043	5.316
4	0.00135	3.205	0.175	5.448	0.0010	3.290	0.158	5.553
5	0.00135	3.205	0.333	5.619	0.0010	3.290	0.308	5.722
6	0.00135	3.205	0.493	5.752	0.0010	3.290	0.464	5.853
7	0.00135	3.205	0.646	5.861	0.0010	3.290	0.613	5.960
8	0.00135	3.205	0.786	5.952	0.0010	3.290	0.751	6.050
9	0.00135	3.205	0.915	6.031	0.0010	3.290	0.878	6.127
10	0.00135	3.205	1.033	6.100	0.0010	3.290	0.995	6.196

Note that $D = 1 - \sqrt{1 - FAR_{combo}(n)} = 1 - \sqrt{1 - ICARL_{combo}^{-1}(n)}$

We illustrate the application of Table 2.2 with Example 2.2.

Example 2.2

Again as in Example 2.1, suppose we are interested in monitoring the average and the standard deviation of the continuous process variable *X* with a Shewhart $\overline{X}$ and an *R* chart, respectively. Samples of size *n* = 5 are taken periodically from the process. Suppose that the IC process mean and standard deviation are known to be 8.53 and 3.36, respectively. Using Table 2.2, the modified $(\overline{X}, R)$ chart limits can be calculated as follows

$$UCL_{xbar} = \mu_0 + 3.205\frac{\sigma_0}{\sqrt{n}} = 8.53 + 3.205 \times \frac{3.36}{\sqrt{5}} = 13.35$$

$$LCL_{xbar} = \mu_0 - 3.205\frac{\sigma_0}{\sqrt{n}} = 8.53 - 3.205 \times \frac{3.36}{\sqrt{5}} = 3.71$$

$$UCL_R = F_W^{-1}(1 - D/2)\sigma_0 = 5.619 \times 3.36 = 18.88$$

$$LCL_R = F_W^{-1}(D/2)\sigma_0 = 0.333 \times 3.36 = 1.12$$

Notice that for *n* = 5 and *ICARL* = 370 the corrected charting constants for the $\overline{X}$ chart are ± 3.205. The value *k* = 3.205 is 6.8% larger than the traditionally used constant of *k* = 3 in a conventional Shewhart chart. In Figure 2.7 (see R code in Appendix 2) we compare the traditional 3-sigma limits with the new modified limits for the Shewhart $\overline{X}$ and *R* charts respectively. For both cases, it can be seen that the corrected limits are wider than the traditional limits and this makes intuitive sense since the wider control limits reduce the false alarm rate and hence shorten the *AICARL* of the scheme, thus mitigating the effects of multiple testing. We encourage practitioners to use the new charting constants in Table 2.2 when implementing the $(\overline{X}, R)$ charting scheme in Case K. This reduces the rate of false alarms, drastically.
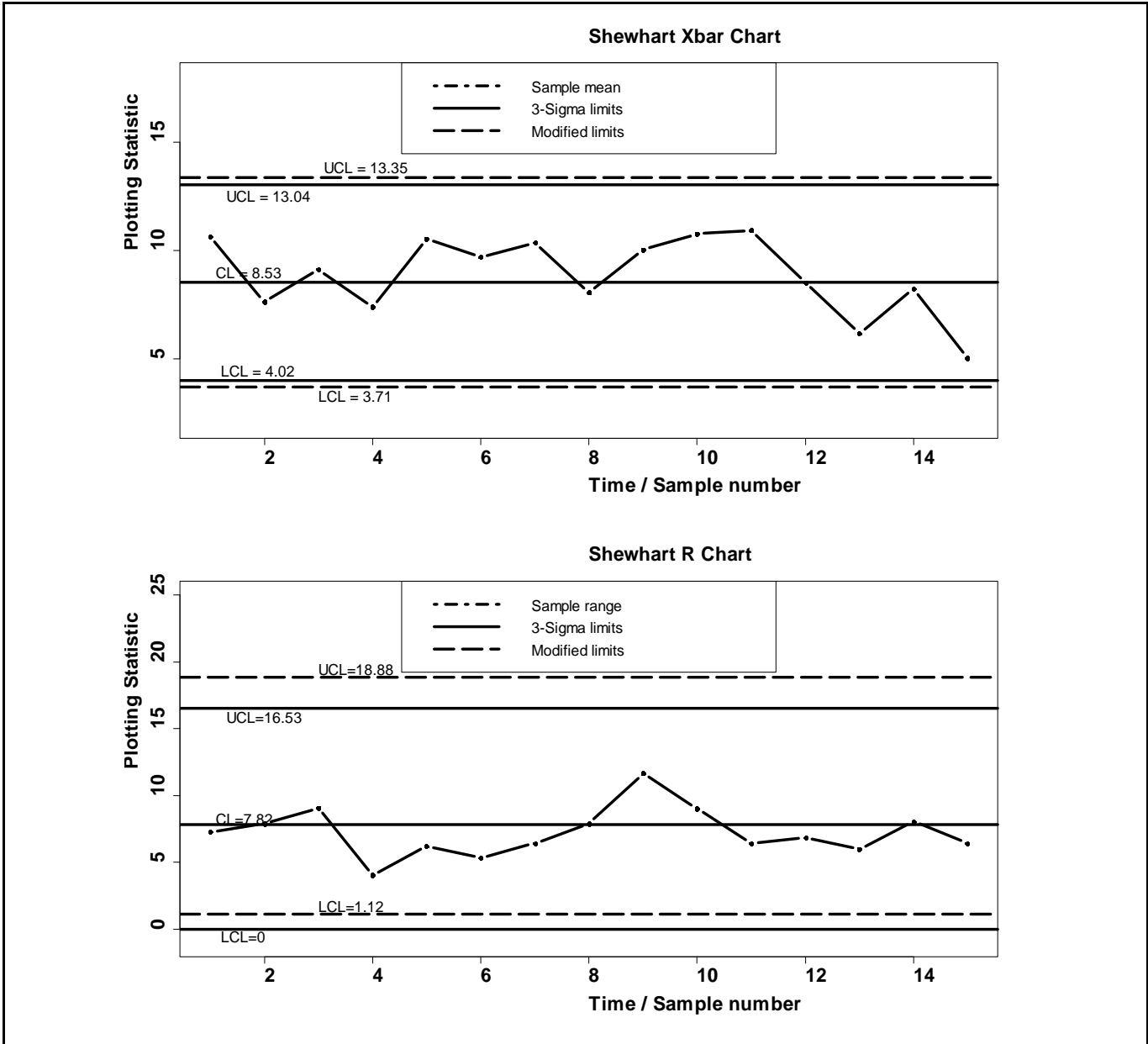
Figure 2.7 Comparison of the standard and corrected $(\overline{X}, R)$ chart limits

2.3   Summary and Conclusions

The Phase II Shewhart $(\overline{X}, R)$ chart scheme for jointly monitoring the process mean and standard deviation is usually implemented using 3-sigma limits for the individual charts. There are two major issues with this. First, it is assumed that the charting statistics are normally distributed. The second issue is multiple testing; since two charts are used at the same time to make decisions about the IC or OOC state of the process the *FAR* of the charting scheme is inflated. We showed the severity of these issues on the IC properties of the $(\overline{X}, R)$ charting scheme by examining the *AFAR* and the *ICARL*. We found that the current practice of using two charts together roughly doubles or triples the *FAR*. This needs to be seriously taken into consideration when designing the combo scheme. Hence, to account for the multiplicity issue, we adjusted the control limits of the individual component charts in such a way that the combo scheme has a specified $ICARL_0$. To correct for the 3-sigma limits issue, we used probability limits in each of the individual control charts. In addition, we provided tables of the charting constants for some nominal in-control average run-lengths and sample sizes to aid in implementing the $(\overline{X}, R)$ chart in practice. We saw that control limits based on our charting constants are wider than the traditional 3-sigma limits. This reduces the rate of false alarms, drastically. Hence, we encourage practitioners to use our charting constants in Table 2.2 and not the 3-sigma limits when implementing the $(\overline{X}, R)$ charting scheme in Case K.

32

2.4   Appendix 2: R Codes

Code for Figure 2.1 : Example of the Case K 3-sigma limits ($\overline{X}, R$) scheme with simulated data

```
set.seed(1442)
data=replicate(15,expr={
rnorm(5,8.53,3.36)})
y=colMeans(data)
x=1:15
plot(x,y,type = 'b', lwd=4, pch = 16, axes = TRUE, xlim = c(1,15), ylim = c(2,17),
cex.axis=1.7,cex.lab=1.7,cex.main=1.7,main="Shewhart Xbar Chart",xlab="Time / Sample
number",ylab="Plotting Statistic",font.lab=2, font.axis=2)
abline(h = c(4.02, 8.53, 13.04), lty = 1, lwd=4)
text(1.2,4.52,'LCL = 4.02',cex=1.3)
text(1.1,9.03, 'CL = 8.53',cex=1.3)
text(1.3,13.54,'UCL = 13.04',cex=1.3)
legend('top',legend=c("Sample mean","3-Sigma limits"),lty=c(4,1),lwd=4,cex=1.3)

set.seed(1442)
data=replicate(15,expr={
rnorm(5,8.53,3.36)})
y= apply(data,2,Range)
x=1:15
plot(x,y,type = 'b', lwd=4, pch = 16, axes = TRUE, xlim = c(1,15), ylim = c(-1,22),
cex.axis=1.7,cex.lab=1.7,cex.main=1.7,main="Shewhart R Chart",xlab="Time / Sample
number",ylab="Plotting Statistic",font.lab=2, font.axis=2)
abline(h = c(0,7.82,16.53), lty = 1, lwd=4)
text(1.2,0.50,'LCL = 0.00',cex=1.3)
text(1.1,8.32, 'CL = 7.82',cex=1.3)
text(1.3,17.03,'UCL = 16.53',cex=1.3)
legend('top',legend=c("Sample Range","3-Sigma limits"),lty=c(4,1),lwd=4,cex=1.3)
```

Code for Figure 2.2 : Example of the Case K 3-sigma limits ($\overline{X}, R$) scheme with simulated data

```
set.seed(19)
data=replicate(15,expr={
rnorm(5,8.53,3.36)})
y=colMeans(data)
x=1:15
plot(x,y,type = 'b', lwd=4, pch = 16, axes = TRUE, xlim = c(1,15), ylim = c(2,17),
cex.axis=1.7,cex.lab=1.7,cex.main=1.7,main="Shewhart Xbar Chart",xlab="Time / Sample
number",ylab="Plotting Statistic",font.lab=2, font.axis=2)
abline(h = c(4.02, 8.53, 13.04), lty = 1, lwd=4)
text(1.2,4.52,'LCL = 4.02',cex=1.3)
text(1.1,9.03, 'CL = 8.53',cex=1.3)
text(1.3,13.54,'UCL = 13.04',cex=1.3)
legend('top',legend=c("Sample mean","3-Sigma limits"),lty=c(4,1),lwd=4,cex=1.3)

set.seed(19)
data=replicate(15,expr={
rnorm(5,8.53,3.36)})
y= apply(data,2,Range)
x=1:15
plot(x,y,type = 'b', lwd=4, pch = 16, axes = TRUE, xlim = c(1,15), ylim = c(-1,22),
cex.axis=1.7,cex.lab=1.7,cex.main=1.7,main="Shewhart R Chart",xlab="Time / Sample
number",ylab="Plotting Statistic",font.lab=2, font.axis=2)
abline(h = c(0,7.82,16.53), lty = 1, lwd=4)
text(1.2,0.50,'LCL = 0.00',cex=1.3)
text(1.1,8.32, 'CL = 7.82',cex=1.3)
text(1.3,17.03,'UCL = 16.53',cex=1.3)
legend('top',legend=c("Sample Range","3-Sigma limits"),lty=c(4,1),lwd=4,cex=1.3)
```

Code for Figure 2.3 :Example of the Case K 3-sigma limits ($\overline{X}, R$) scheme with simulated data

```
set.seed(387)
data=replicate(15,expr={
rnorm(5,8.53,3.36)})
y=colMeans(data)
x=1:15
plot(x,y,type = 'b', lwd=4, pch = 16, axes = TRUE, xlim = c(1,15), ylim = c(2,17),
cex.axis=1.7,cex.lab=1.7,cex.main=1.7,main="Shewhart Xbar Chart",xlab="Time / Sample
number",ylab="Plotting Statistic",font.lab=2, font.axis=2)
abline(h = c(4.02, 8.53, 13.04), lty = 1, lwd=4)
text(1.2,4.52,'LCL = 4.02',cex=1.3)
text(1.1,9.03, 'CL = 8.53',cex=1.3)
text(1.3,13.54,'UCL = 13.04',cex=1.3)
legend('top',legend=c("Sample mean","3-Sigma limits"),lty=c(4,1),lwd=4,cex=1.3)

set.seed(387)
data=replicate(15,expr={
rnorm(5,8.53,3.36)})
y= apply(data,2,Range)
x=1:15
plot(x,y,type = 'b', lwd=4, pch = 16, axes = TRUE, xlim = c(1,15), ylim = c(-1,22),
cex.axis=1.7,cex.lab=1.7,cex.main=1.7,main="Shewhart R Chart",xlab="Time / Sample
number",ylab="Plotting Statistic",font.lab=2, font.axis=2)
abline(h = c(0,7.82,16.53), lty = 1, lwd=4)
text(1.2,0.50,'LCL = 0.00',cex=1.3)
text(1.1,8.32, 'CL = 7.82',cex=1.3)
text(1.3,17.03,'UCL = 16.53',cex=1.3)
legend('top',legend=c("Sample Range","3-Sigma limits"),lty=c(4,1),lwd=4,cex=1.3)
```

Code for Figure 2.4 : Example of the Case K 3-sigma limits ($\overline{X}, R$) scheme with simulated data

```
set.seed(15)
data=replicate(15,expr={
rnorm(5,8.53,3.36)})
y=colMeans(data)
x=1:15
plot(x,y,type = 'b', lwd=4, pch = 16, axes = TRUE, xlim = c(1,15), ylim = c(2,17),
cex.axis=1.7,cex.lab=1.7,cex.main=1.7,main="Shewhart Xbar Chart",xlab="Time / Sample
number",ylab="Plotting Statistic",font.lab=2, font.axis=2)
abline(h = c(4.02, 8.53, 13.04), lty = 1, lwd=4)
text(1.2,4.52,'LCL = 4.02',cex=1.3)
text(1.1,9.03, 'CL = 8.53',cex=1.3)
text(1.3,13.54,'UCL = 13.04',cex=1.3)
legend('top',legend=c("Sample mean","3-Sigma limits"),lty=c(4,1),lwd=4,cex=1.3)
data=replicate(15,expr={
rnorm(5,8.53,3.36)})
y= apply(data,2,Range)
x=1:15
plot(x,y,type = 'b', lwd=4, pch = 16, axes = TRUE, xlim = c(1,15), ylim = c(-1,22),
cex.axis=1.7,cex.lab=1.7,cex.main=1.7,main="Shewhart R Chart",xlab="Time / Sample
number",ylab="Plotting Statistic",font.lab=2, font.axis=2)
abline(h = c(0,7.82,16.53), lty = 1, lwd=4)
text(1.2,0.50,'LCL = 0.00',cex=1.3)
text(1.1,8.32, 'CL = 7.82',cex=1.3)
text(1.3,17.03,'UCL = 16.53',cex=1.3)
legend('top',legend=c("Sample Range","3-Sigma limits"),lty=c(4,1),lwd=4,cex=1.3)
```

Code for Figure 2.5 : Cumulative run-length probabilities for the 3-sigma R chart

```
x=1:1000
y=pgeom(x,0.0027)
plot(x,y,type = 'l', lwd=3, cex.axis=1.7,cex.lab=1.7,cex.main=1.7,main="Cumulative Run-length
probabilities for the 3-Sigma R chart",xlab="Run-Length",ylab="Cumulative Probability",font.lab=2,
font.axis=2)
far=c(0.00460,0.00437,0.00538)
for (i in 1:length(far)){
lines(x,pgeom(x,far[i]),lty=i+1,lwd=4,col=i+1,cex=5)}
legend('right',legend=c("Nominal","n=5","n=10","n=100"),lty=c(1,2,3,4),lwd=3,col=c(1,2,3,4),cex=1.3
)
```

Code for Figure 2.6 : Cumulative run-length probabilities for the ($\overline{X}$, R) scheme

```
x=1:1000
y=pgeom(x,0.0027)
plot(x,y,type = 'l', lwd=3, cex.axis=1.7,cex.lab=1.7,cex.main=1.7,main="Cumulative Run-length
probabilities for the (Xbar,R) scheme",xlab="Run-Length",ylab="Cumulative Probability",font.lab=2,
font.axis=2)
far=c(0.00729,0.00706,0.00806)
for (i in 1:length(far)){
lines(x,pgeom(x,far[i]),lty=i+1,lwd=4,col=i+1,cex=5)}
legend('right',legend=c("Nominal","n=5","n=10","n=100"),lty=c(1,2,3,4),lwd=3,col=c(1,2,3,4),cex=1.3
)
```

Code for Table 2.1 : The *AFAR*, *ICARL* and %diff for the 3-sigma *R* chart

```
n=c(3,4,5,6,7,8,9,10,15,50,100)

AFAR=function(n){
d2=function(n){
pt=function(w){1-ptukey(w,n,Inf)}
integrate(pt,lower=0,upper=Inf)[[1]]}
EW2=function(n){
ptt=function(a){(1-ptukey(sqrt(a),n,Inf))}
integrate(ptt,lower=0,upper=Inf)[[1]]}
d3=function(n){
sqrt(EW2(n)-d2(n)^2)}
D4=d2(n)+3*d3(n)
D3=d2(n)- 3*d3(n)
DD3=max(c(D3,0))
1-ptukey(D4,n,Inf)+ptukey(DD3,n,Inf)}

AFARrchart=numeric(length(n))
for (i in 1:length(n)) {
AFARrchart[i]= AFAR(n[i])}

ICARLrchart=AFARrchart^-1
Percent_dif=((AFARrchart-0.0027)/0.0027)
Results=cbind(AFARrchart,Percent_dif,ICARLrchart)
rownames(Results)=c( 3, 4, 5, 6, 7, 8, 9, 10, 15, 50, 100)
Results
write.table(Results, "clipboard",sep="\t",col.names=NA)
```

Code for Table 2.1 : The *AFAR*, *ICARL* and %diff for the 3-sigma ($\overline{X}, R$) scheme

```
n=c(3,4,5,6,7,8,9,10,15,50,100)

AFAR=function(n){
d2=function(n){
pt=function(w){1-ptukey(w,n,Inf)}
integrate(pt,lower=0,upper=Inf)[[1]]}
EW2=function(n){
ptt=function(a){(1-ptukey(sqrt(a),n,Inf))}
integrate(ptt,lower=0,upper=Inf)[[1]]}
d3=function(n){
sqrt(EW2(n)-d2(n)^2)}
D4=d2(n)+3*d3(n)
D3=d2(n)- 3*d3(n)
DD3=max(c(D3,0))
1-ptukey(D4,n,Inf)+ptukey(DD3,n,Inf)}

AFARrchart=numeric(length(n))
for (i in 1:length(n)) {
AFARrchart[i]= AFAR(n[i])}
ICARLrchart=AFARrchart^-1
AFARxbar=1-pnorm(3,0,1)+pnorm(-3,0,1)
ICARLxbar=AFARxbar^-1
AFARxbar_rchart=1-(1-AFARrchart)*(1-AFARxbar)
ICARLxbar_rchart=AFARxbar_rchart^-1
Percent_dif=((AFARxbar_rchart-0.0027)/0.0027)
Results=cbind(AFARxbar_rchart,Percent_dif,ICARLxbar_rchart)
rownames(Results)=c( 3, 4, 5, 6, 7, 8, 9, 10, 15, 50, 100)
Results
write.table(Results, "clipboard",sep="\t",col.names=NA)
```

Code for Table 2.2 : Calculation of the new Case K charting constants

```
ICARL=c(370,500)
D=numeric(length(ICARL))
D[1]=1-sqrt(1-ICARL[1]^-1)
D[2]=1-sqrt(1-ICARL[2]^-1)
n=c(3,4,5,6,7,8,9,10)
Cons=matrix(nrow=length(n),ncol=8)
for (i in 1:length(n)){
Cons[i,]=c(D[1],qnorm(1-D[1]/2,0,1),qtukey(D[1]/2,n[i],Inf),qtukey(1-D[1]/2,n[i],Inf), D[2],qnorm(1-
D[2]/2,0,1),qtukey(D[2]/2,n[i],Inf),qtukey(1-D[2]/2,n[i],Inf))}
rownames(Cons)= c(3,4,5,6,7,8,9,10)
Cons
write.table(Cons, "clipboard",sep="\t",col.names=NA)
```

Code for Figure 2.7 : Example of the Case modified limits ($\overline{X}, R$) scheme with simulated data

```
set.seed(15)
data=replicate(15,expr={
rnorm(5,8.53,3.36)})
y=colMeans(data)
x=1:15
plot(x,y,type = 'b', lwd=4, pch = 16, axes = TRUE, xlim = c(1,15), ylim = c(2,18),
cex.axis=1.7,cex.lab=1.7,cex.main=1.7,main="Shewhart Xbar Chart",xlab="Time / Sample
number",ylab="Plotting Statistic",font.lab=2, font.axis=2)
abline(h = c(4.02, 8.53, 13.04), lty = 1, lwd=4)
text(1.2,4.52,'LCL = 4.02',cex=1.3)
text(1.1,9.03, 'CL = 8.53',cex=1.3)
text(1.3,12.54,'UCL = 13.04',cex=1.3)
abline(h = c(3.71, 13.35), lty = 5, lwd=4)
text(3,3.31,'LCL = 3.71',cex=1.3)
text(3.1,13.85,'UCL = 13.35',cex=1.3)
legend('top',legend=c("Sample mean","3-Sigma limits","Modified limits"),lty=c(4,1,5),lwd=4,cex=1.3)

set.seed(15)
data=replicate(15,expr={
rnorm(5,8.53,3.36)})
y= apply(data,2,Range)
x=1:15
plot(x,y,type = 'b', lwd=4, pch = 16, axes = TRUE, xlim = c(1,15), ylim = c(-1,25),
cex.axis=1.7,cex.lab=1.7,cex.main=1.7,main="Shewhart R Chart",xlab="Time / Sample
number",ylab="Plotting Statistic",font.lab=2, font.axis=2)
abline(h = c(0,7.82,16.53), lty = 1, lwd=4)
text(1.2,-0.50,'LCL=0',cex=1.3)
text(1.1,8.32, 'CL=7.82',cex=1.3)
text(1.3,15.95,'UCL=16.53',cex=1.3)
abline(h = c(1.12, 18.88), lty = 5, lwd=4)
text(3,1.77,'LCL=1.12',cex=1.3)
text(3,19.50,'UCL=18.88',cex=1.3)
legend('top',legend=c("Sample range","3-Sigma limits","Modified limits"),lty=c(4,1,5),lwd=4,cex=1.3)
```

Chapter 3

The $(\overline{X}, R)$ charting scheme when standards are unknown (Case U)

3.1   Introduction

In this chapter, we consider the $(\overline{X}, R)$ charting scheme when process parameters are unknown (Case U) and are to be estimated from reference Phase I data. Most practitioners make use of the Case K control limits in Expressions (2.1) and (2.2) when monitoring the process mean and process standard deviation, respectively, even though the Phase 1 estimates $\hat{\mu}_0$ and $\hat{\sigma}_0$ are used in place of μ_0 and σ_0 to construct the charts. These control limits are incorrect because their *AICARL* can be a lot much shorter (see Table 3.1) than what is nominally expected due to the effects of multiple testing, the standard use of the 3-sigma limits and parameter estimation. Parameter estimation is known to degrade control chart performance (see for example Jensen et al. (2006)). This must be disturbing to all, since it means a lot more false alarms in Case U than what we have observed in Case K (Chapter 2). This, in turn, implies a lot more faulty decisions and possible work stoppages, thus rendering the control charting scheme wasteful, costly and useless.

In the sections that follow, we show that the standard Case U $(\overline{X}, R)$ charting scheme results in highly inflated false alarm rates relative to what is nominally expected and relative to Case K. We then present the corrected or adjusted $(\overline{X}, R)$ charting scheme. This involves finding the correct charting constants accounting for the effects of multiple (joint) charting, the use of 3-sigma limits in individual component charts along with parameter estimation.

3.2   Correcting the control limits

In order to maintain a specified or nominal IC average run-length $(ICARL_0)$ or nominal false alarm rate (FAR_0) for the combo $(\overline{X}, R)$ chart in Case U, it is necessary to make modifications to the $\overline{X}$ and R charts (control limits) so that the effects of parameter estimation are correctly accounted for together with the effects of multiple testing. We accomplish this by first using the conditioning technique developed in Chakraborti (2000), then applying the correction due to multiple testing (see Chapter 2) and finally using the probability limits.

41

We now review the conventional $(\overline{X}, R)$ scheme in Case U showing that the application of the scheme results in much shorter *AICARL* than what is nominally expected and also relative to what we saw in Case K (Chapter 2). However, since the properties of the Case U charting scheme are a function of the properties of its individual component charts, we describe the individual component charts first and then give the properties of the combo scheme later.

3.2.1   The Shewhart $\overline{X}$ control chart

When process parameters are unknown, they must be estimated from Phase I data. Let X_{ij}, $i=1,2,\ldots,m$ and $j=1,2,\ldots,n$ denote IC Phase I data from the normal distribution with unknown mean μ and unknown standard deviation σ, where m is the number of subgroups and n is the subgroup size.

The plotting statistic for the $\overline{X}$ chart is the sample mean $\overline{X}_i$ $i=m+1, m+2,\ldots$. Recall that the IC distribution of the sample mean is normal with mean $\hat{\mu}_0$ and variance $\hat{\sigma}_0^2/n$. This result together with a FAR_0 are used to define the $\overline{X}$ chart limits. Thus, for an $FAR_0 = 0.0027$ (or, $ICARL_0 = 370.40$, the control limits of the estimated 3-sigma Shewhart $\overline{X}$ chart are given in Montgomery (2013), Chapter 6, as

$$LCL_{xbar} = \overline{\overline{X}} - \frac{3}{d_2\sqrt{n}}\overline{R} = \overline{\overline{X}} - A_3\overline{R}$$

$$UCL_{xbar} = \overline{\overline{X}} + \frac{3}{d_2\sqrt{n}}\overline{R} = \overline{\overline{X}} + A_4\overline{R}$$

(3.1)

where $\overline{\overline{X}}$ is the grand average of the Phase I subgroup averages, $\overline{R}$ is the average of Phase I sample ranges and the charting constant 3 is the $100\left[1 - \frac{FAR_0}{2}\right]^{th}$ percentile of the standard normal distribution. Note that, the plotting statistic $\overline{X}_i$ can be transformed to $Z_i = \dfrac{\overline{X}_i - \mu}{\sigma/\sqrt{n}}$, which can be used as a plotting statistic for the following equivalent set of limits

$$L\hat{C}L_{xbar} = \frac{Z}{\sqrt{m}} - 3\frac{c\sqrt{U}}{\sqrt{v}}$$

$$U\hat{C}L_{xbar} = \frac{Z}{\sqrt{m}} + 3\frac{c\sqrt{U}}{\sqrt{v}}$$

(3.2)

where $Z = \sqrt{mn}(\overline{\overline{X}} - \mu)/\sigma$ is the standard normal variable, $U = \frac{v\overline{R}^2}{c^2 d_2^2 \sigma^2}$ is approximately a chi-squared variable having v degrees of freedom, the constant c depends on v, which is a function of m and n.

The *AFAR* is given by

$$AFAR_{xbar} = \int_0^\infty \int_{-\infty}^\infty AFAR_{xbar}(z,u)\,\phi(z)\,g(u)\,dzdu$$
$$= \int_0^\infty \int_{-\infty}^\infty \left[1 - \Phi\left(U\hat{C}L_{xbar}\right) + \Phi\left(L\hat{C}L_{xbar}\right)\right]\phi(z)\,g(u)\,dzdu$$

(3.3)

where Φ denotes the cdf of the standard normal distribution, ϕ denotes the density function of the standard normal distribution, g represents the density function of the chi-squared distribution and $AFAR_{xbar}(z,u)$ is the conditional attained false alarm rate. However, when control limits are estimated, the attained false alarm rate is a poor measure of control chart performance, see Jensen et al. (2006). In this case, the run-length distribution and its properties are the recommended control chart performance measures. Hence, the IC run-length cdf for the Shewhart $\overline{X}$ chart with 3-sigma limits is given by

$$P(N \le t) = 1 - \int_0^\infty \int_{-\infty}^\infty \left[\Phi\left(U\hat{C}L_{xbar}\right) - \Phi\left(L\hat{C}L_{xbar}\right)\right]^t \varphi(z)g(u)dzdu$$

(3.4)

and its mean, the *AICARL*, can be written as

$$AICARL_{xbar} = \int_0^\infty \int_{-\infty}^\infty \left[AFAR_{xbar}(z,u)\right]^{-1} \varphi(z)g(u)dzdu$$

(3.5)

where N denotes the run-length variable and $t = 0,1,2,3,...$. Figure 3.1 (see the corresponding R code in Appendix 3) shows the IC run-length cdf of the 3-sigma limits $\overline{X}$ chart for Case U (for $m = $ 5, 15, 30 and 100) and compares it to the 3-sigma limits $\overline{X}$ chart for Case K. It can be seen that, for small N and small m, the run-length cdf's for Case U are steeper than the Case K cdf, particularly when $m = 5$. This means more short runs will be issued in Case U than in Case K and this translates

43

to a lot more false alarms for Case U compared to Case K. Furthermore, for large N but small m, the Case U cdf's are below the Case K cdf. This is caused by a few very large values of N that occur with parameter estimation (see Quesenberry (1993)). These very large values of N can be viewed as outliers, which pull the *AICARL* towards them, making it appear very large (see Table 3.1) than it really is. This can lead to the misunderstanding of chart properties. In summary, parameter estimation causes the Case U $\overline{X}$ chart to issue a lot more false alarms relative to Case K.

Table 3.1 (see the corresponding R code in Appendix 3) shows the *AICARL* of the $\overline{X}$ chart for different values of m. As mentioned before, it can be seen that for small m, the *AICARL's* are much larger than the $ICARL_0 = 370$ in Case K. In addition, both Table 3.1 and Figure 3.1 show that when m is increased the IC run-length distribution of the Case U $\overline{X}$ chart approaches the Case K geometric distribution with parameter $FAR_0 = 0.0027$. However, as seen in Table 3.1, this is not the case for the R chart and the $(\overline{X}, R)$ combo charting scheme. We discuss these next.
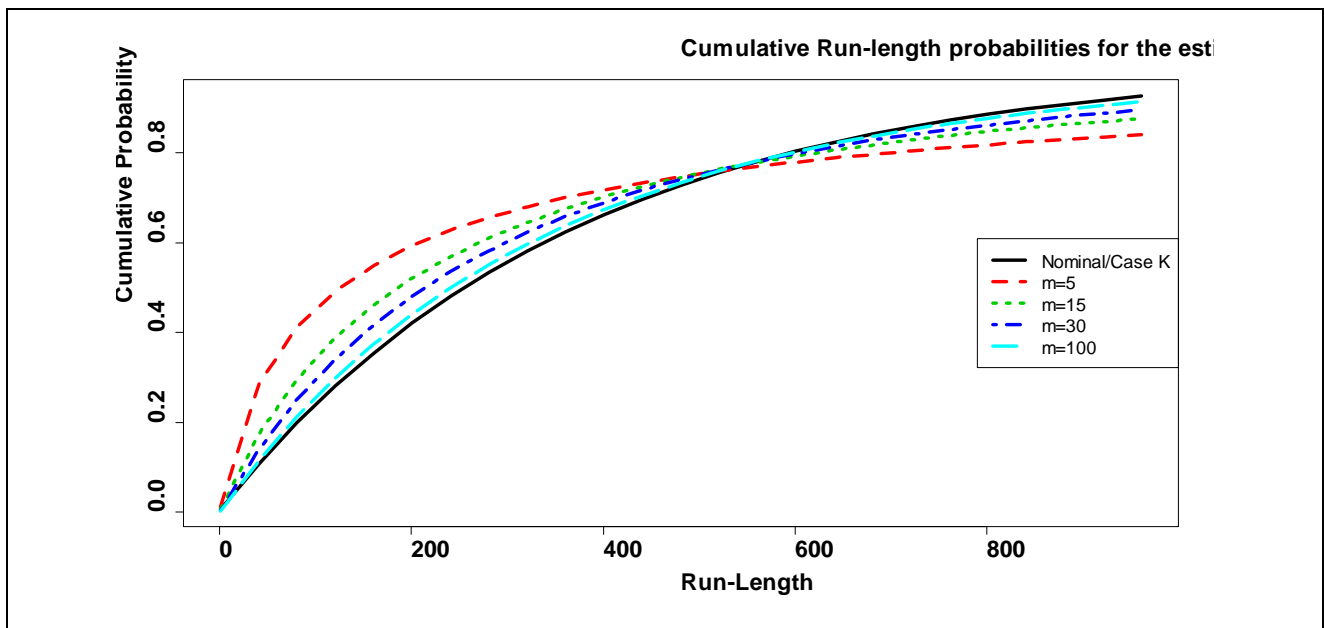
Figure 3.1. Comparison of the run-length cdf's of the Case U and Case K Shewhart 3-sigma $\overline{X}$ chart when $n = 5$

44

Table 3.1. The *AICARL* values for the $(\overline{X}, R)$ combo chart and its component charts when $n = 5$

m	$\overline{X}$ **chart**	R **chart**	$(\overline{X}, R)$ **chart**
10	624	1000	349
20	453	422	211
30	417	332	182
50	395	278	162
100	381	245	149
500	372	222	139
Case K	370	217	137

3.2.2 The Shewhart R control chart

The estimated 3-sigma Shewhart $\overline{X}$ control chart limits given in Expressions 3.1 and 3.6 depend on the unknown standard deviation parameter σ. Thus, one must ensure that σ is IC and that it stays IC before estimating it and using it to construct the $\overline{X}$ control chart. This is why it is recommended to run the R chart for the standard deviation, simultaneously, with the $\overline{X}$ chart.

The plotting statistic for the R chart is the sample range R_i. The IC distribution of R_i is approximated by the normal distribution: $R_i \sim N(\hat{\sigma}_0 d_2, \hat{\sigma}_0 d_3)$ where d_2, d_3 are constants that we defined in Chapter 2 page 23. Using this approximation along with $FAR_0 = 0.0027$ (or $ICARL_0 = 370.40$), the lower and upper control limits of the Shewhart 3-sigma R chart are given in Montgomery (2013), Chapter 6, as

$$L\hat{C}L_R = \left(1 - \frac{3d_3}{d_2}\right)\overline{R}$$

and $$\hspace{4cm} (3.6)$$

$$U\hat{C}L_R = \left(1 + \frac{3d_3}{d_2}\right)\overline{R}$$

45

respectively. These control limits can be equivalently written as

$$L\hat{C}L_R = \left(1 - \frac{3d_3}{d_2}\right)\frac{c\sqrt{U}}{\sqrt{v}} \qquad U\hat{C}L_R = \left(1 + \frac{3d_3}{d_2}\right)\frac{c\sqrt{U}}{\sqrt{v}} \tag{3.7}$$

the plotting statistic, in this case, is the sample relative range $W_i = \dfrac{R_i}{\hat{\sigma}_0}$.

The *AFAR* can be expressed as

$$AFAR_R = \int_0^\infty AFAR_R(u)g(u)du = \int_0^\infty \left[1 - F_W\left(U\hat{C}L_R\right) + F_W\left(L\hat{C}L_R\right)\right]g(u)du \tag{3.8}$$

where $AFAR_R(u)$ is the conditional attained false alarm rate. The IC run-length cdf and the *AICARL* for these limits can be written as

$$P(N \le t) = 1 - \int_0^\infty \left[F_W\left(U\hat{C}L_R\right) - F_W\left(L\hat{C}L_R\right)\right]^t g(u)du \tag{3.9}$$

and

$$ICARL_R = \int_0^\infty \left[AFAR_R(u)\right]^{-1} g(u)du. \tag{3.10}$$

Figure 3.2 (see the corresponding R code in Appendix 3) shows the IC run-length cdf of the Case U 3-sigma Shewhart *R* chart (for $m = 5$, 15, 30 and 100) and compares it to that of the Case K 3-sigma Shewhart *R* chart as well as the nominally expected results. It can be seen that the IC run-length cdf for Case K is much steeper than the geometric distribution with parameter $FAR_0 = 0.0027$ (nominal). This discrepancy is due to the common practice of approximating the distribution of the plotting statistic by the normal distribution along with using the 3-sigma limits. It can also be seen that for small *N* and *m*, short runs appear much more frequently for the Case U *R* charts than the Case K *R* chart. Further, both the Case K and Case U results are far different to the nominally expected results. Furthermore, it can be observed that when the number of subgroups *m* is increased, the Case U IC run-length performance approaches that of Case K. However, note that the Case K results are themselves unacceptable, due to the effects of using the normal approximation and the usual 3-sigma *R* chart limits.

Moreover, it can be seen from Table 3.1 that when m is increased and n is kept constant (say, $n = 5$) the *AICARL* performance in Case U approaches the *AICARL* = 217 value of Case K, which in turn is far shorter than the nominally expected 370 value. Thus, for fixed n, increasing m corrects for parameter estimation but does not correct for the effects of using the normal approximation and the 3-sigma limits.
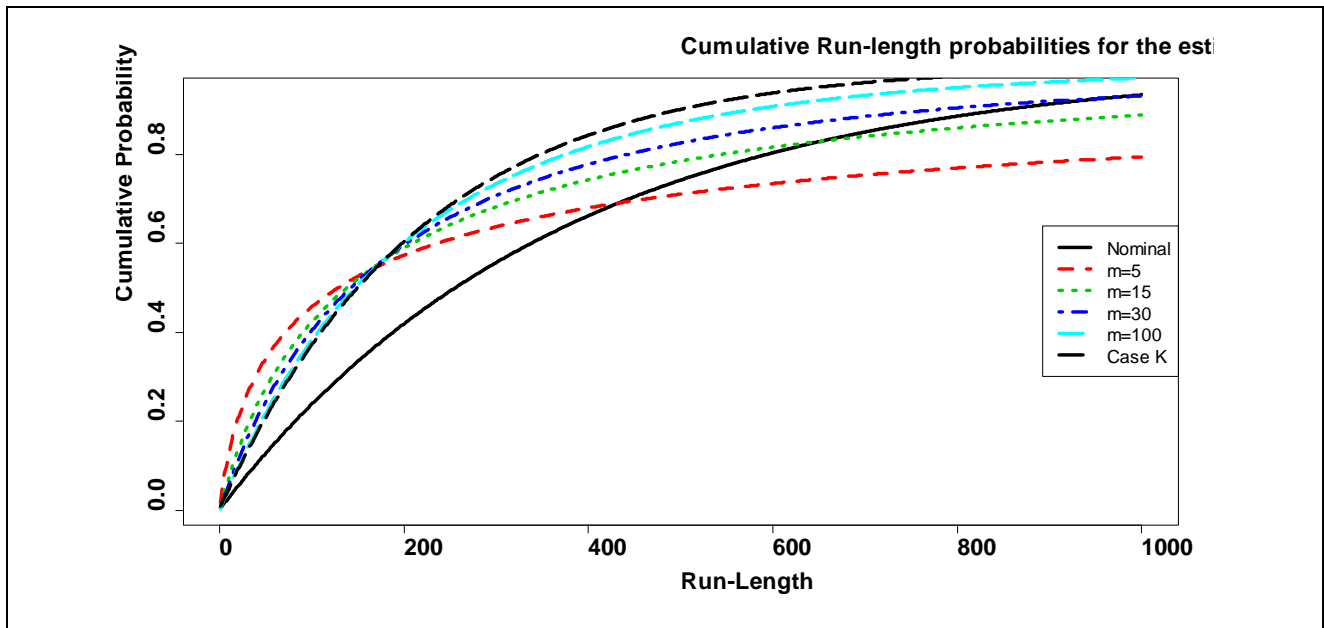
Figure 3.2. Comparison of the IC run-length cdf for the Case U and Case K Shewhart 3-sigma R chart when $n = 5$

In summary, the effect of parameter estimation and using the normal approximation along with 3-sigma limits is highly problematic, particularly when the number of subgroups m is small. Next we discuss the effects of multiple testing.

3.2.3   Effects of multiple testing

As noted before, in practice, the Shewhart 3-sigma $\overline{X}$ chart and a spread chart such as the R chart are used together to make decisions about the status (IC or OOC) of a process. This combo charting scheme gives a signal when at least one of the two component charts, the $\overline{X}$ or the R chart, signals. The *AFAR* for this combo $(\overline{X}, R)$ scheme, in Case U, can be calculated as follows

$$AFAR_{combo} = \int_0^\infty \int_{-\infty}^\infty AFAR_{combo}(z, u)\phi(z)g(u)dzdu \tag{3.11}$$

47

where $AFAR_{combo}(z,u)$ is the conditional attained false alarm rate. Using the independence of $\overline{Y}_i$ and R_i, this conditional false alarm rate can be written as

$$
\begin{aligned}
& AFAR_{combo}(z,u) \\
& = 1 - P\left[\left(L\hat{C}L_{xbar} < \overline{Y}_i < U\hat{C}L_{xbar}, \; L\hat{C}L_R < R_i < U\hat{C}L_R\right) | IC\right] \\
& = 1 - \left[1 - AFAR_{xbar}(z,u)\right]\left[1 - AFAR(u)\right] \\
& = 1 - \left[1 - ICARL_{xbar}^{-1}(z,u)\right]\left[1 - ICARL_R(u)^{-1}\right]
\end{aligned}
\tag{3.12}
$$

However, as mentioned earlier, the false alarm rate is not a recommended control chart performance or design measure in Case U (see Quesenberry (1993) and Jensen et al. (2006)). Therefore, to study the properties of the conventional Case U $(\overline{X},R)$ charting scheme, we evaluate the run-length distribution.

Thus, the IC run-length cdf of the estimated 3-sigma $(\overline{X},R)$ scheme can be expressed as

$$
P(N \le t) = 1 - \int_0^\infty \int_{-\infty}^\infty \left[\left(\Phi\left(U\hat{C}L_{xbar}\right) - \Phi\left(L\hat{C}L_{xbar}\right)\right) * \left(F_W\left(U\hat{C}L_R\right) - F_W\left(L\hat{C}L_R\right)\right)\right]^t \phi(z)g(u)dzdu
\tag{3.13}
$$

and its mean is

$$
ICARL_{combo} = \int_0^\infty \int_{-\infty}^\infty \left[AFAR_{combo}(z,u)\right]^{-1} \phi(z)g(u)dzdu
\tag{3.14}
$$

Figure 3.3 (see the corresponding R code in Appendix 3) shows the IC run-length cdf's for the 3-sigma $(\overline{X},R)$ scheme in Case U and compares it with the Case K cdf and the cdf of the geometric distribution with parameter $FAR_0 = 0.0027$. It can be seen that for small m, there are more short runs for the Case U chart than for the Case K chart. Both the Case K and Case U results are different from the geometric distribution with parameter $FAR_0 = 0.0027$. Therefore, parameter estimation exacerbates the effects of multiple testing and the effects of using 3-sigma limits, particularly for small m. This means a lot more false alarms for the estimated limits charts, unless m is very large.

In addition, Table 3.1 shows the *AICARL* for the Case U and Case K 3-sigma $(\overline{X},R)$ combo chart scheme. It can be seen that when m is increased and n kept constant (say, $n = 5$), the *AICARL* performance for Case U approaches the *AICARL* = 137 value for Case K, which in turn is roughly 3 times lower than the nominally expected 370.4 value. Thus, for a fixed value of n, increasing m to a

48

larger value corrects for parameter estimation but does nothing to correct the serious effects of multiple testing and those of using the normal approximation along with the 3-sigma limits. In short the current practice of using two charts together in Case U is to roughly reduce the *ICARL* by 3 times from its nominally expected value, thus tripling the number of false alarms. Obviously, this needs to be seriously taken into consideration when designing and applying the two chart scheme.
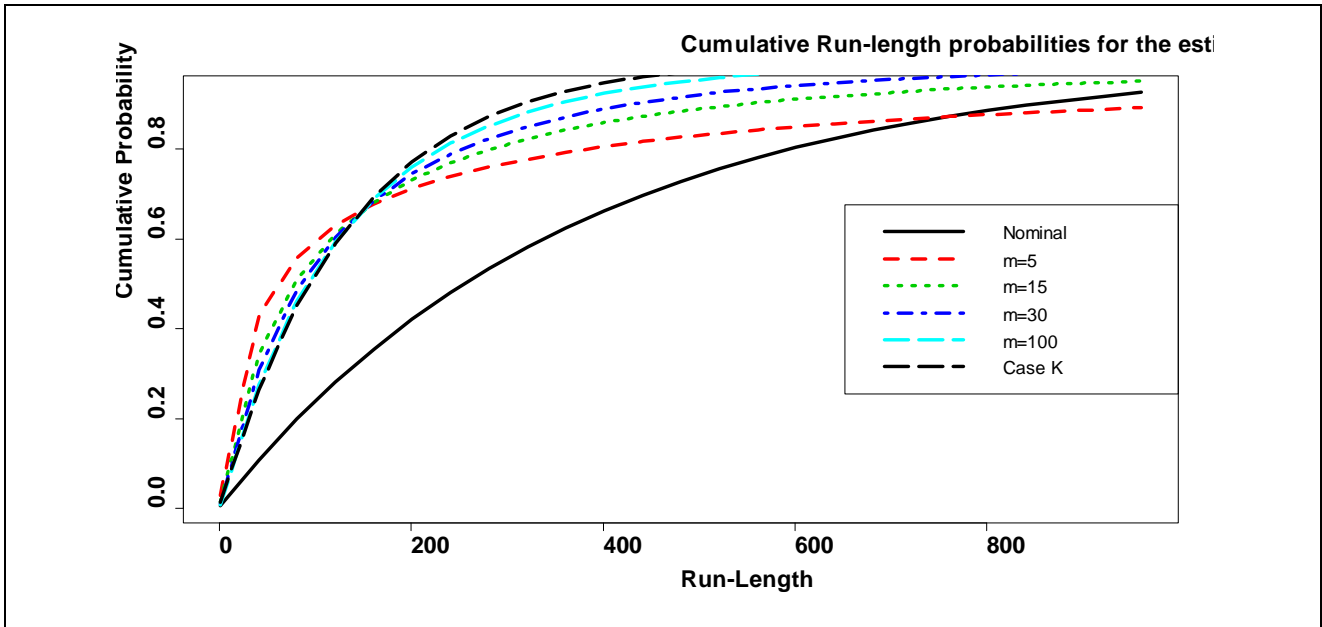
Figure 3.**3**. Comparison of the IC run-length cdf of the Case U and Case K Shewhart 3-sigma $\left(\overline{X}, R\right)$ charting scheme when $n = 5$

3.2.4 New control limits adjusted for 3-sigma and multiplicity effects

We understand the need to select the control limits on the individual charts in a way which accounts for the additional variability caused by parameter estimation and also corrects for multiple testing as a function of the available data. We accomplish this by first using the conditioning technique developed in Chakraborti (2000), then applying the correction due to multiple testing (as in the parameters known case, see Chapter 2) and finally using the probability limits. This is described next.

Recall that the IC average run-length of the estimated limits $\left(\overline{X}, R\right)$ scheme is

$$ICARL_{combo} = \int_0^\infty \int_{-\infty}^\infty \left[AFAR_{combo}(z,u)\right]^{-1} \phi(z)g(u)dzdu$$

49

Note that, by averaging the $\left[AFAR_{combo}(z,s)\right]^{-1}$ over the distributions of the parameter estimates, the effects of parameter estimation are accounted for. Further, by using the joint distribution of $\overline{Y}_i$ and R_i in the following expression,

$$AFAR_{combo}(z,u) = 1 - P\left[\left(L\hat{C}L_{xbar} < \overline{Y}_i < U\hat{C}L_{xbar}, L\hat{C}L_R < R_i < U\hat{C}L_R\right)| IC\right]$$

the multiplicity issue is also accounted for. But, the R chart limits $L\hat{C}L_R$ and $U\hat{C}L_R$ are still inappropriate because they are based on an incorrect assumption that $R_i \sim N(\hat{\sigma}_0 d_2, \hat{\sigma}_0 d_3)$. Thus, we replace them with the following probability limits

$$L\tilde{C}L_R = \frac{c\sqrt{u}}{\sqrt{v}} F_W^{-1}\left(\frac{p}{2}\right) \qquad U\tilde{C}L_R = \frac{c\sqrt{u}}{\sqrt{v}} F_W^{-1}\left(1 - \frac{p}{2}\right)$$

where $p = FAR_0$. As a result the conditional attained false alarm rate for the combo scheme is now

$$
\begin{aligned}
& AFAR_{combo}(z,u) \\
& = 1 - P\left[\left(L\hat{C}L_{xbar} < \overline{Y}_i < U\hat{C}L_{xbar}, \; L\tilde{C}L_R < R_i < U\tilde{C}L_R\right)/ IC\right] \\
& = 1 - \left[\Phi\left(\frac{z}{\sqrt{m}} + \frac{c\sqrt{u}}{\sqrt{v}}\Phi^{-1}\left(1 - \frac{p}{2}\right)\right) - \Phi\left(\frac{z}{\sqrt{m}} - \frac{c\sqrt{u}}{\sqrt{v}}\Phi^{-1}\left(1 - \frac{p}{2}\right)\right)\right] \times \\
& \qquad \left[F_W\left(\frac{c\sqrt{u}}{\sqrt{v}} F_W^{-1}\left(1 - \frac{p}{2}\right)\right) - F_W\left(\frac{c\sqrt{u}}{\sqrt{v}} F_W^{-1}\left(\frac{p}{2}\right)\right)\right]
\end{aligned}
$$
(3.15)

To emphasize the dependence of $AFAR_{combo}(z,u)$ and therefore the dependence of the $ICARL_{combo}$ on $p = FAR_0$ of the component charts, we write $AFAR_{combo}(z,u,p)$ and $ICARL_{combo}(p)$, respectively.

Noting that $ICARL_{combo}(p)$ is a function of p, we find the value of p that corresponds to the specified $ICARL_{combo}(p) = A$ for some given values of m and n. We do this by evaluating the integrals below using R coding given in Appendix 3,

$$
\begin{aligned}
& \int_0^\infty \int_{-\infty}^\infty \left[AFAR_{combo}(z,u,p)\right]^{-1} \phi(z)g(u)dzdu = ICARL_{combo}(p) \\
& \int_0^\infty \int_{-\infty}^\infty \left[AFAR_{combo}(z,u,p)\right]^{-1} \phi(z)g(u)dzdu = A \\
& \int_0^\infty \int_{-\infty}^\infty \left[AFAR_{combo}(z,u,p)\right]^{-1} \phi(z)g(u)dzdu - A = 0.
\end{aligned}
$$
(3.16)

50

Once p is found, the correct probability control limits for the $\overline{X}$ and R charts are found from the corresponding percentiles of the standard normal distribution and the distribution of the relative range, respectively. Some results are shown in Table 3.2.

Table 3.2. New chart constants for the Case U Shewhart $\left(\overline{X}, R\right)$ combo scheme for an ICARL = A = 370, 500 and n = 5, 10; m = 5, 10, 20, 30, 50, 75, 100

n	m	ICARL=A=370				ICARL=A=500			
		p	$\overline{X}$ chart	R chart		p	$\overline{X}$ chart	R chart	
5	5	0.001025	3.284	0.310	5.713	0.000758	3.368	0.287	5.814
	10	0.001164	3.248	0.320	5.670	0.000862	3.332	0.297	5.772
	20	0.001256	3.226	0.327	5.645	0.000929	3.311	0.303	5.747
	30	0.001290	3.218	0.329	5.636	0.000955	3.303	0.305	5.737
	50	0.001318	3.212	0.331	5.628	0.000975	3.298	0.306	5.73
	75	0.001331	3.209	0.331	5.625	0.000985	3.295	0.307	5.727
	100	0.001337	3.208	0.332	5.623	0.00099	3.293	0.307	5.725
Case K		0.00135	3.205	0.333	5.619	0.0010	3.290	0.308	5.722
10	5	0.000855	3.334	0.976	6.245	0.000627	3.420	0.940	6.341
	10	0.00103	3.282	0.999	6.186	0.000758	3.368	0.962	6.282
	20	0.001163	3.248	1.014	6.148	0.000857	3.334	0.977	6.244
	30	0.001217	3.235	1.020	6.134	0.000899	3.32	0.982	6.229
	50	0.001267	3.223	1.025	6.121	0.000936	3.309	0.987	6.217
	75	0.001294	3.217	1.027	6.114	0.000957	3.303	0.99	6.21
	100	0.001308	3.214	1.029	6.111	0.000967	3.3	0.991	6.206
Case K		0.001350	3.205	1.033	6.100	0.0010	3.290	0.995	6.196

Notice that when *m* is increased, the values of *p* in Table 3.2 approach the Case K value (shown on the last row in Table 3.2). This implies that when *m* is large say *m* = 500, one can use the corrected Case K chart constants in Table 2.2 to construct the estimated limits $(\overline{X}, R)$ combo chart scheme.

Finally, we illustrate how Table 3.2 can be used to implement the Case U $(\overline{X}, R)$ combo scheme. We then compare these modified Case U $(\overline{X}, R)$ limits to the conventional Case U 3-sigma $(\overline{X}, R)$ limits and the modified Case K $(\overline{X}, R)$ limits. Recall that, the conventional Case U 3-sigma $(\overline{X}, R)$ limits have not been corrected for parameter estimation, poor normal approximation and multiple testing; whereas the modified Case K $(\overline{X}, R)$ limits have been corrected for the effect of multiple testing and using 3-sigma limits (since there is no parameter estimation in Case K).

Example 3.1

Again, suppose we are interested in monitoring the average and standard deviation of the normally distributed characteristic *X* with a Shewhart $\overline{X}$ and R chart, respectively. Suppose *m* = 5 subgroups of size *n* = 5 are used to estimate the unknown process parameters. Suppose the parameter estimates are 8.53 and 3.36 for the mean and standard deviation, respectively. Using Table 3.2, the control limits of the modified Case U $(\overline{X}, R)$ charting scheme are given by

$$U\hat{C}L_{xbar} = \overline{\overline{X}} + 3.284 \times \frac{\overline{R}}{d_2\sqrt{n}} = 8.53 + 3.284 \times \frac{3.36}{\sqrt{5}} = 13.47$$

$$L\hat{C}L_{xbar} = \overline{\overline{X}} - 3.284 \frac{\overline{R}}{d_2\sqrt{n}} = 8.53 - 3.284 \times \frac{3.36}{\sqrt{5}} = 3.60$$

$$U\hat{C}L_R = F_W^{-1}(1 - D/2)\frac{\overline{R}}{d_2} = 5.713 \times 3.36 = 19.20$$

$$L\hat{C}L_R = F_W^{-1}(D/2)\frac{\overline{R}}{d_2} = 0.310 \times 3.36 = 1.04.$$

Notice that for *n* = 5, *m* = 5 and *ICARL* = 370 the charting constant for the $\overline{X}$ chart is *k* = 3.284. This value is 2.5% larger than the charting constant *k* = 3.204 for the modified Case K limits, and 9.3% larger than the conventional charting constant *k* = 3.

In Figure 3.4, we compare the modified Case K limits to the modified Case U limits for the Shewhart $\overline{X}$ and *R* charts respectively. From both charts, it can be seen that, for small *m*, the

52

modified Case U limits are slightly wider than the modified Case K limits. This mitigates the effects of parameter estimation. It can be shown that when *m* is increased the modified Case U limits approach the modified Case K limits. Hence for large *m* the corrected Case K charting constants in Table 2.2 can be used to construct the modified Case U control limits.
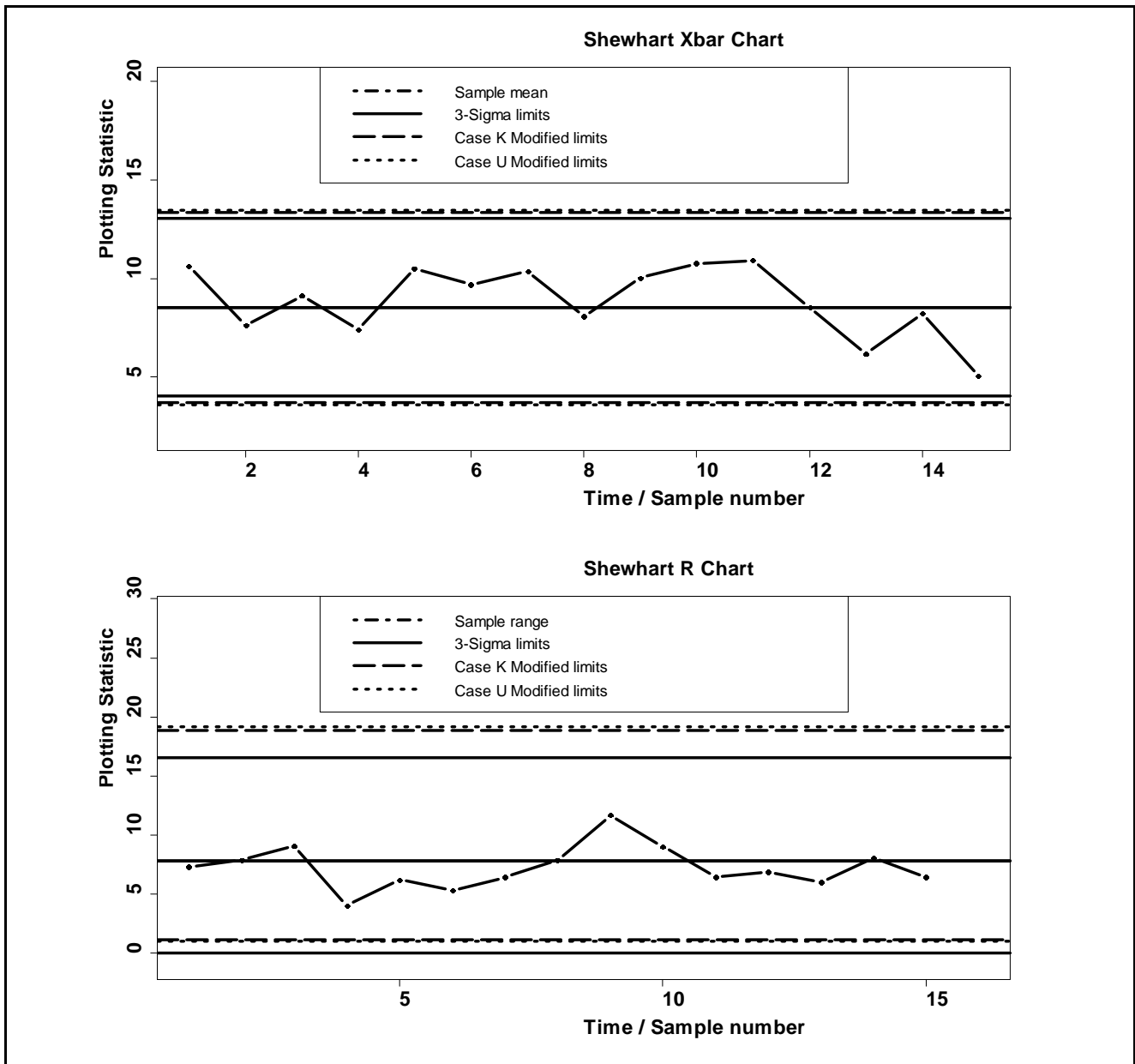
Figure 3.4. Comparison of the standard and modified Shewhart $\overline{X}$ and *R* chart limits in Case K and Case U

53

3.3 Summary and Conclusions

The Phase II Shewhart $(\overline{X}, R)$ chart scheme for jointly monitoring the process mean and standard deviation is usually implemented using 3-sigma limits for the individual charts. There are three major issues with this. First, it is assumed that the charting statistics are normally distributed. The second is multiple testing; since two charts are used at the same time to make decisions about the in-control state of the process the *FAR* of the scheme is inflated. The last issue is the effect of parameter estimation which is known to degrade chart performance. We showed the severity of these issues on the IC properties of the $(\overline{X}, R)$ charting scheme by examining the *AFAR* and the *ICARL*. We found that the current practice of using the two chart $(\overline{X}, R)$ charting scheme in Case U roughly reduces the *ICARL* by 3 times from its nominally expected value, thus tripling the number of false alarms. This needs to be seriously taken into consideration when designing the combo scheme. Thus, we derived the new charting constants taking proper account of all these three issues. We accomplished this by first using the conditioning technique developed in Chakraborti (2000), then we applied the correction due to multiple testing and finally we used the probability limits. In addition, we provided tables of the charting constants for some nominal in-control average run-lengths and sample sizes to aid in the implementing the $(\overline{X}, R)$ chart in practice. The control limits based on our charting constants are wider than those of the traditional 3-sigma limits and the modified Case K limits in Table 2.2. This reduces the rate of false alarms, drastically. Hence, we encourage practitioners to use our charting constants in Table 3.2 instead of the standard 3-sigma limits when implementing the $(\overline{X}, R)$ charting scheme in Case U.

54

3.4 Appendix 3: R Code

Code for Figure 3.1 : Cumulative run-length probabilities for the estimated limits 3-sigma $\overline{\overline{X}}$ chart

```
n=5
m=c(5,15,30)
q=seq(1,1000,40)
d2=function(n){
pt=function(w){1-ptukey(w,n,Inf)}
integrate(pt,lower=0,upper=Inf)[[1]]}
d2=d2(n)
EW2=function(n){
ptt=function(a){(1-ptukey(sqrt(a),n,Inf))}
integrate(ptt,lower=0,upper=Inf)[[1]]}
d3=function(n){
sqrt(EW2(n)-d2^2)}
d3=d3(n)

library(cubature)
CRL=function(m,a){
M=function(m){
d3^2/(m*d2^2)}
r=function(m){
(-2+2*sqrt(1+2*M(m)))^-1}
t=function(m){
M(m)+1/(16*r(m)^3)}
v=function(m){
(-2+2*sqrt(1+2*t(m)))^-1}
cc=function(m){
1+(1/(4*v(m)))+(1/(32*v(m)^2))-(5/(128*v(m)^3))}
uclxbar=function(x){x[1]/sqrt(m)+qnorm(1-a/2,0,1)*cc(m)*sqrt(x[2])/sqrt(v(m))}
lclxbar=function(x){x[1]/sqrt(m)-qnorm(1-a/2,0,1)*cc(m)*sqrt(x[2])/sqrt(v(m))}
MPNS=numeric(length(q))
for (i in 1:length(q)){
PNS=function(x){(pnorm(uclxbar(x),0,1)-pnorm(lclxbar(x),0,1))^q[i]}
CPNS=function(x){ PNS(x)*dnorm(x[1],0,1)*dchisq(x[2],v(m))}
b=qchisq(0.99999,v(m))
MPNS[i]=adaptIntegrate(CPNS,c(-100,0),c(100,b),tol=1e-10)[[1]]}
MPNS}

y=pgeom(q,0.0027)
plot(q,y,type = 'l', lwd=3, cex.axis=1.7,cex.lab=1.7,cex.main=1.7,main="Cumulative Run-length
probabilities for the estimated limits 3-Sigma Xbar chart",xlab="Run-Length",ylab="Cumulative
Probability",font.lab=2, font.axis=2)

for (j in 1:length(m)){
lines(q, (1-CRL(m[j],0.0027)),lty=j+1,lwd=4,col=j+1,cex=5)}
legend('right',legend=c("Nominal/Inf","m=5","m=15","m=30"),
lty=c(1,2,3,4),lwd=3,col=c(1,2,3,4),cex=1.3)
```

55

Code for Table 3.1 : ICARL's for the Case U 3-sigma $\overline{X}$ chart

```
n=5
m=c(10,20,30,50,100,500)
d2=function(n){
pt=function(w){1-ptukey(w,n,Inf)}
integrate(pt,lower=0,upper=Inf)[[1]]}
d2=d2(n)
EW2=function(n){
ptt=function(a){(1-ptukey(sqrt(a),n,Inf))}
integrate(ptt,lower=0,upper=Inf)[[1]]}
d3=function(n){
sqrt(EW2(n)-d2^2)}
d3=d3(n)

library(cubature)
ICARL=function(m,a){
M=function(m){
d3^2/(m*d2^2)}
r=function(m){
(-2+2*sqrt(1+2*M(m)))^-1}
t=function(m){
M(m)+1/(16*r(m)^3)}
v=function(m){
(-2+2*sqrt(1+2*t(m)))^-1}
cc=function(m){
1+(1/(4*v(m)))+(1/(32*v(m)^2))-(5/(128*v(m)^3))}
uclxbar=function(x){x[1]/sqrt(m)+qnorm(1-a/2,0,1)*cc(m)*sqrt(x[2])/sqrt(v(m))}
lclxbar=function(x){x[1]/sqrt(m)-qnorm(1-a/2,0,1)*cc(m)*sqrt(x[2])/sqrt(v(m))}
AFAR=function(x){1-pnorm(uclxbar(x),0,1)+pnorm(lclxbar(x),0,1)}
CFAR=function(x){ AFAR(x)^-1*dnorm(x[1],0,1)*dchisq(x[2],v(m))}
b=qchisq(0.99999,v(m))
adaptIntegrate(CFAR,c(-100,0),c(100,b),tol=1e-10)}

ICARLxbar=numeric(length(m))
for (i in 1:length(m)) {
ICARLxbar[i]= ICARL(m[i],0.0027)[[1]]}
Percent_dif=((ICARLxbar-370.40)/370.40)
Results=cbind(ICARLxbar,Percent_dif)
rownames(Results)= c(10,20,30,50,100,500)
Results
write.table(Results, "clipboard",sep="\t",col.names=NA)
```

56

Code for Table 3.1 : ICARL's for Case U 3-sigma *R* chart

```
n=5
m=c(10,20,30,50,100,500)
d2=function(n){
pt=function(w){1-ptukey(w,n,Inf)}
integrate(pt,lower=0,upper=Inf)[[1]]}
d2=d2(n)
EW2=function(n){
ptt=function(a){(1-ptukey(sqrt(a),n,Inf))}
integrate(ptt,lower=0,upper=Inf)[[1]]}
d3=function(n){
sqrt(EW2(n)-d2^2)}
d3=d3(n)

library(cubature)
ICARL=function(m,a){
M=function(m){
d3^2/(m*d2^2)}
r=function(m){
(-2+2*sqrt(1+2*M(m)))^-1}
t=function(m){
M(m)+1/(16*r(m)^3)}
v=function(m){
(-2+2*sqrt(1+2*t(m)))^-1}
cc=function(m){
1+(1/(4*v(m)))+(1/(32*v(m)^2))-(5/(128*v(m)^3))}
uclrchart=function(x){(d2+qnorm(1-a/2)*d3)*cc(m)*sqrt(x)/sqrt(v(m))}
lclrchart=function(x){(d2- qnorm(1-a/2)*d3)*cc(m)*sqrt(x)/sqrt(v(m))}
DD3=max(c(lclrchart(x),0))
AFAR=function(x){1-ptukey(uclrchart(x),n,Inf)+ptukey(DD3,n,Inf)}
CFAR=function(x){ AFAR(x)^-1*dchisq(x,v(m))}
b=qchisq(0.99999,v(m))
adaptIntegrate(CFAR,c(0),c(b),tol=1e-10)}

ICARLrchart=numeric(length(m))
for (i in 1:length(m)) {
ICARLrchart[i]= ICARL(m[i],0.0027)[[1]]}
Percent_dif=((ICARLrchart-370.40)/370.40)
Results=cbind(ICARLrchart,Percent_dif)
rownames(Results)= c(10,20,30,50,100,500)
Results
write.table(Results, "clipboard",sep="\t",col.names=NA)
```

Code for Table 3.1 : ICARL's for Case U 3-sigma ($\overline{X}, R$) chart scheme in Table 3.1

```
n=5
m=c(10,20,30,50,100,500)
d2=function(n){
pt=function(w){1-ptukey(w,n,Inf)}
integrate(pt,lower=0,upper=Inf)[[1]]}
d2=d2(n)
EW2=function(n){
ptt=function(a){(1-ptukey(sqrt(a),n,Inf))}
integrate(ptt,lower=0,upper=Inf)[[1]]}
d3=function(n){
sqrt(EW2(n)-d2^2)}
d3=d3(n)

library(cubature)
ICARL=function(m,a){
M=function(m){
d3^2/(m*d2^2)}
r=function(m){
(-2+2*sqrt(1+2*M(m)))^-1}
t=function(m){
M(m)+1/(16*r(m)^3)}
v=function(m){
(-2+2*sqrt(1+2*t(m)))^-1}
cc=function(m){
1+(1/(4*v(m)))+(1/(32*v(m)^2))-(5/(128*v(m)^3))}
uclxbar=function(x){x[1]/sqrt(m)+qnorm(1-a/2,0,1)*cc(m)*sqrt(x[2])/sqrt(v(m))}
lclxbar=function(x){x[1]/sqrt(m)-qnorm(1-a/2,0,1)*cc(m)*sqrt(x[2])/sqrt(v(m))}
PNSxbar=function(x){pnorm(uclxbar(x),0,1)-pnorm(lclxbar(x),0,1)}
uclrchart=function(x){(d2+qnorm(1-a/2,0,1)*d3)*cc(m)*sqrt(x[2])/sqrt(v(m))}
lclrchart=function(x){(d2-qnorm(1-a/2,0,1)*d3)*cc(m)*sqrt(x[2])/sqrt(v(m))}
PNSrchart=function(x){ptukey(uclrchart(x),n,Inf)-ptukey(max(c(lclrchart(x),0)),n,Inf)}
AFAR=function(x){1-PNSxbar(x)*PNSrchart(x)}
CFAR=function(x){ AFAR(x)^-1*dnorm(x[1],0,1)*dchisq(x[2],v(m))}
b=qchisq(0.99999,v(m))
adaptIntegrate(CFAR,c(-100,0),c(100,b),tol=1e-10)}

ICARLxbarrchart=numeric(length(m))
for (i in 1:length(m)) {
ICARLxbarrchart[i]= ICARL(m[i],0.0027)[[1]]}
Percent_dif=((ICARLxbarrchart-370.40)/370.40)
Results=cbind(ICARLxbarrchart,Percent_dif)
rownames(Results)= c(10,20,30,50,100,500)
Results
write.table(Results, "clipboard",sep="\t",col.names=NA)
```

Code for Figure 3.2 : Cumulative run-length probabilities for the estimated 3-sigma *R* chart

```
n=5
m=c(5,15,30,100)
q=seq(1,1000,40)
d2=function(n){
pt=function(w){1-ptukey(w,n,Inf)}
integrate(pt,lower=0,upper=Inf)[[1]]}
d2=d2(n)
EW2=function(n){
ptt=function(a){(1-ptukey(sqrt(a),n,Inf))}
integrate(ptt,lower=0,upper=Inf)[[1]]}
d3=function(n){
sqrt(EW2(n)-d2^2)}
d3=d3(n)

library(cubature)
CRL=function(m,a){
M=function(m){
d3^2/(m*d2^2)}
r=function(m){
(-2+2*sqrt(1+2*M(m)))^-1}
t=function(m){
M(m)+1/(16*r(m)^3)}
v=function(m){
(-2+2*sqrt(1+2*t(m)))^-1}
cc=function(m){
1+(1/(4*v(m)))+(1/(32*v(m)^2))-(5/(128*v(m)^3))}
uclrchart=function(x){(d2+qnorm(1-a/2)*d3)*cc(m)*sqrt(x)/sqrt(v(m))}
lclrchart=function(x){(d2- qnorm(1-a/2)*d3)*cc(m)*sqrt(x)/sqrt(v(m))}
MPNS=numeric(length(q))
for (i in 1:length(q)){
PNS=function(x){
(ptukey(uclrchart(x),n,Inf)-ptukey(max(c(lclrchart(x),0)),n,Inf))^q[i]}
CPNS=function(x){ PNS(x)*dchisq(x,v(m))}
b=qchisq(0.99999,v(m))
MPNS[i]=adaptIntegrate(CPNS,c(0),c(b),tol=1e-10)[[1]]}
MPNS}

y=pgeom(q,0.0027)
plot(q,y,type = 'l', lwd=3, cex.axis=1.7,cex.lab=1.7,cex.main=1.7,main="Cumulative Run-length
probabilities for the estimated 3-Sigma R chart",xlab="Run-Length",ylab="Cumulative
Probability",font.lab=2, font.axis=2)

for (j in 1:length(m)){
lines(q, (1-CRL(m[j],0.0027)),lty=j+1,lwd=4,col=j+1,cex=5)}
legend('right',legend=c("Nominal","m=5","m=15","m=30","m=100"),
lty=c(1,2,3,4,5),lwd=3,col=c(1,2,3,4,5),cex=1.3)
legend('right',legend=c("Nominal","m=5","m=15","m=30","m=100"),
lty=c(1,2,3,4,5),lwd=3,col=c(1,2,3,4,5),cex=1.3)
```

Code for Figure 3.3 : Cumulative run-length probabilities for the estimated 3-sigma ($\overline{X}, R$) scheme

```
n=5
m=c(5,15,30,100)
q=seq(1,1000,40)
d2=function(n){
pt=function(w){1-ptukey(w,n,Inf)}
integrate(pt,lower=0,upper=Inf)[[1]]}
d2=d2(n)
EW2=function(n){
ptt=function(a){(1-ptukey(sqrt(a),n,Inf))}
integrate(ptt,lower=0,upper=Inf)[[1]]}
d3=function(n){
sqrt(EW2(n)-d2^2)}
d3=d3(n)

library(cubature)
CRL=function(m,a){
M=function(m){
d3^2/(m*d2^2)}
r=function(m){
(-2+2*sqrt(1+2*M(m)))^-1}
t=function(m){
M(m)+1/(16*r(m)^3)}
v=function(m){
(-2+2*sqrt(1+2*t(m)))^-1}
cc=function(m){
1+(1/(4*v(m)))+(1/(32*v(m)^2))-(5/(128*v(m)^3))}
uclxbar=function(x){x[1]/sqrt(m)+qnorm(1-a/2,0,1)*cc(m)*sqrt(x[2])/sqrt(v(m))}
lclxbar=function(x){x[1]/sqrt(m)-qnorm(1-a/2,0,1)*cc(m)*sqrt(x[2])/sqrt(v(m))}
PNSxbar=function(x){pnorm(uclxbar(x),0,1)-pnorm(lclxbar(x),0,1)}
uclrchart=function(x){(d2+qnorm(1-a/2,0,1)*d3)*cc(m)*sqrt(x[2])/sqrt(v(m))}
lclrchart=function(x){(d2-qnorm(1-a/2,0,1)*d3)*cc(m)*sqrt(x[2])/sqrt(v(m))}
PNSrchart=function(x){ptukey(uclrchart(x),n,Inf)-ptukey(max(c(lclrchart(x),0)),n,Inf)}
MPNS=numeric(length(q))
for (i in 1:length(q)){
JPNS=function(x){(PNSxbar(x)*PNSrchart(x))^q[i]}
CJPNS=function(x){ JPNS(x)*dnorm(x[1],0,1)*dchisq(x[2],v(m))}
b=qchisq(0.99999,v(m))
MPNS[i]=adaptIntegrate(CJPNS,c(-100,0),c(100,b),tol=1e-10)[[1]]}
MPNS}

y=pgeom(q,0.0027)
plot(q,y,type = 'l', lwd=3, cex.axis=1.7,cex.lab=1.7,cex.main=1.7,main="Cumulative Run-length
probabilities for the estimated 3-Sigma (Xbar,R) scheme",xlab="Run-Length",ylab="Cumulative
Probability",font.lab=2, font.axis=2)
m=c(5,15,30,100)
for (j in 1:length(m)){
lines(q, (1-CRL(m[j],0.0027)),lty=j+1,lwd=4,col=j+1,cex=5)}
legend('right',legend=c("Nominal","m=5","m=15","m=30","m=100"),
lty=c(1,2,3,4,5),lwd=3,col=c(1,2,3,4,5),cex=1.3)
```

60

Code for Table 3.2 : Calculation of Case U charting constants (A=370)

```
n=10
m=37
aa=seq(from=0.001238,to=0.001240,length.out=3)
d2=function(n){
pt=function(w){1-ptukey(w,n,Inf)}
integrate(pt,lower=0,upper=Inf)[[1]]}
d2=d2(n)
EW2=function(n){
ptt=function(a){(1-ptukey(sqrt(a),n,Inf))}
integrate(ptt,lower=0,upper=Inf)[[1]]}
d3=function(n){
sqrt(EW2(n)-d2^2)}
d3=d3(n)

library(cubature)
ICARL=function(m,a){
M=function(m){
d3^2/(m*d2^2)}
r=function(m){
(-2+2*sqrt(1+2*M(m)))^-1}
t=function(m){
M(m)+1/(16*r(m)^3)}
v=function(m){
(-2+2*sqrt(1+2*t(m)))^-1}
cc=function(m){
1+(1/(4*v(m)))+(1/(32*v(m)^2))-(5/(128*v(m)^3))}
uclxbar=function(x){x[1]/sqrt(m)+qnorm(1-a/2,0,1)*cc(m)*sqrt(x[2])/sqrt(v(m))}
lclxbar=function(x){x[1]/sqrt(m)-qnorm(1-a/2,0,1)*cc(m)*sqrt(x[2])/sqrt(v(m))}
PNSxbar=function(x){pnorm(uclxbar(x),0,1)-pnorm(lclxbar(x),0,1)}
uclrchart=function(x){qtukey(1-a/2,n,Inf)*cc(m)*sqrt(x[2])/sqrt(v(m))}
lclrchart=function(x){qtukey(a/2,n,Inf)*cc(m)*sqrt(x[2])/sqrt(v(m))}
PNSrchart=function(x){ptukey(uclrchart(x),n,Inf)-ptukey(lclrchart(x),n,Inf)}
AFAR=function(x){1-PNSxbar(x)*PNSrchart(x)}
CFAR=function(x){ AFAR(x)^-1*dnorm(x[1],0,1)*dchisq(x[2],v(m))}
b=qchisq(0.99999,v(m))
adaptIntegrate(CFAR,c(-100,0),c(100,b),tol=1e-10)[[1]]}


ICARLxbar_rchart=numeric(length(aa))
Const=matrix(nrow=length(aa),ncol=3)
for (j in 1:length(aa)){
Const[j,]=c(qnorm(1-aa[j]/2),qtukey(aa[j]/2,n,Inf),qtukey(1-aa[j]/2,n,Inf))
ICARLxbar_rchart[j]=ICARL(m,aa[j])}
ICARL370=ICARLxbar_rchart-370
Results1=cbind(ICARL370,rep(m,length(aa)),aa,Const)
colnames(Results1)=c("ICARL370","m","p","Xbar","SprL","SprU")
Results1
write.table(Results1, "clipboard",sep="\t",col.names=NA)
```

61

Code for Table 3.2 : Calculation of Case U charting constants (A=500) in Table 3.2

```
n=5
m=5
aa=seq(from=0.000758,to=0.000760,length.out=3)
d2=function(n){
pt=function(w){1-ptukey(w,n,Inf)}
integrate(pt,lower=0,upper=Inf)[[1]]}
d2=d2(n)
EW2=function(n){
ptt=function(a){(1-ptukey(sqrt(a),n,Inf))}
integrate(ptt,lower=0,upper=Inf)[[1]]}
d3=function(n){
sqrt(EW2(n)-d2^2)}
d3=d3(n)

library(cubature)
ICARL=function(m,a){
M=function(m){
d3^2/(m*d2^2)}
r=function(m){
(-2+2*sqrt(1+2*M(m)))^-1}
t=function(m){
M(m)+1/(16*r(m)^3)}
v=function(m){
(-2+2*sqrt(1+2*t(m)))^-1}
cc=function(m){
1+(1/(4*v(m)))+(1/(32*v(m)^2))-(5/(128*v(m)^3))}
uclxbar=function(x){x[1]/sqrt(m)+qnorm(1-a/2,0,1)*cc(m)*sqrt(x[2])/sqrt(v(m))}
lclxbar=function(x){x[1]/sqrt(m)-qnorm(1-a/2,0,1)*cc(m)*sqrt(x[2])/sqrt(v(m))}
PNSxbar=function(x){pnorm(uclxbar(x),0,1)-pnorm(lclxbar(x),0,1)}
uclrchart=function(x){qtukey(1-a/2,n,Inf)*cc(m)*sqrt(x[2])/sqrt(v(m))}
lclrchart=function(x){qtukey(a/2,n,Inf)*cc(m)*sqrt(x[2])/sqrt(v(m))}
PNSrchart=function(x){ptukey(uclrchart(x),n,Inf)-ptukey(lclrchart(x),n,Inf)}
AFAR=function(x){1-PNSxbar(x)*PNSrchart(x)}
CFAR=function(x){ AFAR(x)^-1*dnorm(x[1],0,1)*dchisq(x[2],v(m))}
b=qchisq(0.99999,v(m))
adaptIntegrate(CFAR,c(-100,0),c(100,b),tol=1e-10)[[1]]}

ICARLxbar_rchart=numeric(length(aa))
Const2=matrix(nrow=length(aa),ncol=3)
for (j in 1:length(aa)){
Const2[j,]=c(qnorm(1-aa[j]/2),qtukey(aa[j]/2,n,Inf),qtukey(1-aa[j]/2,n,Inf))
ICARLxbar_rchart[j]=ICARL(m,aa[j])}
ICARL500=ICARLxbar_rchart-500
Results2=cbind(ICARL500,rep(m,length(aa)),aa,Const2)
colnames(Results2)=c("ICARL-500","m","p","Xbar","SprL","SprU")
Results2
write.table(Results2, "clipboard",sep="\t",col.names=NA)
```

Code for Figure 3.4 : The ($\overline{\overline{X}}, R$) scheme's with simulated data

```
set.seed(15)
data=replicate(15,expr={
rnorm(5,8.53,3.36)})
y=colMeans(data)
x=1:15
plot(x,y,type = 'b', lwd=4, pch = 16, axes = TRUE, xlim = c(1,15), ylim = c(2,18),
cex.axis=1.7,cex.lab=1.7,cex.main=1.7, main="Shewhart Xbar Chart",xlab="Time / Sample
number",ylab="Plotting Statistic",font.lab=2, font.axis=2)
abline(h = c(8.53), lty = 1, lwd=4)
text(1.1,9.03, 'CL=8.53',cex=1.3)
abline(h = c(3.71, 13.35), lty = 5, lwd=4)
text(1.1,4.21,'LCL=3.71',cex=1.3)
text(1.2,12.85,'UCL=13.35',cex=1.3)
abline(h = c(3.60, 13.47), lty = 3, lwd=4)
text(3,3.10,'LCL=3.60',cex=1.3)
text(3,13.97,'UCL=13.47',cex=1.3)
legend('top',legend=c("Sample mean","Case K Modified limits","Case U Modified
limits"),lty=c(4,5,3),lwd=4,cex=1.3)


set.seed(15)
data=replicate(15,expr={
rnorm(5,8.53,3.36)})
y= apply(data,2,Range)
x=1:15
plot(x,y,type = 'b', lwd=4, pch = 16, xlim = c(1,16), ylim = c(-1,27),
cex.axis=1.7,cex.lab=1.7,cex.main=1.7, main="Shewhart R Chart",xlab="Time / Sample
number",ylab="Plotting Statistic",font.lab=2, font.axis=2)
abline(h = c(7.82), lty = 1, lwd=4)
text(1,8.45, 'CL=7.82',cex=1.3)
abline(h = c(1.12, 18.88), lty = 5, lwd=4)
text(1.2,1.81,'LCL=1.12',cex=1.3)
text(1.3,18.38,'UCL=18.88',cex=1.3)
abline(h = c(1.04, 19.20), lty = 3, lwd=4)
text(3,0.60,'LCL=1.04',cex=1.3)
text(3,19.84,'UCL=19.20',cex=1.3)
legend('top',legend=c("Sample range","Case K Modified limits","Case U Modified
limits"),lty=c(4,5,3),lwd=4,cex=1.3)
```

Chapter 4

Literature review: Non-standard applications of SPC

4.1   Introduction

Traditionally SPC charts have been used for process monitoring and improvement in manufacturing, for example, Qiu (2014) discuss a number of examples. However, recently applications of control charts have been reported outside manufacturing in biology (see, e.g., Pazhayamadom et al. (2013)), medicine (see, e.g., Chen and Huang (2014)), athletics (see, e.g., Cox and Dunn (2002)), finance (see, e.g., Yi et al. (2006)) and other areas. In this chapter, we review some reported non-standard applications of SPC charts from 2001 to 2012 and highlight the reported benefits and problems associated with these applications. Moreover, this chapter serves as a prelude to the case study presented in Chapter 5. The case study presented in Chapter 5 can be seen as a non-standard application of SPC, since it applies the $\left(\overline{X}, R\right)$ charting scheme we developed in Chapter 3 to student evaluation of teaching (SET) survey data.

MacCarthy and Wasusri (2001) gave a detailed overview of the literature on non-standard applications of SPC up to the year 2000. In their paper they identified *four* application domains, namely:

   i.   engineering, industrial and environmental applications (43%),

  ii.   healthcare applications (31%),

 iii.   general service sector applications (17%),

 iv.   statistical applications / forecasting (9%).

After conducting our own overview of the literature on non-standard applications of SPC from the year 2000 to 2012 we identified *six* application domains, namely:

   i.   engineering, industrial and environmental applications (20%),

  ii.   healthcare applications (31%),

 iii.   general service sector applications (17%),

 iv.   statistical applications / forecasting (2%),

    v.   animal production (28%),

    vi.   everyday situations (2%).

Thus, we have identified *two* additional domains over and above those identified by MacCarthy and Wasusri (2001), namely animal production and everyday situations. Firstly, we will focus on the two additional domains that we have identified. It should be noted that our overview included the years 2000 to 2012, since in the year 2013 the focus of this dissertation shifted to the joint monitoring scheme presented in Chapters 2 and 3.

4.1.1   Animal production applications

The primary objective of animal production SPC applications has been to monitor, control and improve animal production processes with examples found in poultry, swine, dairy and others. Examples include monitoring disease incidence, milk production, reproductive performance and water intake. For instance, the outbreak of a disease can spread fast within a group of animals and if it is not detected and treated immediately the outcome might include losses such as increased mortality and economic losses. Data is usually ratio scaled, non-normally distributed with correlation and is gathered from the process itself (i.e. it is usually not simulated data). The types of control charts used are mostly the more advanced charts such as residuals-based Shewhart, CUSUM, EWMA and multivariate charts. A major problem in animal production SPC applications is data correlation. De Vries and Reneau (2010) gave a detailed systematic review of the application of SPC in animal production applications to the year 2009. Here, we give some examples and we briefly mention some of the key contributions and ideas and a few of the more recent developments in the area; the literature on SPC methods applied to animal production applications continues to grow at a rapid pace.

Quimby et al. (2001) used a two-sided parametric CUSUM chart for monitoring the feeding behaviour of steers in order to minimize economic loss by predicting morbidity. Individual animals were considered as the experimental units and an animal was recorded as either absent or present at the feed bunk every 5.25 seconds. Although a two-sided chart was used in this study, a one-sided approach was used since a signal (that is, an animal being categorized as morbid) is given when a charting statistic plots on or below the *LCL*. This is due to the fact that appetite typically decreases with the onset of disease. Current methods of detecting disease include visual appraisal by feedlot pen riders, however, the authors concluded that only using visual appraisal is not effective. This was proven by doing two trials at a commercial feedlot and finding that the CUSUM chart detected

65

animal morbidity on approximately 4.5 days and 3.7 days earlier than pen riders, for the first and second trial, respectively, which will allow for medical intervention approximately 4.1 days earlier.

De Vries and Conlin (2003) considered the timely signalling of changes in estrous detection ratio (EDR) and, accordingly, applied control charting techniques to animal fertility. Since control charts for EDR can be based on the normal or binomial distribution, the authors considered the individuals chart (X chart) based on the normal distribution and the fraction nonconforming chart (p chart) based on the binomial distribution for the Shewhart-type chart (for the detection of larger shifts) and the CUSUM-type chart (for the detection of smaller shifts), respectively. They found that CUSUM-type charts detected changes in estrous detection ratio faster than Shewhart-type charts; which is to be expected. Following their 2003 paper, De Vries and Conlin (2005) stated that the performance of control charts in dairy production systems is largely unknown and, to gain some more insight, they used a Monte Carlo simulation model of a dairy production system. The main objective was to compare the performance of a wide variety of plausible control chart designs that are applied to dairy production systems. Again it was found that CUSUM-type charts detected changes faster than Shewhart-type charts; which is not surprising. The ideal would of course be to use a combination of a Shewhart chart and a CUSUM chart for good detection of both large and small changes.

When considering the monitoring of animal health problems, Lukas et al. (2005) used two Shewhart-type charts, namely the individuals chart and the moving range chart, and ran them separately to monitor subclinical mastitis incidence (i.e. the inflammation of breast tissue incidence) in a dairy herd. More specifically, the objective of their study was to examine the relationship between monthly Dairy Herd Improvement (DHI) subclinical mastitis, new infection rate estimates and daily bulk tank somatic cell count (BTSCC). They concluded that control charting techniques detected a change in BTSCC (as a result of subclinical mastitis) earlier than the official control authority that did tests on a monthly basis. More recently Lukas et al. (2009) used a CUSUM chart to monitor disease onset. Daily milk yield (MY) and milk electrical conductivity (MEC) were monitored. The authors used two autoregressive models based on a subset of healthy cow records to address the problem of autocorrelation between individuals cow MY and MEC readings. It was noted that although a signalling event can't indicate the type of disease that is emerging, the charts were shown to be effective in early detection of disease onset giving the herd manager an advantage in terms of time to fight off the emerging disease. It should be noted, at this point, that although the reader may not be familiar with all the terminology used in the animal health discipline, the point we are trying to get across is that SPC techniques have moved far beyond manufacturing into other areas, such as animal health problems, and that the literature continues to grow at a rapid pace. An

66

example of (perhaps) a more well-known health problem (specifically, a bacterium) that causes fever and food poisoning is Salmonella.

Baum et al. (2005) used the parametric Shewhart $\overline{X}$ chart to evaluate the serological responses of three groups of pigs infected with three Salmonella serovars (one serovar per group). For more applications of SPC techniques to animal health problems the reader is referred to Reneau and Kinsel (2001), Grennstam (2005), Pastell and Madsen (2008) and the references therein.

Mertens et al. (2008) used a CUSUM chart based on residuals to monitor egg weight in order to minimize economic loss. A non-linear model was developed to detect the natural increasing trend of the egg weight with the increasing hen age. This trend was then subtracted from the measured egg weight and the residual values were inserted into the CUSUM statistic. The results showed that utilizing a CUSUM chart enables us to quickly detect a decrease in the average egg weight. The Mertens et al. (2008) paper ushered in a succession of papers on the use of control charts in monitoring livestock production. Following the 2008 paper, Mertens et al. (2009) cautioned that the well-known parametric CUSUM chart is based on certain assumptions such as the underlying process distribution being normal and the observations being independent and identically distributed. The problem is that statistical properties of livestock production processes often do not comply with the basic assumptions of control charts. For example, data originating from livestock production processes typically display autocorrelation between successive observations, for instance, the age of an animal can have an effect. Mertens et al. (2009) used Engineering Process Control (EPC) strategies as a possible solution. Without going into too much detail here, EPC is basically a model based process adjustment. The reader is referred to Del Castillo (2002) for more information, however, for our purposes it is only important to note that by the use of EPC a control chart can be constructed based on corrected data (where corrected data refers to the data after autocorrelation has been removed by means of modelling). In conclusion, the combination of the principles of EPC and SPC, referred to as synergistic control, can be used to monitor livestock production processes. More recently, following the 2009 paper, Mertens et al. (2011) gave a review on the most important aspects, recommendations, drawbacks and opportunities for the development and performance of control charts use for monitoring livestock production processes. In Table 1 of their paper they provided a list of all the publications where control charting techniques have been used up to the year 2009.

67

St-Pierre and Cobanov (2007a, b) used the parametric Shewhart $\overline{X}$ chart for monitoring the nutritional composition of forage. Different designs were used by varying the sample size, sampling frequency and the width of the control limits. The authors observed that there is some association between nutrients. Thus, there is a need to expand the method from a univariate approach, in which each composition element is monitored separately, to a multivariate approach in which relationships between composition elements are factored in the monitoring process.

Davis et al. (2008) used a Shewhart $\overline{X}$ chart to monitor the effects of a Bacillus-based direct-fed microbial feed supplement on growth performance of pigs. Average daily gain (ADG) and gain to feed ratio (G:F) were monitored under experimental conditions. Their study demonstrated that SPC can be used to measure the outcome of implementing new technologies in a commercial swine production facility. However, the potential effect of seasonality on measurements still needs to be addressed when using SPC in a swine production facility.

Cornou et al. (2008) used a CUSUM chart based on residuals to monitor estrous and health disorders of group housed sows fed by electronic sow feeders. A dynamic linear model of water intake and a dynamic linear model of eating rank were created and used to predict estrous, lameness and other health disorders. Differences between the predicted values of the model and the observations were monitored. The chart signals when residuals exceed some defined parameters. It was concluded that the CUSUM chart is more sensitive than trained expert personnel in the detection of estrous, lameness and other health disorders.

Krieter et al. (2008) applied parametric CUSUM and EWMA charts to quickly detect process changes in swine production. The authors concluded that these control charting procedures are useful tools to trace deviations in commercial swine farming. Madsen and Kristensen (2005) used a parametric CUSUM chart to monitor the condition of piglets by monitoring their water consumption and studying the drinking behaviour, since changes in drinking patterns are usually the first visual signs that pigs are experiencing some kind of stress.

SPC techniques have been used in the past as a way to monitor milk quality (see, for example, Reneau (2000) and Fuhrman (2002)). More recently, Wallace (2009) used the Shewhart individuals chart with probability limits for monitoring dairy milking management systems. Parlor indicators (milk production, flow rate, milking duration) were monitored. SPC is ideally suited to monitor milk quality, since milk-related data are not only easy to collect but it is also collected on a daily

68

basis (frequently collected). Wallace (2009) concluded that SPC can be used to signal emerging problems, evaluate the positive or negative impact of change in management practise or implementation of a new product. The only disadvantage noted by the author was that collecting suitable data for SPC control charting techniques was problematic since most computerised milking systems provide "snap shots" of the most recent data. Furthermore it was noted that if SPC is to be useful as a part of any production system the idea of continuous improvement must be embraced.

Fraile et al. (2009) used the Shewhart individuals chart to monitor the effect of treatment with phytosterols in three herds of pigs with porcine respiratory disease complex. The performance measures were culls (%), feed efficiency, mortality (%) and average daily gain (ADG). The study showed that the use of SPC techniques is viable in pig production when formal studies are not feasible. For instance, it is possible to compare the performance of a process by using SPC techniques to examine data collected before and after a change has been introduced.

Clearly, from all the examples / publications above and the references therein it is clear that the literature on SPC methods applied to animal production applications continues to grow at a rapid pace.

4.1.2   Everyday situations

Bamford and Greatbanks (2005) applied Shewhart individuals charts to monitor everyday personal processes. Processes monitored included (i) a shopping activity, (ii) washing dishes, (iii) swimming, (iv) commuting to and from university and (v) visiting a doctor. The performance measures for each of the activities were (i) time taken to complete a shopping spree, (ii) time taken to wash dishes, (iii) the time taken to swim 250m, (iv) time taken to commute to and from university and (v) patients' waiting time. The charts gave a better understanding of the process monitored. For example, for the shopping activity it was found that it is best to shop on a Monday before late afternoon, using a basket not a trolley, with a list of items to buy and shopping alone or with no more than one friend. The authors remarked that other tools like flow charts, pie charts, Pareto charts, cause and effect diagrams, scatter graphs and histograms could be used together with the control charts to optimise the analyses. Each of these methods highlights data in its own way, and together they give the best analyses and process understanding.

4.1.3 Healthcare applications

"This group covers three types of applications: monitoring the performance of a healthcare process such as asthma in a patient, the performance of a healthcare unit such as a pneumonia clinic, and monitoring patient/user satisfaction levels with a particular healthcare unit such as an outpatient clinic" MacCarthy and Wasusri, 2001. Many of the studies use attributes data gathered directly from the process, so predominantly Shewhart attribute charts are used. Major problem with this application type is that data might be cross-correlated and this suggests the use of the more advanced multivariate charts in addition to the univariate charts. Thor et al. (2007) gave a detailed systematic review of the application of SPC in healthcare improvement up to the year 2007. Here, we briefly mention some of the key contributions and ideas and a few of the more recent developments in the area; the literature on healthcare improvement continues to grow at a rapid pace.

Curran et al. (2008) showed the use of Shewhart charts to monitor and reduce the number of ward-acquired methicillin-resistant staphylococcus aureus (WA-MRSA). The chart helped to indicate when and where incident control teams should focus their efforts to investigate causes of WA-MRSA increases. Charts assisted in determining the hospital epidemiology of antimicrobial-resistant alert organisms. They improved communication between incident control teams and ward managers regarding infection prevention and control performance. All participants valued using SPC techniques as a feedback system and many stated that they would continue using it after this study for future infection control quality improvement.

Dzik et al. (2008) used a Shewhart p chart to monitor errors in patient specimen collection. The performance measures used were the proportion of mislabelled samples and the proportion of miscollected samples. The authors created a template in Microsoft Excel where the practitioner simply has to input the number of mislabelled samples, the number of miscollected samples, the sample size and the date and at that point the Shewhart p chart for the proportion of errors is constructed. They refer to this as an SPC spreadsheet (see Appendix 4 below). They reported that the SPC tool can be a practical means to establish a regional or national performance standard and that the participating hospitals found the SPC spreadsheet easy to implement and an appropriate tool to monitor the performance of the sample labelling and collection process.

Canel et al. (2010) used the Shewhart c chart to monitor patient record assembly times. They reported that the implementation of SPC charts reduced the amount of time a record stayed in the

70

health information management department from 9 to 7.6 days and decreased the average time taken to file a patient's completed record in permanent file from 6.1 to 3.3 days. In addition, they reported that everyone accepted then implementation of SPC techniques in their department, except for one employee who was hostile to change.

Wirtschafter et al. (2010) used a Shewhart u chart to monitor central line-associated bloodstream infection (CLABSI) among new born babies and to test the effect of the collaborative to reduce neonatal central line-associated blood stream infections. They concluded, based on the SPC methodology, that their collaborative was associated with special cause variation. However, they did not have a randomized control group and hence could not rule out other explanations for the CLABSI rate change. In addition, their baseline (Phase I) and follow up periods were shorter than desirable for SPC purposes. They only had eight points in the Phase I which is much smaller than what is recommended in the literature (see, for example, Chakraborti et al. (2009)).

Pujar et al. (2010) used a Shewhart individuals chart with runs-rules to monitor weekly seizure frequency due to epilepsy and also to evaluate the effectiveness of drug interventions. According to the study, SPC techniques helped assess seizure fluctuations in individuals with epilepsy and objectively assessed whether a drug intervention has led to a change in seizure frequency. However, SPC charts are generated using expensive statistical packages like SPSS and Minitab and may not be easily available especially in resource poor countries. A limitation of this study was that it did not have enough data to analyze seizure types separately. An idea for future research could be to apply a moving range chart to the data to get the variance IC before running the individuals control chart for monitoring location. It is highly recommended in the literature to have two control charts, one for monitoring the location and one for monitoring the spread.

Correia and Oliveira (2010) used univariate and multivariate charts (see Section 1.10.4) with variable control limits to monitor chronic respiratory patients. The measures used were oxygen partial pressure and carbon dioxide partial pressure. The authors observed that the control chart with varying limits explicitly showed the tendency for worsening or improving of the patient's health status, throughout time. Furthermore, the charts permitted the identification of abnormal values for the corresponding phase in the patient's health status, at each time instant.

Weib and Atzmüller (2010) applied an EWMA chart using attributes data to monitor medical diagnosis by medical examiners. The proportion of cases where an examiner has given correct diagnosis was used in the EWMA statistic. The implementation of the SPC approach provided an

71

easy and intuitive overview on the documentation behaviour of different examiners. For more information of EWMA charts using attributes data the reader is referred to Trevanich and Bourke (1993).

Kottner and Halfens (2010) used the Shewhart p chart to monitor the prevalence of hospital acquired pressure ulcers in the Netherlands. The charting statistic was the proportion of patients with pressure ulcers. Chi-square trend tests were also done and conflicting outcomes resulted, for instance, the chi-square trend tests indicated downward trends (i.e. prevalence rates decreased) in four hospitals, whereas the Shewhart p charts indicated the presence of common causes of variation only for these four hospitals. Although the uses of SPC control charting techniques have many advantages, there are some limitations, for example, even if processes are under statistical control, the values of the measured indicators are not automatically clinically acceptable or desired.

Duclos and Voirin (2010) monitored the observed proportion of postoperative complications per month in a healthcare unit using a Shewhart p chart. The chart enabled practitioners to continuously undertake a critical examination of the care delivered. Control charts could also work complementary to randomized controlled trials in providing evidence on the impact of safety improvement interventions. However, they warned that although the Shewhart p chart was conceived to be user friendly for non-experts, previous knowledge is still required for design. They listed the rarity of events and confounding factors such as patient case-mix as some of the fundamental differences between monitoring a healthcare process and monitoring a manufacturing process.

Perla et al. (2011) used a Shewhart individuals chart to monitor the percentage of unreconciled medication in a health facility. They concluded that Shewhart charts have many advantages such as (i) the display data in such a manner as to make process improvement visible, (ii) they determine whether changes resulted in improvement, (iii) they determine if gains made by the improvement are still holding, and (iv) they allow for a sequential view of data versus a stagnant view.

Correia et al. (2011) used both univariate and multivariate charts (see Section 1.10.4) to monitor chronic respiratory patients. In this case, oxygen and carbon dioxide partial pressure were used together with the body mass index as performance indicators. Multivariate charts were used since there is some cross-correlation between performance measures. The reason for the inclusion of univariate charts is that it is highly recommended in the literature to use univariate charts along with

72

multivariate charts, since one of the disadvantages to using the latter is the fact that there is some difficulty in identifying when an OOC state has occurred.

4.1.4   Engineering, industrial and environmental applications

"Many of the studies in this group focus on monitoring the performance of a critical piece of equipment or machinery or a complex piece of instrumentation, either through variables or attributes data that is generated directly from the process or indirectly through a measure that is associated with the process in some way. Some of the studies focus on the use of SPC for optimal maintenance planning in industry. Some of the studies are concerned with monitoring the level of environmental variables such as the concentration of pollutants in industrial processes or in physical environment. Typically the emphasis is on hazardous or safety critical variables but applications also extend to monitoring concentrations of mineral deposits." MacCarthy and Wasusri (2001). Major issues here are the definition of IC and OOC, and data is usually correlated, so the more advanced residual-based Shewhart, CUSUM, EWMA and multivariate charts are predominantly used.

Shehab and Schlegel (2000) used several control charts to monitor the performance of workers on various human performance tasks. They considered Shewhart-type charts for detection of larger changes (threshold control) and CUSUM-type and EWMA-type charts for detection of smaller changes (deviation control). They considered both attributes and variables charts for discrete and continuous performance measures, respectively. They considered charts for monitoring location, e.g. the Shewhart $\overline{X}$ chart, and they also considered charts for monitoring spread, e.g. the Shewhart R and S charts. Specifically, the following control charts were considered: (i) Shewhart p chart for fraction nonconforming, (ii) the Shewhart $\overline{X}$ chart, (iii) the Shewhart R chart, (iv) the Shewhart S chart, (v) the CUSUM $\overline{X}$ chart and (vi) the EWMA $\overline{X}$ chart. The performance measures monitored included reaction time (RT), root mean square error (RMS), lambda (LM), percentage incorrect (PI) and control losses (CL). These are called readiness to perform indicators (RTP). RTP testing is undertaken to identify changes in an individual's performance that may be due to exposure to risk factors such as the use of alcohol and / or drugs, fatigue and sleep loss. To give an illustration of why the use of SPC techniques is feasible in these situations, let us consider the case where there is a noticeable deterioration in an individual's performance because of drug use. Traditional methods of testing for drug use include drug screenings, however, a lot of controversy surround drug screenings since they are deemed to be an invasion of privacy and intrusive. In order

73

to avoid such difficulties, efforts have turned towards the use of SPC techniques. A major challenge posed by the use of computer based RTP testing is identifying an effective method of analysing and interpreting performance data in order to make individualized judgements. The authors concluded that by adapting SPC control charting techniques to the monitoring of human performance in industry it will make the process of screening workers, for the presence of risk factors, more readily implemented. As a result, the health and safety of the workforce will be improved. Furthermore, they advocated the use of SPC techniques over that of traditional statistical analyses since the latter is typically based on pooling observations across participants creating a masking effect (the reader is referred to the discussion on rational subgrouping and masking effects in Section 1.7).

MacCarthy and Wasusri (2002) applied the Shewhart chart based on residuals, the traditional EWMA individuals chart and the EWMA chart based on residuals to detect disturbances in production planning and scheduling. When monitoring time-related measures, in operational systems, problems arise such as autocorrelated data (see Section 1.4.2). The Shewhart and EWMA charts based on residuals were used to address the problem of autocorrelation since residuals are assumed to be iid normal. The authors stated that the traditional EWMA individuals chart was used since it has been shown to be robust to autocorrelated data (see Borror et al. (1999)). However, on the contrary, Human et al. (2011) recently showed that the traditional EWMA chart can lack in-control robustness and their findings call into question routine applications of the traditional EWMA chart in practice. However, these finding were only published in 2011 and, consequently, this information was not known to MacCarthy and Wasusri in 2002. Using these three control charts, MacCarthy and Wasusri (2002) monitored differences between planned flow time per job and actual flow time per job; the difference between target output per day and actual output per day. They concluded that control charting techniques provide visibility which helps to control production planning and scheduling. In addition, it assists management to prioritize and decide on the disturbances to be eliminated. However, they acknowledged that it will take practitioners some time to understand, construct and interpret control charts correctly as SPC techniques are not well-known in all operational systems. In addition, control charts cannot guarantee that the organization is operating efficiently. It can only show how the organization is and has been operating. Another drawback is that performance measures used to construct control charts in production planning and scheduling, can only be obtained after the job has been done. Therefore, investigation and corrective action cannot be taken at the time the job is being produced and there may be longer time lags.

74

Corbett and Pan (2002) used the CUSUM chart to evaluate environmental performance. Specifically, they monitored emissions data since pollution is well-known to have a huge economic impact as well as an environmental impact. The chart was used to monitor nitrate concentration levels. They found the chart to be a useful risk management tool and recommended it to other practitioners who may want to identify processes that are at risk of provoking compliance problems. They also recommended it to regulators, since it contains useful information for enforcement. They mentioned that there are new and detailed environmental performance data being gathered because of the trend towards adopting environmental management systems standards. Therefore applying quantitative methods like SPC is becoming easier than before. However, environmental control is based on upper one-sided specification limits e.g. nitrate concentrations may not exceed a certain upper specification limit. This calls for more research on the problem of lower and upper one-sided specification limits. Furthermore, the design of the control chart is complicated by the dependence of specification limits on legislation. For example, one could be monitoring the process using daily emissions data with no specification limits on daily emissions themselves by having only an upper limit on total monthly emissions. In addition, data used in environmental monitoring are likely to be multivariate (see Section 1.10.4) and correlated (see Section 1.4.2) which is problematic since multivariate control charting techniques are not well-known amongst practitioners and it is difficult to implement and having autocorrelated data brings its own problems since the use of standard control charting techniques (based on independent observations) become questionable.

Masson et al. (2005) used Shewhart charts to monitor the performance of the ion chromatography method. Chloride and nitrate concentrations were monitored. The charts allowed evaluation of quality performance during a time period that can lead to immediate changes in the procedure. Masson et al. (2005) concluded that the charts were a way to demonstrate accuracy and precision of the instrument method and that the charts could be used to verify the performance of the laboratory at any desired moment.

Masson (2007) used a Shewhart $\overline{X}$ chart with warning limits to monitor the performance of the liquid chromatography method. Phosphate concentration was monitored. In Shewhart-type charts the control limits are typically placed at distances of 3 standard deviations (of the charting statistic) above and below the *CL*. Since it is well-known that Shewhart-type charts are relatively insensitive in the detection of small shifts, warning limits can be added to the chart which are typically placed at distances of 2 standard deviations (of the charting statistic) above and below the *CL*. A signal is then given if two consecutive points plot between the warning and control limits or if one point plots on or beyond the control limits. These control charting techniques were used to check whether

75

the performance of the analytical procedure was maintained or, rather, how well it was maintained, when it is used in routine analysis. Masson (2007) warned that statistical control does not imply that the system is performing within the analytical quality required, but only that it is stabilized. This implies that if the analytical procedure is based on mistaken assumptions, the analytical results will be wrong even if no statistical variations are reported by the SPC chart.

Bateman et al. (2009) used two Shewhart-type charts, namely the individuals chart and the moving range chart, and ran them separately to monitor camera image variation. Pixel values were used to construct these control charts. The chart acted as a tool for yielding anomalies in image data. It made it possible to pinpoint inconsistent images such that it is potentially possible to establish a stochastic feature from the image data that acts as a fingerprint for that device. This can benefit camera identification research. One year later a similar study was done by these authors (see Bateman et al. (2010)), with the difference being that in their 2010 paper they implemented the Western Electric Rules (1956) into the Shewhart individuals chart to increase the sensitivity of detecting small shifts and they also applied the parametric EWMA chart to the data.

Nakahati et al. (2010) made use of the multivariate Shewhart Hotelling's T^2 and Runger's U^2 charts together with univariate Shewhart charts for health monitoring of aircraft horizontal stabilizer systems. The reader is referred to Section 1.10.4 for a discussion on univariate and multivariate control charts. The system temperature and the average value of motor current were used as performance measures. They concluded that using univariate SPC charts alone can lead to mistaken detection of emerging failures since the monitored variables vary as a function of other variables such as operational and environmental conditions. Therefore the use of multivariate SPC charts was deemed more appropriate.

Tasdemir (2012) used two Shewhart-type charts, namely the individuals chart and the moving range chart, and ran them separately to monitor a coal washing plant. Moisture content and ash content were used as performance measures. The author noted that most data in the mineral and mining industries are correlated. In the case of autocorrelation, when traditional charts are applied, a very high false alarm rate will probably cause process personnel to waste effort in unproductive searches for special causes. This can lead to a loss of confidence in the control chart, and even to the process monitoring being discontinued. In order to prevent this Tasdemir (2012) adjusted the data before using it to construct the charts. The reader is referred to Section 1.4.2 to see how to deal with autocorrelated data. Basically, an appropriate time series model is fitted to the autocorrelated

76

observations and Tasdemir (2012) identified the ARIMA (1,0,1) model for moisture content and the ARIMA (0,1,2) model for ash content to be the best for removing autocorrelation.

4.1.5   Statistical applications

The objective in this application is to give accurate forecasts by detecting non-random points using control charts. The data (residuals/ forecast errors) is usually ratio scale data, normal and independently distributed. The data is gathered from process of fitting the forecasting model. Usually traditional Shewhart mean and range charts are used. CUSUM and EWMA charts are also used.

Lotze and Shmueli (2009) compared the forecasting accuracy of three forecasting models using the traditional Shewhart mean and range charts.

4.1.6   General service applications

The main objective of applying SPC charts in this domain is to evaluate customer satisfaction and expectations and to help detect the root cause of extraordinary levels of satisfaction and dissatisfaction for individual customers. Data are typically gathered from surveys and are mostly ordinal. Problems include skewed data, time between surveys (time may be too long), correlation between questions and variable large sample size. However, even though the data are ordinal and skewed, many studies in this group still use the traditional Shewhart $\overline{X}$ and R charts regardless. Our case study in the next chapter (Chapter 5) explores this problem and offers some suggestions.

Marks and O'Connell (2003) used two Shewhart-type charts to analyse data from student evaluations of teaching. This was in response to the dangerous practise of relying on a single number to evaluate a teacher's performance or to allege that one individual's performance is superior to the other. They plotted the average of the students' responses to the statement: "The instructor was excellent (independent of how you feel about the course)" on the first chart. Using the other chart, they monitored the residuals from a regression model relating the average instructor rating to the expected grade. The purpose of pre-adjusting data through a regression model and plotting the residuals was to remove, from the average ratings, the bias due to the expected grade. Consequently, the performance of an individual whose scores are OOC on both charts cannot be explained by expected grade and therefore is worthy of note. The authors mentioned that SPC charts might provide an antidote for much of the tension and anxiety surrounding teaching evaluations,

77

misuse of the ratings by administrators and the pressure to rely on manipulative practices in pursuit of higher scores. However, Ding et al. (2006) observed that their charts did not include any time element; their approach was just a series of hypothesis tests shown graphically over instructors instead of over time. Therefore, their results conveyed no information regarding how well each instructor performs. Note that in their application Marks and O'Connell (2003) did not keep the spread chart, as recommended in literature, when they monitored the process mean.

Pettersson (2004) used the Shewhart chart for binomial data to monitor churn rate. Churn is a process of a customer replacing one provider of a service or merchandise for another. The chart displayed the proportion of churners in a group of at risk customers. They concluded that statistical methods (including control charting techniques) can increase detection power by decreasing the number of false alarms. In a nutshell, statistical methods will save time and money in the churn management area. However, their major concern was that the stakeholders were likely to be limited in their ability to apply and interpret control charts effectively. SPC charts were compared with data mining techniques for understanding churn. The main difference found was the lack of timeliness in data mining. Data mining results are only valid at one specific time point, and neither comparisons over time nor the repeated decisions, that are key in SPC, are possible in the data mining paradigm. Another criticism levelled against data mining techniques was the lack of information about significance level and the power of the results generated by the analysis.

Scordaki and Psarakis (2005) proposed that the multivariate Shewhart Hotelling's T^2 chart be used as an alternative to using several univariate Shewhart individuals charts in monitoring the performance of salesmen. One reason being that sales of a salesman are cross correlated with sales from other salesmen, since the sales of each one are influenced by the state of the market. Furthermore, sales data are autocorrelated since they are influenced by seasonality market patterns. Therefore making use of the traditional Shewhart individuals chart is inappropriate. Monitoring the ratio of the weekly total sales of a salesman to the total sales of the week instead of the raw sales on a multivariate Shewhart Hotelling's T^2 chart takes account of both issues. The authors believe that the use of SPC procedures in commercial companies may be a valuable tool in the machinery of the managers in evaluating employees, departments and services.

Maguad (2005, 2006) used a Shewhart $\overline{X}$ chart for monitoring a teacher's performance. The charting statistic was the average of the students' responses to the following question (which was presented in the format of a five point strongly agree to strongly disagree Likert scale): "Independent of the course, what is your overall rating of this instructor's performance?" The

78

author's proposal was motivated by a number of limitations in the conventional analysis of responses to such questions. Conventionally, such responses have been analysed by comparing the class average for the question to the group average (the group may be a department or an entire institution). But what does it really mean when an instructor's performance is below or above the group average? In other words, is this difference due to common cause variation or assignable cause variation? Conventional analysis methods fail to distinguish between these types of variation. Hence, conventional performance evaluations fail to discriminate between factors that are within the instructor's control and system determined factors. Consequently, conventional performance evaluations create a shortage of winners within the educational institution and do little to motivate teachers or enhance their satisfaction. It was concluded that using SPC charts to monitor teachers' performance will help the academic institution to understand which problems are attributable to the system and which ones are attributable to special causes. It will also help to assess classroom processes to determine whether or not the system needs intervention. Furthermore, it will help the administration to discover which teachers are performing outside the limits of variation of the system on either the good side or poor side and which ones are performing within the calculated limits of differences attributable to the system so that appropriate responses can be crafted to address the needs of different groups of teachers. Note that in their application of the $(\overline{X}, R)$ charting scheme Maguad (2005, 2006) ignored the multiplicity issue and the non-normality of their survey scales.

Ding et al. (2006) compared the Shewhart individuals chart, the modified p chart and the z-score chart to analyse student evaluation of teaching data. The overall teaching effectiveness variable, on the five point strongly agree to strongly disagree Likert scale, was used in all three cases. For both the Shewhart individuals chart and the z-score chart, overall teaching effectiveness was treated as a continuous variable and an average instructor teaching effectiveness was computed, standardized (in the case of the z-score chart) and plotted. For the modified p chart, the proportion that strongly agreed or agreed was monitored. The authors advocated the use of the modified p chart because it utilized distributions that were appropriate for categorical data and was relatively easy to program. In addition, its control limits varied with the sample size. The only drawback of the modified p chart is the fact that, since it is not well established in literature, it is unknown to most practitioners.

Morgan and Dewhurst (2007) used a Shewhart $\overline{X}$ chart to monitor the performance of supermarket chain's problem suppliers. Their application was motivated by (i) the need for a performance analysis tool that will be effective in enhancing buyer/supplier relationships in the food retailing

79

environment, and (ii) the fact that huge economic losses can be incurred if, for example, the delivery is not on time or the product is damaged. Current tools based on descriptive statistics do not add much management value in understanding the time relatedness of the data analysed. However, they are useful in exploring performance targets and understanding the scope of performance variations. The performance measures monitored in this study were Supplier Service (SS) and On Shelf Availability (OSA) which were calculated as follows:

(i) SS (%) = (Received volume) / (Total order volume) ✖ 100, and

(ii) OSA (%) = (Products in store stock) / (Products required in store stock) ✖ 100.

Phrased simply SS is a measure of the efficiency of supply operations from the supplier to the supermarket and OSA is a measure of the efficiency of 'back-of-shop' to 'front-of-shop' operations. Morgan and Dewhurst (2007) concluded that the application of control charting techniques is valuable in managing supplier relationships and that they enabled meaningful problem solving dialogues to be established. However, by only focussing on poorly performing suppliers the lack of balance in the sample limited the extent of their generalizations from the analysis. An idea for future research could be to look at the performance of suppliers that perform poorly, adequately and exceptionally.

Cadden et al. (2008) used the Shewhart $\overline{X}$ chart to monitor and improve teacher effectiveness. They also investigated what measure should be used as a standard by which an instructor's performance should be evaluated. This was a response to the lack of clear guidance on how to interpret SET results in order to make comparative evaluations of the instructor's performance. The authors believe that SPC charts offer a new method for a comprehensive evaluation of teaching effectiveness. In addition, they can allow for the consideration of possible additional explanatory variables such as the course taught, course and student status, expected grade and class size. However, the scores of teaching ability and other items in their assessment instrument are not normally distributed and, accordingly, an idea for future research could include considering some sort of transformation of the data or the use of nonparametric control chart techniques (see Section 1.10.2). Note that in their application of the $\left(\overline{X}, R\right)$ charting scheme Cadden et al. (2008) ignored the multiplicity issue and the non-normality of their survey scales.

Hanna (2009) used a Shewhart $\overline{X}$ chart in monitoring the management of education department resources. Hanna (2009) monitored the number of lost Basic Life Support: Health Care Provider (BLS HCP) training slots. The author concluded by stating that unlike column and line charts, SPC charts have interpretation guidelines that may be used to determine whether processes and outcomes

80

should be investigated. Also, SPC charts were effective presentation tools that enabled them to graphically display information for audiences. They were instrumental in reducing the number of lost BLS HCP slots, and therefore reduced costs.

The underlying process distributions of service processes are usually non-normal or unknown and, consequently, control charts that do not depend on a particular distributional assumption are desirable (see Section 1.10.2). Accordingly, Yang et al. (2012) used a nonparametric Shewhart-type mean chart and an arcsine transformed nonparametric EWMA-type chart for monitoring service processes with unknown distributions. The performances of these charts were compared to the traditional EWMA $\overline{X}$ chart, the traditional Shewhart $\overline{X}$ chart and a modification of the latter called the transformed $\overline{X}$ chart. Service quality was monitored by considering service time. Yang et al. (2012) concluded that the arcsine transformed nonparametric EWMA-type chart outperformed all the other charts and should therefore be used in practice.

4.2   Summary and Conclusion

We reviewed non-standard applications of SPC charts reported in the literature from the year 2001 to 2012, inclusive. We classified these applications into six groups according to the domain to which control chart techniques have been applied (see Table 4.1 below). For each group we described the nature of the application along with the objectives, data characteristics, data sources and control charts used (see Table 4.2 below). Further, we have highlighted the benefits and problems associated with the non-standard applications. Some of the benefit mentioned are that SPC charts can (i) help distinguish special from common cause variation, saving time and costs associated with process monitoring. (ii) help distinguish whether process interventions led to anticipated improvements (iii) help determine if gains made by improvement are still holding (iv) provide a common language for process improvement (v) help stakeholders learn about their process, enabling them to make informed decisions based on facts (vi) enable valuable prediction of future process performance. A major concern about the non-standard applications was that common SPC charts are not well suited to non-normal or correlated cases that exist with the type of data. It is clear that there is a great opportunity to make significant research contributions to these application areas. Thus, in Chapter 5 we present a case study that applies the Phase II $\left(\overline{X}, R\right)$ charting scheme, we developed in Chapter 3, to SET survey data.

Our findings are summarized in Tables 4.1 and 4.2.

Domain	Specific application
Health care	Dzik et al. (2008): Monitoring errors in patient specimen collection
	Curran et al. (2008): Monitoring and reducing the number of ward-acquired methicillin-resistant staphylococcus aureus (WA-MRSA))
	Canel et al. (2010): Monitoring patient record assembly times
	Wirtschafter et al. (2010): Monitoring central line-associated bloodstream infection (CLABSI) among new born babies to reducing neonatal central line associated blood stream infections.
	Pujar et al. (2010): Monitoring seizure frequency and evaluating drug interventions
	Correia and Oliveira (2010): Monitoring chronic respiratory patients
	Weib and Atzmüller (2010): Monitor medical diagnosis by medical examiners
	Kottner and Halfens (2010): Monitoring the prevalence of hospital acquired pressure ulcers
	Duclos and Voirin (2010): Monitoring postoperative complications
	Perla et al. (2011): Monitoring unreconciled medication
	Correia et al. (2011): Monitoring chronic respiratory patients
Animal production	Quimby et al. (2001): Monitoring the feeding behaviour of steers
	De Vries and Conlin (2003): Monitoring estrous of a dairy herd
	Lukas et al. (2005): Monitoring subclinical mastitis incidence
	Baum et al. (2005): Evaluating the serological responses of pigs infected with Salmonella serovas
	Madsen and Kristensen (2005): Monitoring and modelling drinking patterns of pigs
	St-Pierre and Cobanov (2007a, b): Monitoring the nutritional composition of forage
	Pastell and Madsen (2008): Detecting lameness in a milking robot
	Mertens et al. (2008, 2009): Monitoring of the average egg weight
	Krieter et al. (2008): Detecting process changes in swine production
	Cornou et al. (2008): Monitoring health disorders of a group of sows
	Lukas et al. (2009): Monitoring disease onset
	Wallace (2009): Monitoring milking management systems
	Fraile et al. (2009): Studying the effect of phytosterols in three herds with porcine respiratory disease complex
Engineering industrial and environmental applications	Cassady et al. (2000): Setting up a preventive maintenance plan
	Shehab and Schlegel (2000): Monitoring human performance on various performance tasks
	Wasusri and MacCarthy (2001): Production planning and scheduling
	Corbett and Pan (2002): Evaluating environmental performance
	Masson et al. (2005): Monitoring performance of the ion chromatography method
	Masson (2007): Monitoring the liquid chromatography method performance
	Bateman et al. (2009): Analysing camera image variations
	Nakahati et al. (2010): Monitoring an aircraft horizontal stabilizer system
	Tasdemir (2012): Monitoring a coal washing plant

General Service Sector	Pettersson (2004): Monitoring churn rate
	Maguad (2006): Assessing the performance in a graduate course
	Maguad (2007): Monitoring teachers performance
	Morgan and Dewhurst (2007): Monitoring the performance of supermarket chain's problem suppliers
	Cadden et al. (2008): Improving teaching effectiveness
	Hanna (2009): Monitoring the management of education resources
	Yang et al. (2012): Monitoring service processes
	Scordaki and Psarakis (2005): Monitoring the performance of a salesman
Statistics (forecasting)	Lotze and Shmueli (2009): Monitoring forecasts
Everyday situations	Bamford and Greatbanks (2005): Monitoring personal everyday activities

Table 4.1. Non-standard SPC applications: Publications from 2000 to 2012 divided into six application domains

Control chart technique	Article and variable plotted
Shewhart control charts	Jatla and Enzenauer (2007): Phacoemulcification time, phacoemulcification power, surgical time Canel et al. (2010): Time to completion Curran et al. (2008): Number of ward-acquired methicillin-resistant staphylococcus aureus (WA-MRSA)) Dzik et al. (2008): proportion of mislabelled samples, proportion of miscollected samples Wirtschafter et al. (2010): Central line associated blood stream infections (CLABSI) rate among new born babies Pujar et al. (2010):Total weekly seizure frequency Correia and Oliveira (2010): Oxygen and carbon dioxide partial pressures Kottner and Halfens (2010): Proportion of patients with pressure ulcers Duclos and Voirin (2010): Proportion of postoperative complications Perla et al. (2011): Proportion of unreconciled medications Pettersson (2004): Proportion of churners in a group of at risk customers Maguad (2006): Overall rating of course Maguad (2007): Overall rating of teacher performance Morgan and Dewhurst (2007): % supplier service, % on shelf availability Cadden et al. (2008): Teaching ability score Hanna (2009): The number of lost training slots Masson et al. (2005): Chloride and nitrate concentrations Masson (2007): Phosphate concentration Bateman et al. (2009): Image mean pixel value Bamford and Greatbanks (2005): Time taken to complete shopping, time taken to swim 250 meters, waiting time at a GP practise, time taken to wash dishes Lukas et al. (2005): Daily bulk tank somatic cell count Baum et al. (2005): Serologic responses St-Pierre and Cobanov (2007a,b): Forage quality Wallace (2009): Parlor data (milk production, flow rate, milking duration) Fraile et al. (2009): % culls, % mortality, feed efficiency, average daily gain Lotze and Shmueli (2009): One-sided Shewhart chart of forecast errors Tasdemir (2012): Shewhart chart of residuals moisture and ash content data
More advanced charts	Hardoon et al. (2006): CUSUM chart for the prostheses revision rate Coory et al. (2008): CUSUM chart for mortality rates Weib and Atzmüller (2010): EWMA chart for the proportion of times an examiner has given correct diagnosis Correia et al. (2011): Multivariate T^2 chart for oxygen partial pressure, carbon dioxide partial pressure and body mass index (BMI) Yang et al. (2012): Arcsine transformed nonparametric EWMA-type chart for monitoring service processes Wasusri and MacCarthy (2001): EWMA chart for differences between planned and flow time per job, differences between planned and actual output per day Corbett and Pan (2002): CUSUM chart for nitrate concentration level Nakahati et al. (2010): Multivariate Shewhart Hotelling's T^2 and Runger's U^2 charts of the system temperature and the average value of motor current Quimby et al. (2001): CUSUM chart to monitor feeding time

	Madsen and Kristensen (2005): CUSUM chart to monitor a linear model of water intake
	Pastell and Madsen (2008): CUSUM chart was used on exponentially smoothed leg weight data
	Mertens et al. (2008): CUSUM chart was used on continuously updated mathematical model of egg weight by age
	Cornou et al. (2008): CUSUM chart used on health disorders data adjusted for eating rank in sows
	Krieter et al. (2008): EWMA and CUSUM charts used on number of piglets born and estrous rate
Both Shewhart and advanced control charts	De Vries and Conlin (2003): Shewhart and CUSUM charts used to monitor estrous detection ratio
	Lukas et al. (2009): A time series model was used to adjust data before Shewhart and CUSUM charts were applied
	Scordaki and Psarakis (2005): Multivariate Shewhart Hotelling's T^2 chart and univariate Shewhart chart to monitor the weekly sales of the salesman
	Shehab and Schlegel (2000): Univariate Shewhart, CUSUM and EWMA charts applied on reaction time (RT), root mean square error (RMS), lambda (LM), percentage incorrect (PI) and control losses (CL).

Table 4.2. Non-standard SPC applications: Publications from 2000 to 2012 divided by the type of control chart applied

85

4.3 Appendix 4: SPC spreadsheet

The template of the SPC spreadsheet created by Dzik et al. (2008).

																						row total	freq.	%
...	PROCESS RUN CHART - MULTIPLE CHARACTERISTICS																							

No.	Labelling defect	Class / Characteristic frequency																				row total	freq.	%
1	Mislabelled																					0	####	#DIV/0!
2	Miscollected																					0	####	#DIV/0!
	Date																					**0**	**####**	**#DIV/0!**
	Sample size																					Sample total:		**0**
	Column totals	0	0	0	0	0	0	0	0	0	0	0	0	0	0	0	0	0	0	0	0	Year:		
	Proportion (p)	####	####	####	####	####	####	####	####	####	####	####	####	####	####	####	####	####	####	####	####	Hospital:		
	Moving Range		####	####	####	####	####	####	####	####	####	####	####	####	####	####	####	####	####	####	####	Ward/Dept:		
Mean proportion * =		**#DIV/0!**				Mean range =		**#DIV/0!**					UCL * =		**#DIV/0!**								

(* Value of Centre line [mean p], UCL to use for next chart)

86

An example of the SPC spreadsheet created by Dzik et al. (2008).

																							row total	fr
		PROCESS RUN CHART - MULTIPLE CHARACTERISTICS																						
		Errors in sample collection and labelling																						
No.	**Labelling defect**	**Class / Characteristic frequency**																					**row total**	**fr**
1	Mislabelled	1	4	3	1	0	3	1	1	0	1	1	1	1	1	1	3	0	1	2	0	26	0.
2	Miscollected	3	0	1	1	1	2	1	2	4	2	1	2	3	1	3	1	3	2	0	1	34	0.
	Date	01/12	02/12	03/12	04/12	05/12	06/12	07/12	08/12	09/12	10/12	11/12	12/12	01/13	02/13	03/13	04/13	05/13	06/13	07/13	08/13	**60**	
	Sample size	100	100	100	100	100	100	100	100	100	100	100	100	100	100	100	100	100	100	100	100	Sample total:	
	Column totals	4	4	4	2	1	5	2	3	4	3	2	3	4	2	4	4	3	3	2	1	Year:	
	Proportion (p)	0.040	0.040	0.040	0.020	0.010	0.050	0.020	0.030	0.040	0.030	0.020	0.030	0.040	0.020	0.040	0.040	0.030	0.030	0.020	0.010	Hospital:	
	Moving Range		0.000	0.000	0.020	0.010	0.040	0.030	0.010	0.010	0.010	0.010	0.010	0.010	0.020	0.020	0.000	0.010	0.000	0.010	0.010	Ward/Dept:	
Mean proportion * =		**0.03000**				**Mean range =**			**0.01211**						**UCL * =**			**0.06220**					

(* Value of Centre line [mean p], UCL to use for next chart)

Control chart from an example by Dzik et al. (2008)

Proportion of erroneous samples
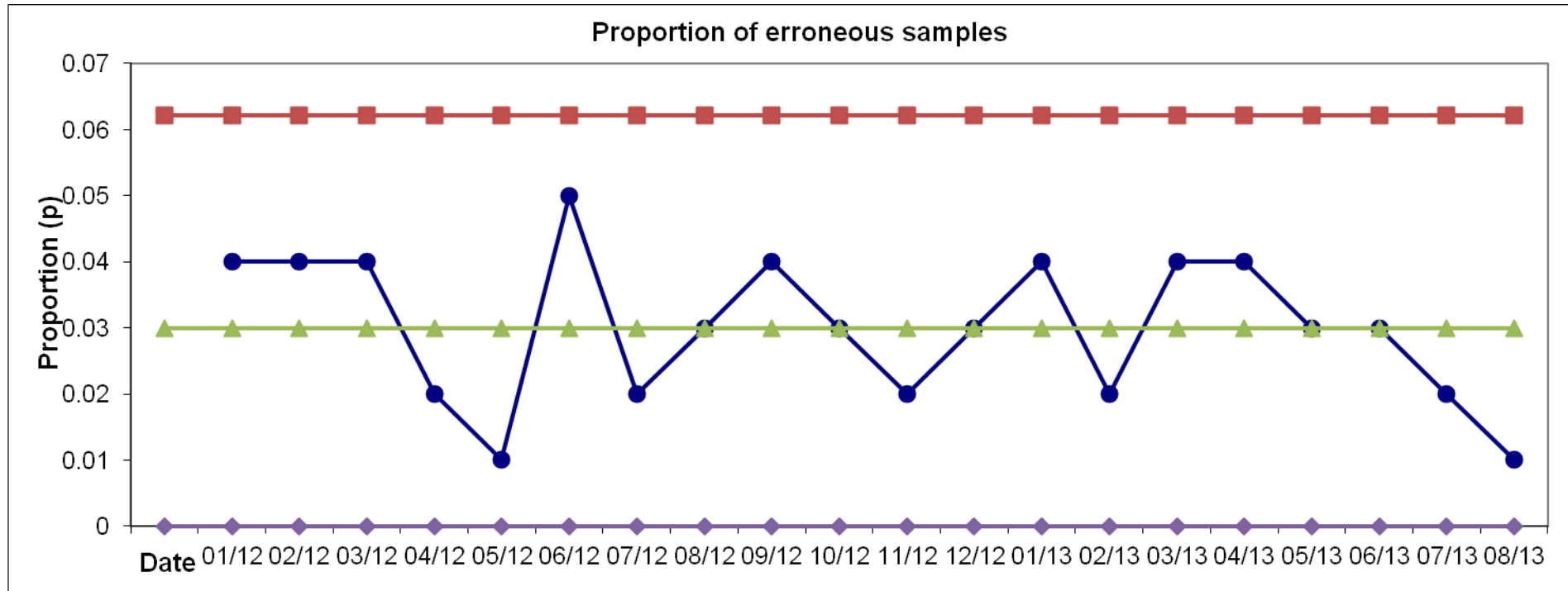
Chapter 5

Case study: Application of the $(\overline{X}, R)$ charting scheme to student evaluation of teaching (SET) survey data

5.1 Introduction

There is a continuing need for publications of case studies showing the benefits of SQC outside the conventional manufacturing domain (Woodall and Montgomery (1993)). In keeping with their spirit, this chapter applies the $(\overline{X}, R)$ charting scheme which we developed in Chapter 3 to student evaluation of teaching (SET) survey data. SET data are used to evaluate, monitor and improve teacher performance as well as student satisfaction levels. Note, SET data can be classified as customer satisfaction survey data and thus this case study can be categorized as a general service sector application, see Section 4.1.6.

Wardell and Candia (1996) showed that applying the standard $(\overline{X}, R)$ charting scheme to customer satisfaction survey data gives too many false alarms. The false alarm inflation was attributed to the non-normality of survey scales. It is known that the control chart constants of the standard Shewhart $\overline{X}$ chart assume that the underlying distribution of the data being measured is normal. Survey scales are at best ordinal and hence observations are not normally distributed. However, this lack of normality can often be redressed by taking large samples and relying on the results of the central limit theorem. Since sample sizes from surveys are usually large, a normal distribution may adequately describe the distribution of the averages of survey responses. This could be the reason why some practitioners (e.g. Marks and O'Connell (2003), Maguad (2005, 2006), Cadden et al. (2008)) continue to use the standard $\overline{X}$ chart even though the survey scales are known to be ordinal and skewed. However, these practitioners overlooked a very important fact, which is, to find the appropriate limits for the $\overline{X}$ chart, a good estimate of the standard deviation must be found. In the case of the $(\overline{X}, R)$ charting scheme this entails finding the value of $\dfrac{\overline{R}}{d_2}$. As stated in Wardell and Candia (1996), the problem is that the unbiased constant d_2 assumes that the individual observations are normally distributed (see the definition of d_2 in Chapter 2 page 23). Since the

89

normality assumption is inappropriate for survey data, $\dfrac{\overline{R}}{d_2}$ may consistently underestimate the population standard deviation and thus cause the limits of the $\overline{X}$ chart to be narrow and the *FAR* to rise.

Further, there are three more issues that might have caused the false alarm inflation and whose effects might not have been known to Wardell and Candia (1996). These issues are (i) the issue of the combined use of the $\overline{X}$ and R charts (multiplicity) and (ii) the issue of using $k = 3$ for the k-sigma limits on the R chart and (iii) the issue of parameter estimation. In Chapters 2 and 3 of this dissertation we have shown analytically how severe these two issues could be on the IC performance of the $\left(\overline{X}, R\right)$ charting scheme. We showed that their effect usually doubles or triples the number of false alarms. This is cause for serious concern.

Furthermore, the application of the $\left(\overline{X}, R\right)$ charting scheme to SET survey data is more cumbersome and complicated than a typical standard application. Wardell and Candia (1996) cited two reasons for this; (i) the fact that subgroup sizes are very large and (ii) the subgroup sizes are rarely equal (usually because response rates vary in surveys). In the literature, control chart constants are usually tabulated for small subgroup sizes and not for large subgroups (say greater than 50). In addition, more work is involved in creating and maintaining control charts when the sample size varies from time to time than when the sample size is constant. In passing, we note that there are two commonly used methods of dealing with variable sample size (see Stapenhurst (2005)). The first method uses only the first n observations of each subgroup to construct a chart, where n is the smallest subgroup size. This is the simplest method, but throws away valuable data. The second method keeps all the data in each subgroup, ignores the fact that n varies and it uses the average value of n in all the calculations. The second method is a little more complex than the previous one; however, it is reasonable when n does not vary too much. Maguad (2005) used the second method. Usually there are many operational variables (items) in a survey dataset and these variables are correlated. In practice, a single operational variable is often studied overtime using SPC charts. However, the multivariate construct complexity of customer satisfaction survey data makes it very dangerous to use individual univariate charts on each individual quality measure (Jensen and Markland (1996)). For example, if we collect and plot three uncorrelated variables, each on a separate univariate control chart (where $FAR_0 = 0.0027$), the overall *AFAR* would be $3 \times 0.0027 = 0.0081$, clearly this is not acceptable. It is even worse if the items are correlated, because the correlation pattern must be investigated before the overall *AFAR* may be assessed.

90

In summary, current and past applications of the $(\overline{X}, R)$ chart to survey data ignore the non-normality of the survey scales, ignore the multiplicity issue, ignore the effects of parameter estimation and do not take advantage of the correlation structure inherent in survey scales (see applications in Marks and O'Connell (2003), Maguad (2005, 2006)); as a result the *FAR* is inflated. In this case study, we take advantage of the correlation structure by using factor analysis to reduce our original 12 survey scales to a single interval scaled factor. We deal with the non-normality by using data transformation. We deal with the multiplicity and parameter estimation issues (in Phase II) by using our own charting constants in Table 3.2. It is because of these reasons that we strongly believe that our application method should lessen the *FAR* inflation and thus should be better than the application methods in Wardell and Candia (1996), Marks and O'Connell (2003) and also Maguad (2005, 2006). Finally we evaluate a single lecturer using the resulting Phase II $(\overline{X}, R)$ charting scheme.

We hope that our case study will provide some guidance to practitioners who want to apply the $(\overline{X}, R)$ charting scheme to survey data in general and more in particular to SET survey data. Next we briefly describe the data that will be used in the case study.

5.2   Description of the data

Table 5.1 Sample of data from the faculty SET database

Lecturer	Q1	Q2	Q3	Q4	Q5	Q6	Q7	Q8	Q9	Q10	Q11	Q12
1	5	5	5	5	4	4	5	5	5	5	5	5
1	4	5	4	4	4	4	5	4	4	4	4	4
1	5	5	5	5	5	4	5	5	4	4	5	5
1	5	5	4	5	5	5	5	4	2	4	5	4
1	5	5	5	5	5	5	4	5	4	5	4	4
1	5	5	5	4	5	4	5	4	4	2	5	5
1	5	5	5	5	5	4	5	5	5	5	4	4
1	5	5	4	5	5	5	5	5	5	5	4	4
1	5	5	5	5	5	5	5	5	5	5	5	5
1	5	4	4	5	4	4	5	5	4	4	4	5

Table 5.1 shows a subset of 10 observations from the SET data set. The first column indicates the evaluated lecturer. In this case lecturer 1 was evaluated. The remaining columns are the questionnaire items that were used in the evaluation process. These items are:

Q1 : the lecture made the purpose of learning clear

91

Q2 : the lecturer prepared well for the learning and teaching activities

Q3 : teaching and learning material supported learning

Q4 : the lecturer communicated effectively

Q5 : the lecturer encouraged student involvement

Q6 : the lecturer encouraged critical thinking

Q7 : the lecturer gave prompt feedback on assessments

Q8 : the lecturer gave appropriate feedback which supports learning

Q9 : the lecturer responded to learning needs

Q10 : the lecturer explained concepts clearly

Q11 : learning activities stimulated my interest in the module

Q12 : the lecturer was available for consultation outside class

Each row in Table 5.1 corresponds to one student who evaluated the lecturer. The students recorded their responses using the following response categories:

1. Strongly Disagree
2. Disagree
3. Neutral
4. Agree
5. Strongly Agree

The number of students evaluating a lecturer varied with the lecturer, the minimum number was 10, the maximum number was 398 and the average was 65.

5.3 Data preparation

In this section, data is prepared for Phase II analysis using the $\left(\overline{X}, R\right)$ charting scheme. This involves factor analysis, calculation of factor scores, transformation of the factor scores to improve their normality and conducting a Phase II analysis on the factor scores to remove outliers – thus ensuring that a set of clean IC data is obtained.

92

5.3.1 Factor analysis

Factor analysis has been used as an analytic tool in educational research. Practitioners use factor analysis for a variety of reasons, such as reducing a large number of items from a questionnaire or survey instrument to a smaller number of components, uncovering latent dimensions underlying the data set, or examining which items have the strongest association with a given factor, etc., see DiStefano et al. (2009).

We subjected our 12 SET data scales to factor analysis using SPSS. The aim was to assess the correlation among them and to reduce them to a manageable set suitable for our control charting purpose. As already mentioned, Jensen and Markland (1996) also used factor analysis to reduce their 22 service quality questionnaire items to 4 factors. Table 5.2 and Figure 5.1 give a summary of our factor analysis. As can be seen in Table 5.1, factor analysis revealed only 1 factor with an eigenvalue exceeding 1, explaining 54% of the variance in the original data. The explained variance of 54% is quite high compared to that given in the study by Jensen and Markland (2006), who extracted and charted 4 factors that explained less than 50% of the original data's variability. Furthermore, an inspection of the scree plot in Figure 5.1 showed a clear break after component 1. Thus we decided to retain only one factor for further analysis even though 46% of the original information will be lost.
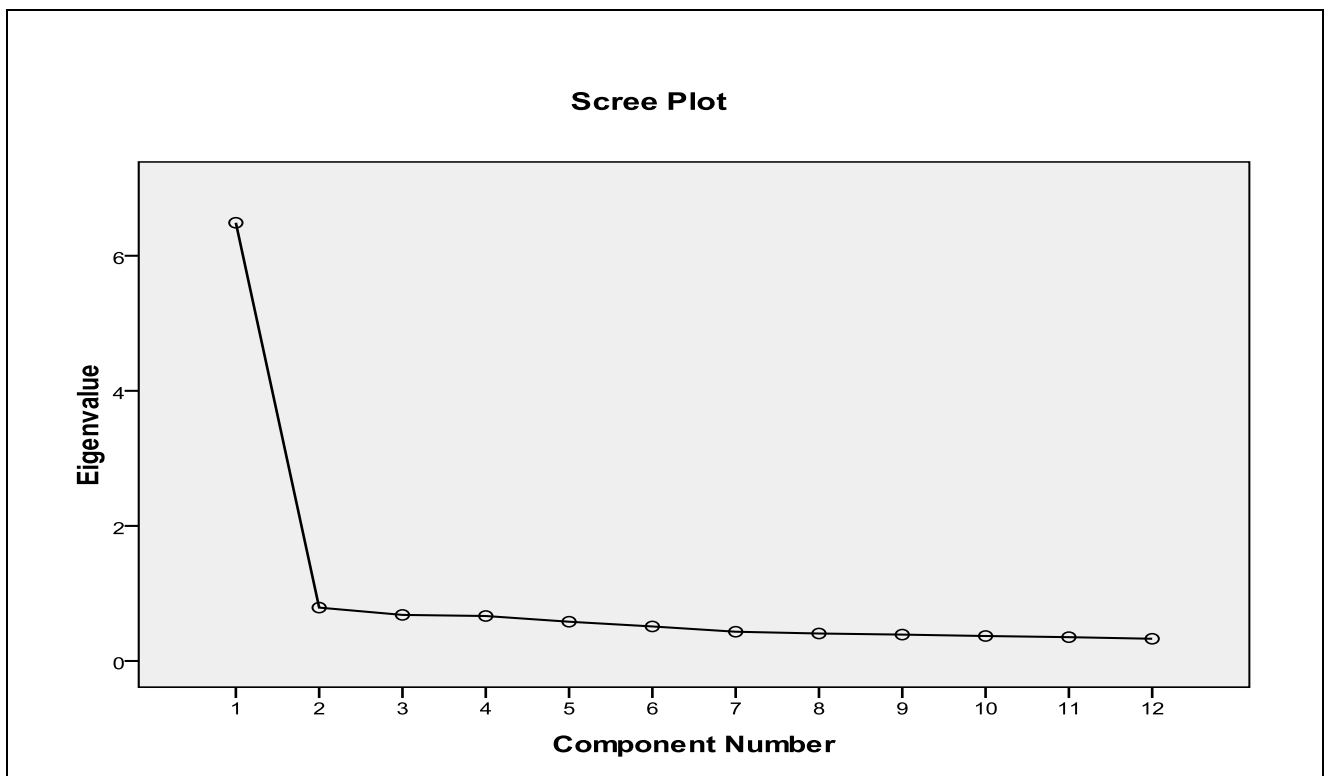

Figure 5.1 The scree plot of the SET data

93

Table 5.2 Total variance of the SET data explained by the components

Component	Initial Eigenvalues			Extraction Sums of Squared Loadings		
	Total	% of Variance	Cumulative %	Total	% of Variance	Cumulative %
1	6.488	54.069	54.069	6.488	54.069	54.069
2	.790	6.584	60.653			
3	.682	5.684	66.337			
4	.666	5.549	71.886			
5	.581	4.843	76.730			
6	.511	4.260	80.990			
7	.433	3.608	84.598			
8	.407	3.389	87.987			
9	.390	3.253	91.241			
10	.370	3.081	94.321			
11	.353	2.938	97.260			
12	.329	2.740	100.000			

Extraction Method: Principal Component Analysis.

5.3.2 Factor scores and data transformation

Factor scores are composite variables which provide information about an individual's placement on the factor (DiStefano et al. (2009)). Once a researcher has used factor analysis and has identified the number of factors or components underlying the data set, he/she may wish to use the information about the factors in subsequent analysis (Gorsuch (1983)). Here, in this dissertation, factor scores are used for control charting purposes. However, we need to calculate them first.

Table 5.3 SET Questionnaire items and their factor loadings

Questionnaire items	Factor loadings
Made purpose of learning clear	.806
Prepared well for the teaching and learning activities	.779
Teaching and supporting material supported learning	.740
Communicated effectively	.762
Encouraged student involvement	.721
Encouraged critical thinking	.716
Gave prompt feedback on assessments	.657
Gave appropriate feedback which supports learning	.752
Responded to learning needs	.768
Explained concepts clearly	.779
Learning activities stimulated my interest in the module	.702
Available for consultation in scheduled hours outside the classroom	.620

Extraction Method: Principal Component Analysis.

94

1 components extracted.

There are various methods of scoring a factor, some of these are the (i) regression technique, (ii) sum technique, (iii) weighted sum technique, (iv) Bartlett technique and (v) Andersin-Rubin technique (see DiStefano et al. (2009)). We opted for the weighted sum technique because its advantage is that the items with the highest factor loading on the factor have the largest influence on the factor score (see DiStefano et al. (2009)). The weighted sum technique multiplies the raw item score by its factor loading and then sums the resulting values across items. Table 5.3 shows the items and their factor loading. It can be seen that the item "made the purpose of learning clear" has the highest loading and thus has the largest impact on the calculated factor scores.
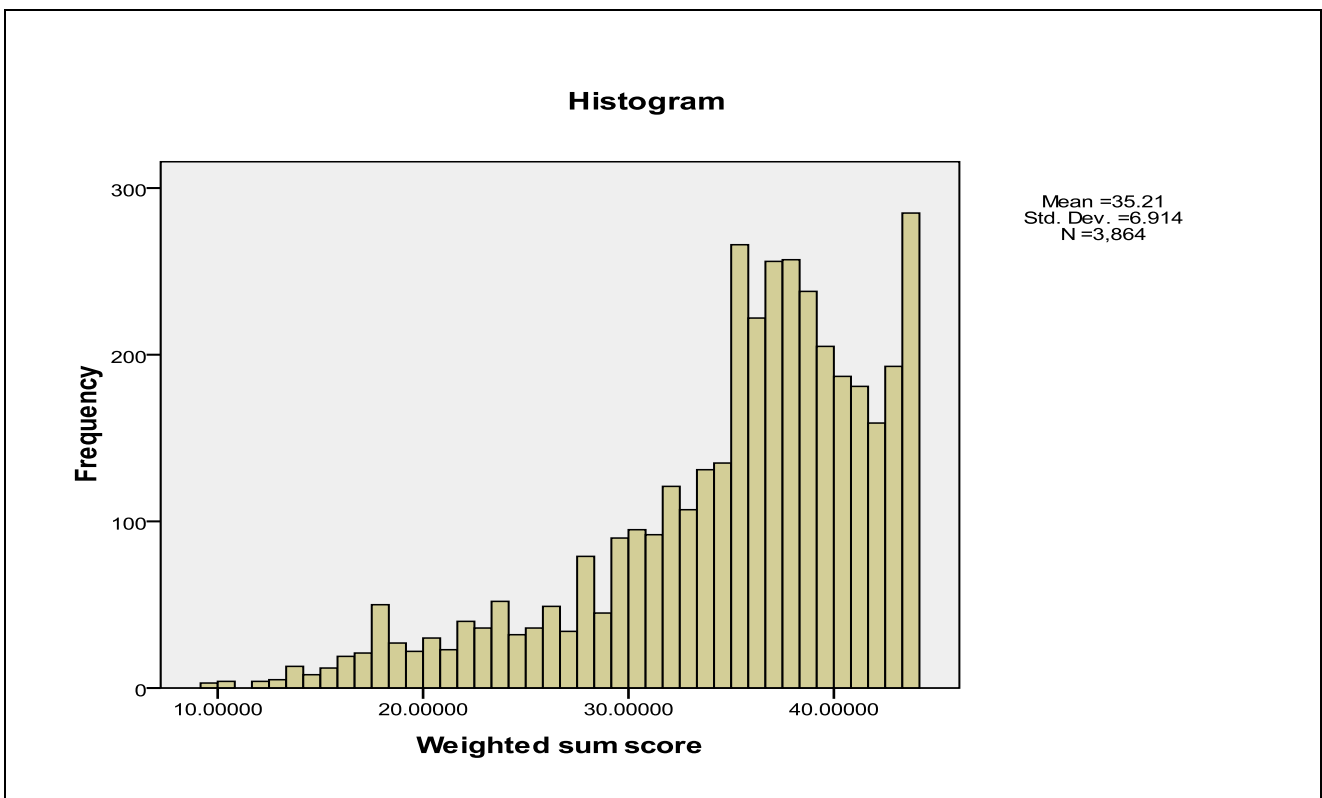
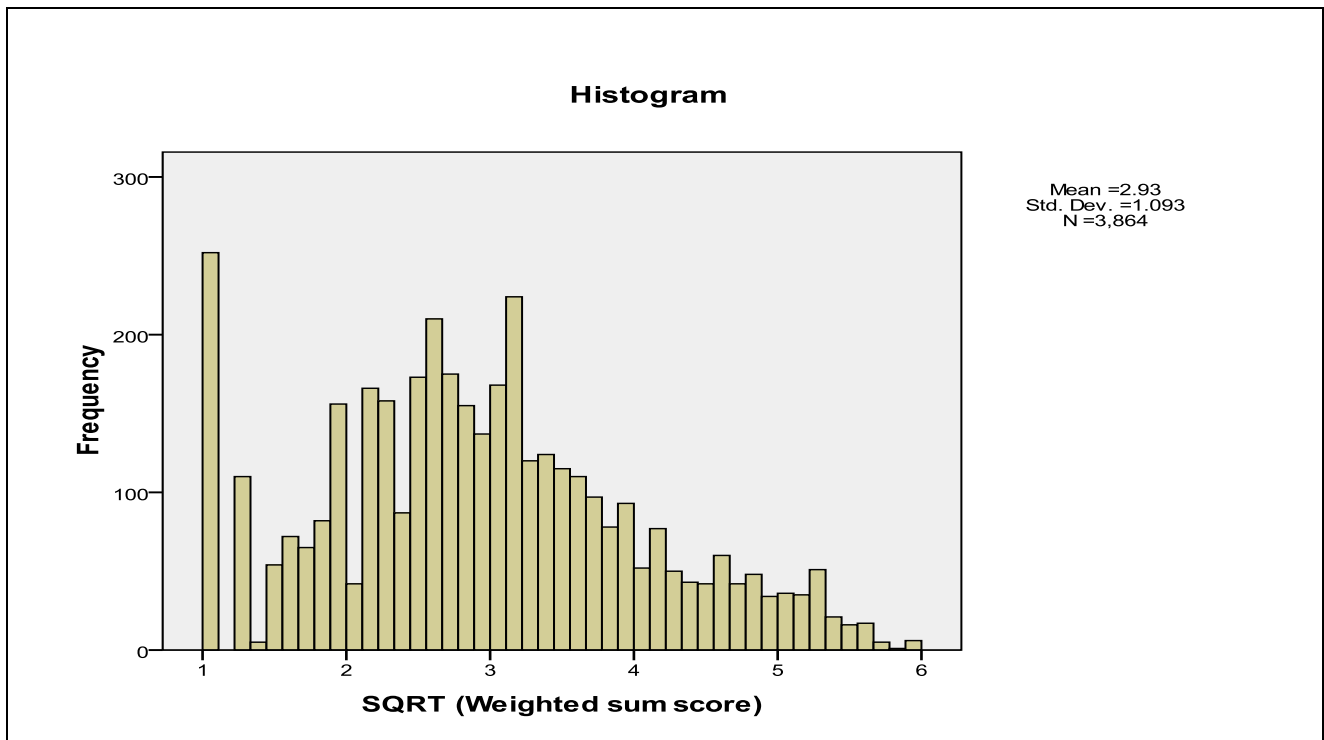**Figure 5.2** Histogram of the SET data factor scores

Since our calculated factor will be analysed using the $\left(\overline{X}, R\right)$ charting scheme, we need to ensure that the factor scores have an approximate normal distribution. Figure 5.2 shows the distribution of the factor scores. It can be seen that the distribution is skewed to the left. Thus we need to improve it to approximate normality. To do this, we employed the square root transformation, which is given by
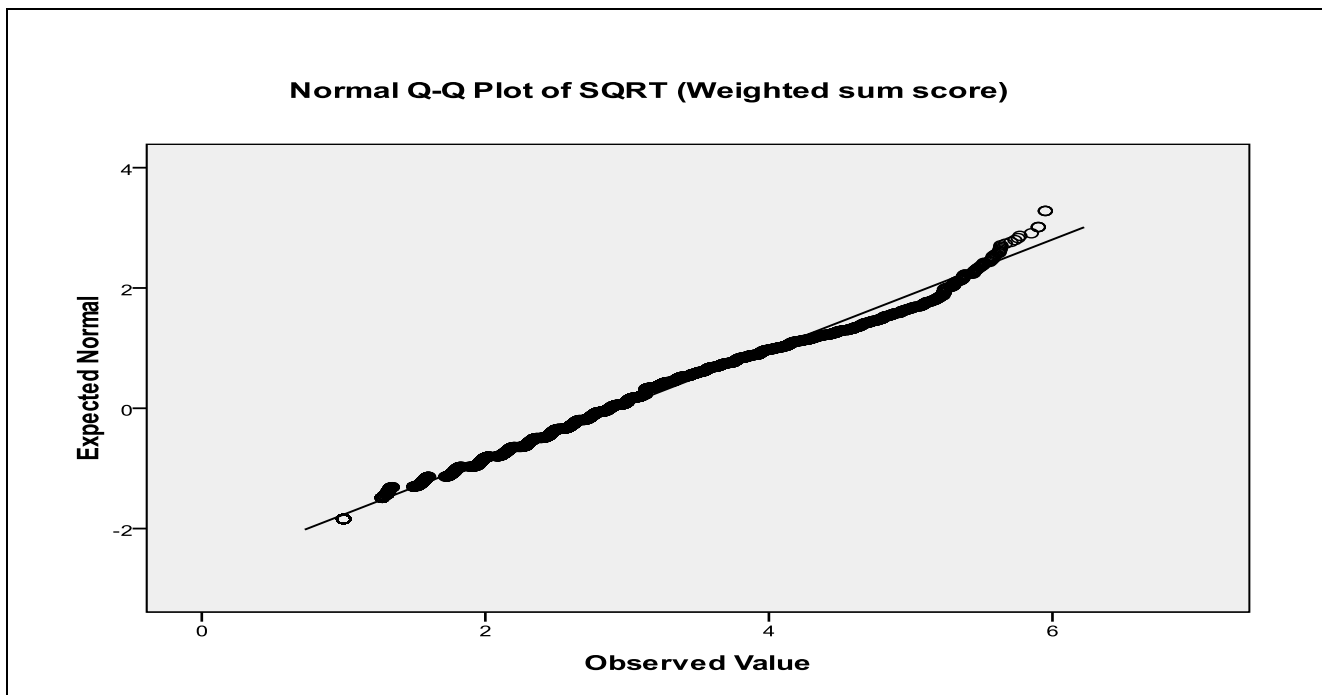
$$\sqrt{K - \text{factor score}}$$

95

where *K* is the maximum value of the weighted factor scores plus 1.

Note that "*K – factor score*" reverses the scale of the factor scores from positive to negative. This has important implications on interpretation, a small value of $\sqrt{K - factor\ score}$ actually means that the person has scored highly on the untransformed factor score. In other words, the student is more satisfied with the classroom performance of the lecturer, the lecturer has responded to the needs of the student, the lecturer is doing well and should possibly get rewarded.

Figure 5.3 Histogram of transformed factor scores of the SET data

Figure 5.4 The QQ-plot of the transformed factor scores of the SET data

Figure 5.3 shows the distribution of the transformed factor scores and Figure 5.4 is their corresponding QQ-plot. It can be seen from both these figures that the transformed factor scores are reasonably normal. Thus, the assumption of normality, which is the main condition required to apply the $\left(\overline{X}, R\right)$ charting scheme, has been reasonably met. Next, we subject the transformed factor scores with Phase I analysis techniques to remove outliers and get a clean set of IC data to estimate the process parameters.

5.3.3 Phase I analysis

The goal of conducting this analysis is to establish the level at which the process is currently performing. Once this level is found and the process is deemed IC, the resulting data can be used to estimate the unknown parameters of the process and estimate the Phase II control limits for lecturer evaluation.

Unfortunately, control charts for joint monitoring in Phase I are absent from the literature so far. Thus we will have to use the currently available charts. For the R chart, we use the control limits and charting constants given in Human et al. (2010) whereas, for the $\overline{\overline{X}}$ chart, we use those given in Champ and Jones (2004). We do this because although their tables do not take into account the joint charting problem (which we discussed in Chapters 2 and 3), these are based on the FAP. Human et al. (2010) defined the control limits for the R chart as

97

$$L\hat{C}L = D_3 \overline{R}$$
$$L\hat{C}L = \overline{R}$$
$$U\hat{C}L = D_4 \overline{R}$$

and provided the tables for D_3 and D_4 values for $FAP = 0.01, 0.05$; $m = 3(1)10, 15, 20, 25, 30, 50$ and $n = 3(1)10$. Champ and Jones (2004) defined the $\overline{X}$ chart limits as

$$L\hat{C}L = \overline{\overline{X}} - k\frac{\overline{R}}{d_2\sqrt{n}}$$
$$\hat{C}L = \overline{\overline{X}}$$
$$U\hat{C}L = \overline{\overline{X}} + k\frac{\overline{R}}{d_2\sqrt{n}}$$

and showed that when $m > 20$, the charting constant k can be found by

$$k = \frac{l}{c}\sqrt{\frac{m-1}{m}}$$

where l is the $1 - \left[1 - (1 - FAP)^{1/m}\right]/2$ quantile of the univariate t-distribution with v degrees of freedom and c is a constant multiplier for the chi-squared approximation of the sampling distribution of $\overline{R}/d_2$.

98
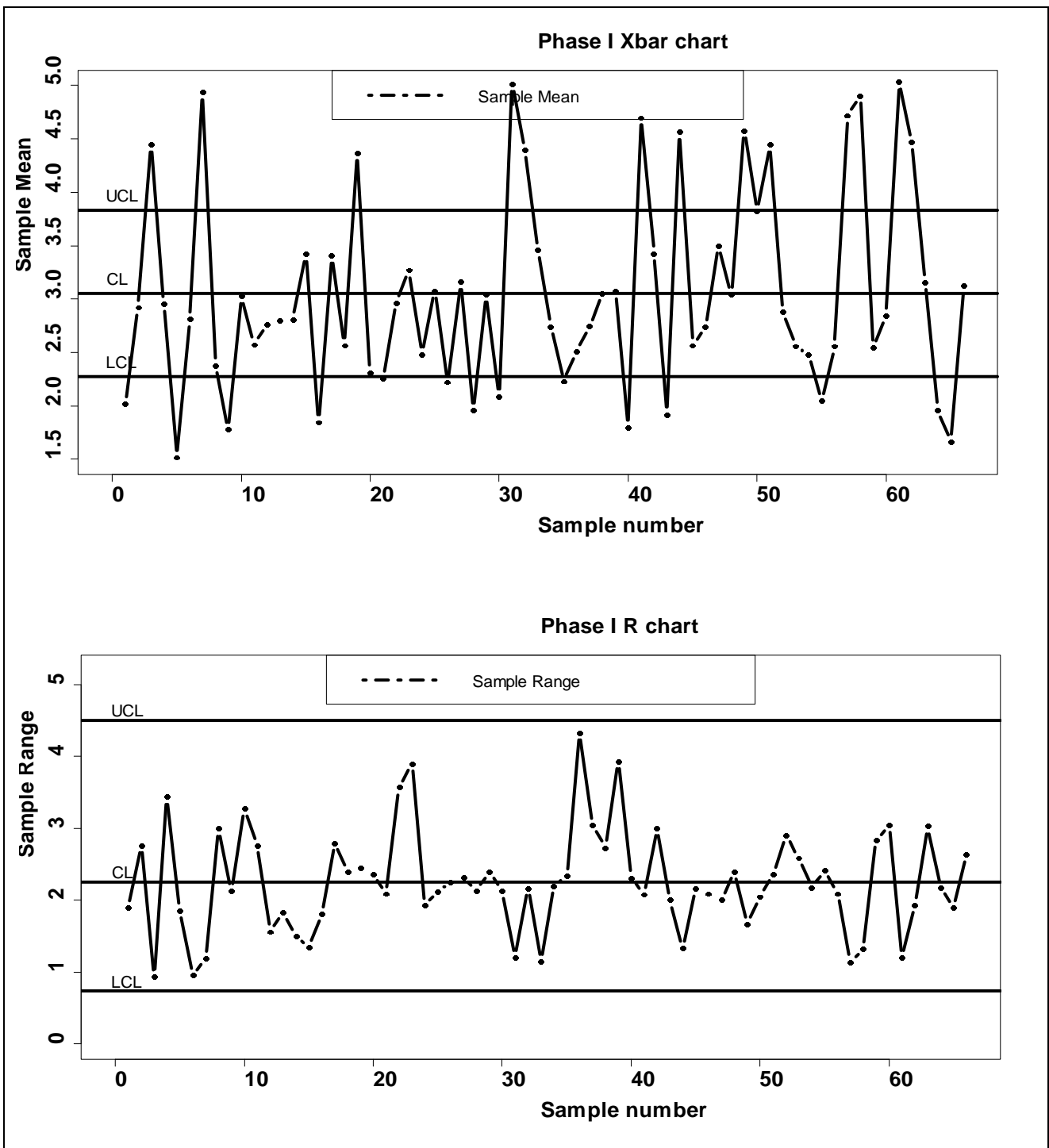
Figure 5.5 Phase I $\left(\overline{X}, R\right)$ scheme of the SET data for $m = 66$, $n = 10$ and a nominal *FAP* = 0.05

An initial Phase I analysis was conducted on the transformed factor scores using 66 lecturers (subgroups). For each lecturer, ten observations were taken and used to calculate the sample range and sample mean. The sample ranges and sample means were used to calculate the mean range and the grand mean as $\overline{R} = 2.25816$ and $\overline{\overline{X}} = 3.05185$, respectively. Figure 5.5 shows the initial results for a nominal *FAP* = 0.05, $m = 66$ and $n = 10$. The associated constants and control limits values are given in Table 5.4. Note that the table provided by Human et al. (2010) was not created for

99

subgroup numbers greater than 50, so we used $m = 50$ to get approximate values of D_3 and D_4. Note, this confirms the concern raised in Wardell and Candia (1996) that common tables of charting constants available in literature do not accommodate for large subgroup numbers and subgroup sizes.

Table 5.4 Constants and control limits of the Phase I $(\overline{X}, R)$ charting scheme for a nominal *FAP* = 0.05 and $n = 10$

|	*R* chart				$\overline{X}$ chart					
	D3	D4	LCL	UCL	v	l	c	k	LCL	UCL
m = 66	0.325	1.995	0.7339	4.50503	492.2209	3.38202	1.00051	3.35461	2.27346	3.83024
m = 39	0.348	1.932	0.88014	4.88632	290.9596	3.24436	1.00086	3.19975	2.07972	3.74284
m = 38	0.348	1.932	0.88454	4.91074	283.5055	3.23752	1.00088	3.19182	2.05363	3.72091

The 66 sample ranges and sample means were plotted simultaneously on the $(\overline{X}, R)$ chart in Figure 5.5. About 27 samples plotted outside the control limits of the $\overline{X}$ chart, meaning that the process was not stable yet. All the subgroups outside the control limits were discarded and the remaining m = 39 samples were used to estimate $\overline{R}$ and $\overline{\overline{X}}$; then the charting process was done again.
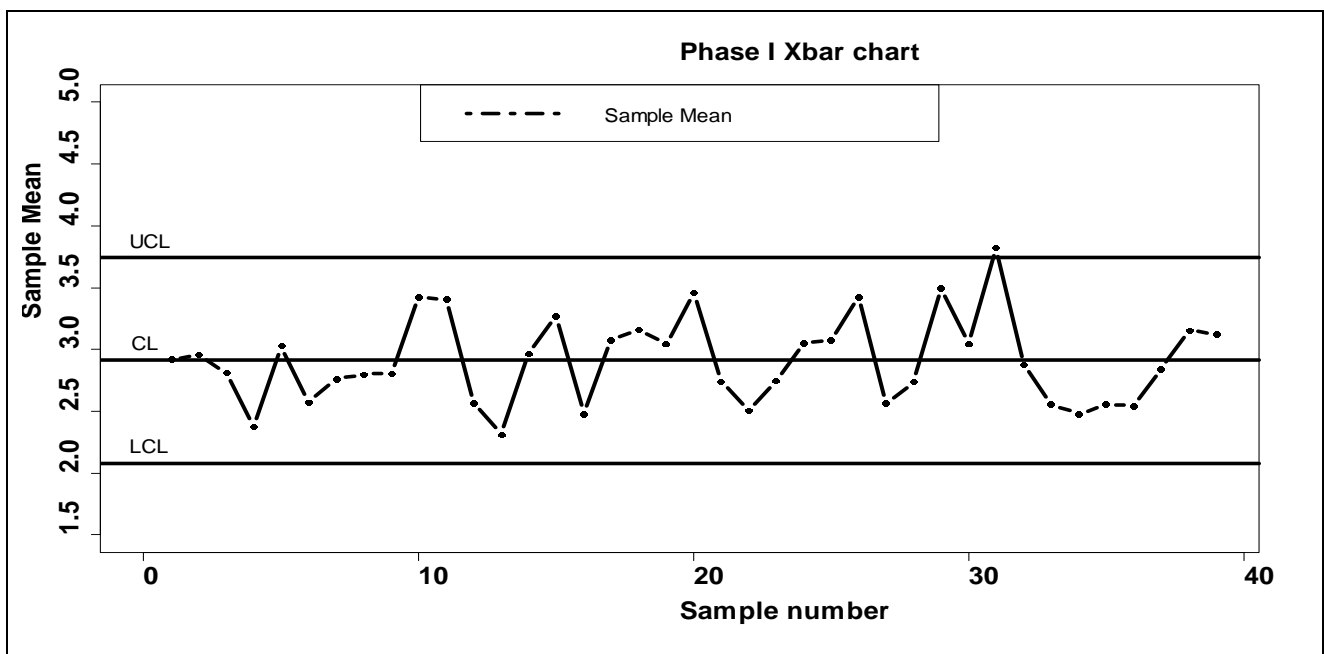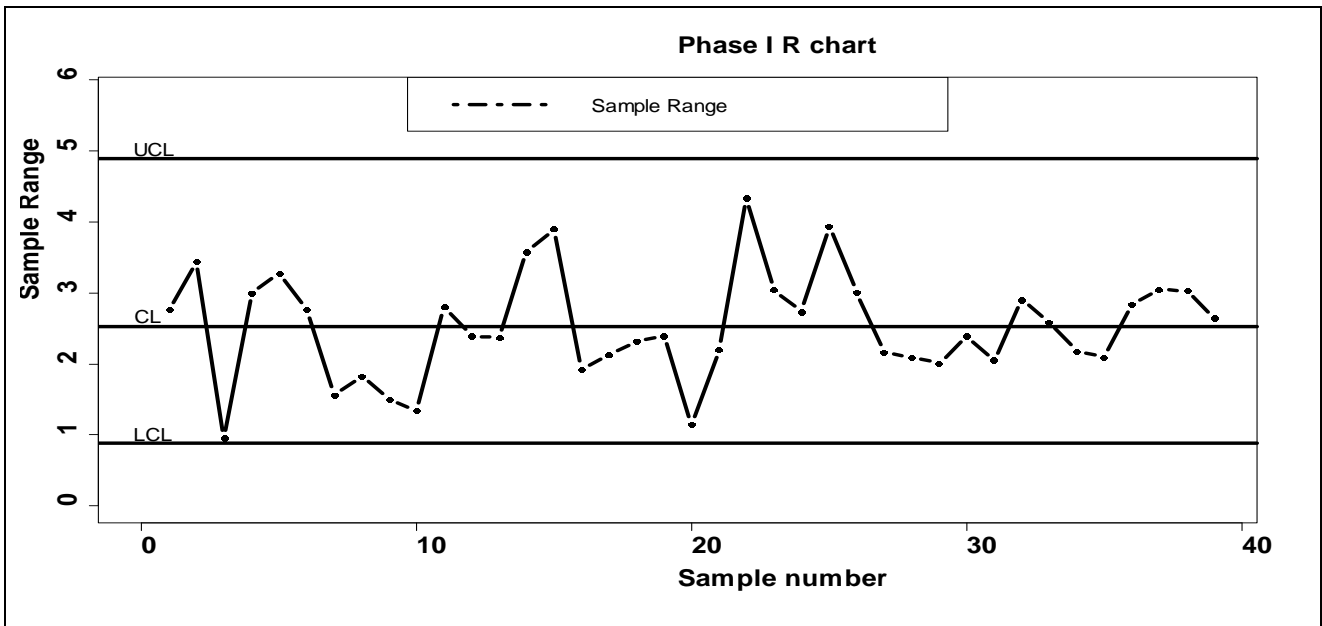
Figure 5.6 Phase I $\left(\overline{X}, R\right)$ scheme of the SET data for $m = 39$, $n = 10$ and a nominal *FAP* = 0.05

Figure 5.6 shows the Phase I $\left(\overline{X}, R\right)$ scheme reconstructed for a nominal *FAP* = 0.05, $m = 39$ and n = 10 with $\overline{R} = 2.52915$ and $\overline{\overline{X}} = 2.91128$. The R chart was constructed using the approximate charting constants D_3 and D_4 that correspond to $m = 30$ (see Table 5.4). Only 1 sample was OOC, as shown by the $\overline{X}$ chart in Figure 5.6. The OOC sample was discarded and the charting procedure was repeated using the remaining $m = 38$ subgroups.
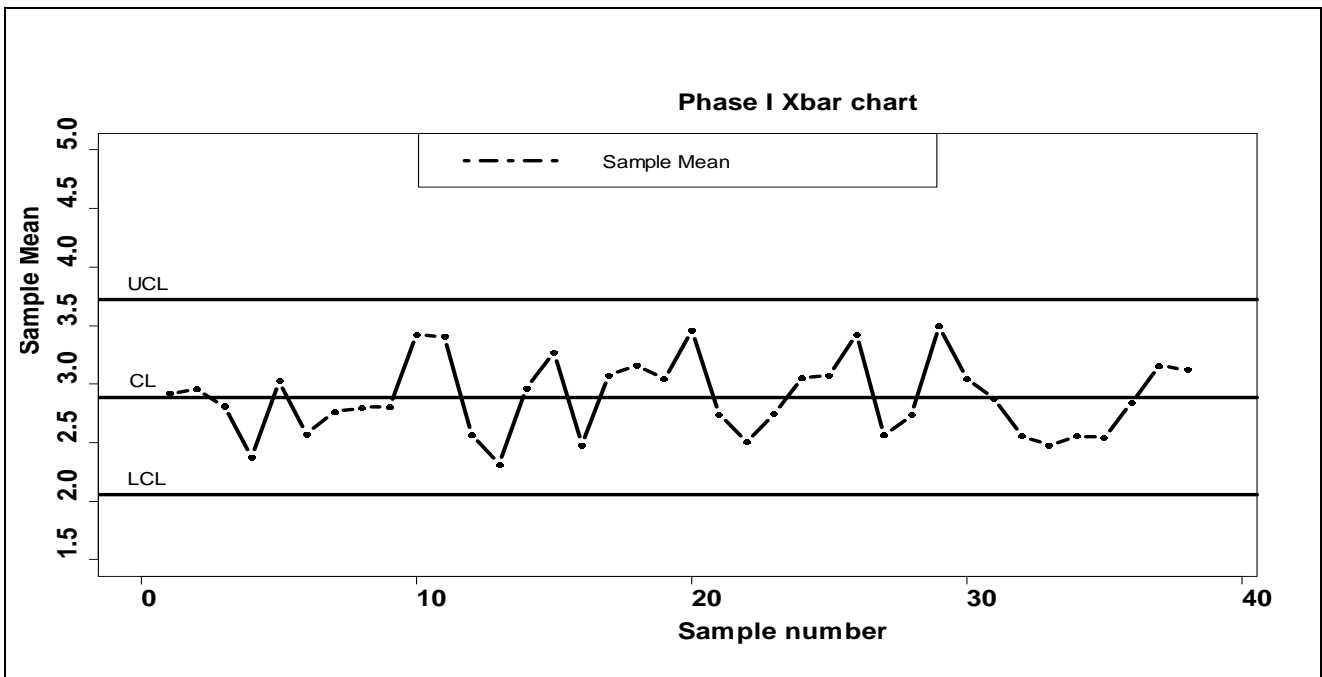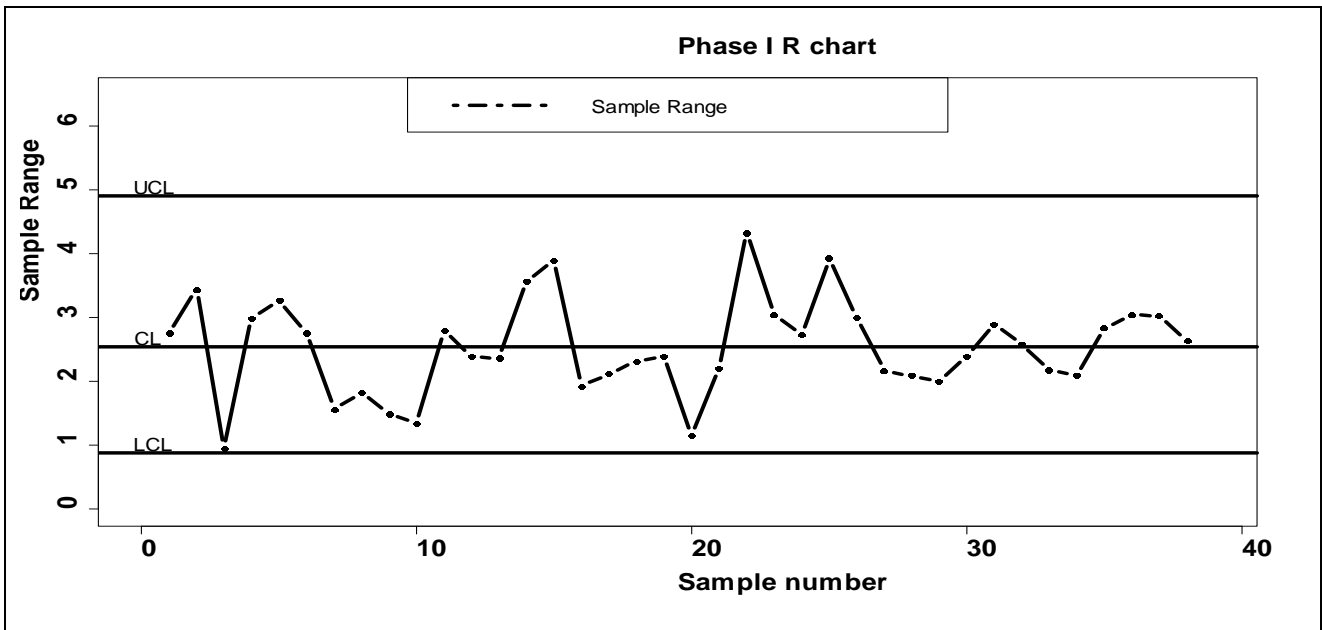
Figure 5.7 Phase I $(\overline{X}, R)$ scheme of the SET data for $m = 38$, $n = 10$ and a nominal $FAP = 0.05$

Figure 5.7 shows the Phase I $(\overline{X}, R)$ scheme reconstructed for the third time for a nominal $FAP = 0.05$, $m = 38$ and $n = 10$ with $\overline{R} = 2.54179$ and $\overline{\overline{X}} = 2.88727$. The associated charting constants and control limits are given in Table 5.4. It can be seen in Figure 5.7 that all the charting statistics plot between the most recent control limits, leading to a decision that the process is IC. This means that the level at which the faculty lecturers are currently performing has been found and the estimates $\overline{R} = 2.54179$ and $\overline{\overline{X}} = 2.88727$ can be used to construct the Phase II $(\overline{X}, R)$ charting scheme for evaluating future performance of the lecturers of the faculty.

5.4 Phase II analysis

For an IC $ARL = 370$, $m = 38$, $n = 10$, $\overline{R} = 2.54179$ and $\overline{\overline{X}} = 2.88727$; the charting constants for the Phase II $(\overline{X}, R)$ are not available in Table 3.2. Using the R programmes given in Appendix 5, the constants were found to be $k = 3.22929$ for the $\overline{X}$ chart, $D_3 = 1.02206$ and $D_4 = 6.12738$ for the lower and upper limits of the R chart, respectively. Thus, the control limits of the Phase II $(\overline{X}, R)$ charting scheme were calculated as follows

102

$$UĈL_{xbar} = \overline{\overline{X}} + k \frac{\overline{R}}{d_2 \sqrt{n}} = 2.88727 + 3.22929 \times \frac{2.54179}{3.07751 \times \sqrt{10}} = 3.73070$$

$$LĈL_{xbar} = \overline{\overline{X}} - k \frac{\overline{R}}{d_2 \sqrt{n}} = 2.88727 - 3.22929 \times \frac{2.54179}{3.07751 \times \sqrt{10}} = 2.04384$$

$$UĈL_R = F_W^{-1}(1 - D/2) \frac{\overline{R}}{d_2} = 6.12738 \times \frac{2.54179}{3.07751} = 5.06075$$

$$LĈL_R = F_W^{-1}(D/2) \frac{\overline{R}}{d_2} = 1.02206 \times \frac{2.54179}{3.07751} = 0.84414$$

Future lecturer performance can be evaluated by plotting the lecturer's data on the above $(\overline{X}, R)$ scheme and to illustrate this, a single lecturer was selected. This lecturer has been evaluated continuously by students for 15 consecutive time points. At each time point a sample of 10 students was taken. Factor scores were calculated and transformed (see Section 5.3.2). Sample ranges and sample means for the transformed factor scores were calculated and plotted on the $(\overline{X}, R)$ chart scheme shown in Figure 5.8. The reader should note that our transformed factor scores are on a negative scale. This means that higher values of the transformed factor scale corresponds to low student satisfaction levels or poor lecturer performance, whereas the lower values correspond to high student satisfaction levels or good lecturer performance.

103
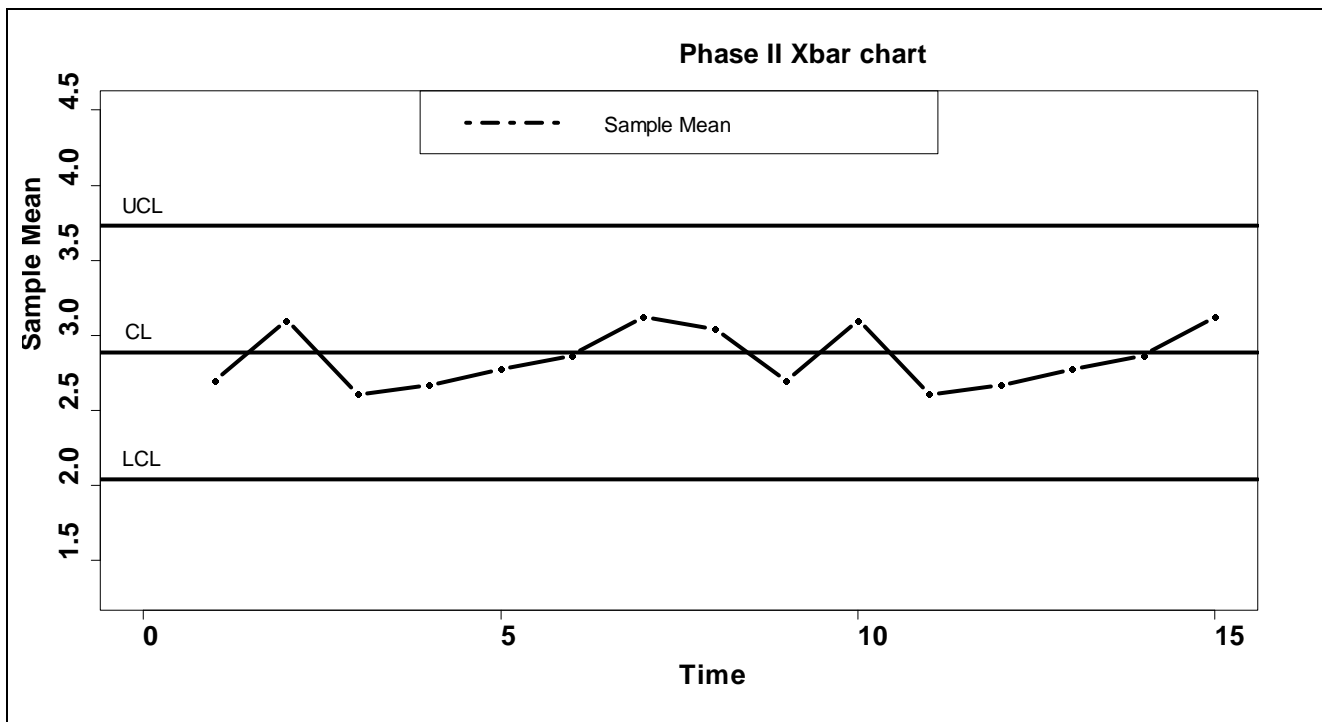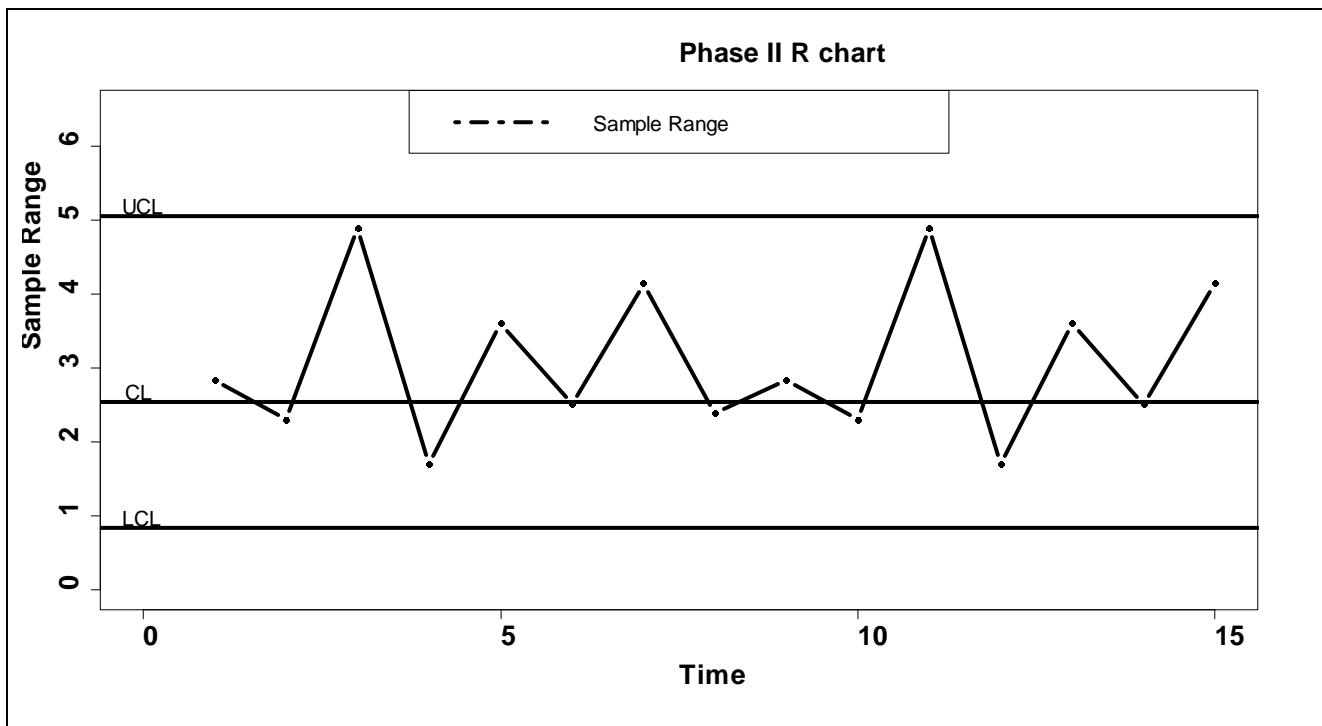
Figure 5.8 The Phase II $\left(\overline{X}, R\right)$ scheme of the SET data evaluated for a specific lecturer

Furthermore, it must be remembered that the *R* chart is plotted and examined first; any point outside the control limits is checked for assignable causes and rejected if one is found. The $\overline{X}$ chart is examined only when the variability of the data is under control. In Figure 5.8, the *R* chart showed no signal at all the time points. The points on the $\overline{X}$ chart are also within the control limits. This means that the lecture's data is consistent with common causes of variation in the system, thus the differences seen in Figure 5.8 between plotted values are not meaningful. They are not due to some special cause or causes. The lecturer is performing within process specifications. Note that without a control chart it would be difficult to tell this. For example, a typical administrator would think that the lectures performance at the first time point on the $\overline{X}$ chart was above average and consequently reward this lecturer, which would be ill-advised and misguided. According to Maguad (2007), a lecturer whose data fall within the control limits of the $\overline{X}$ chart should not be ranked or compared with other faculty lecturers whose data also fall within the same control limits. Their differences arise almost entirely from the actions of the system and are not due to individual performance differences. However lecturers whose data point plots below the *LCL* (which would be above the *UCL* in our $\overline{X}$ chart in Figure 5.8) require individualised help. For example, they could be sent for a training course or a counselling session to help restore their confidence (Maguad (2007)). For others, it may be an offer to move to a more suitable position within the organisation. Faculty members whose data point plots above the *UCL* (below the *LCL* in our $\overline{X}$ chart in Figure 5.8)

104

deserve recognition. They could be models and mentors for other faculty members and consequently, help raise the process average for continual improvement (Maguad (2007)).

5.5   Summary and conclusion

In this chapter, factor analysis was used to reduce 12 ordinal scaled SET items to a single interval scaled factor. Then, factor scores were calculated and their normality improved by the square root transformation. The transformed normal factor scores were subjected to Phase I and Phase II analyses using the $(\overline{X}, R)$ charting scheme. For the Phase II analysis, we used the new charting constants we developed in Chapter 3 to account for the effects of multiplicity, 3-sigma limits and parameter estimation. We strongly believe that the method we have outlined above, which involves condensing the data, forcing normality on the data and using the charting constants in Chapter 3 should lessen the *FAR* inflation. However, as can be seen in Section 5.4, our chart is not that easy to interpret. Research still needs to be done to sort out the joint charting issue in Phase I.

105

5.6 Appendix 5: R Code

Code for Figure 5.5

```
y=c(1.89240,2.76205,0.93294,3.44207,1.85517,0.95097,1.19174,2.99700,2.13081,3.27504,2.76165
,1.56524,1.82951,1.49734,1.34360,1.80844,2.79736,2.39696,2.44960,2.36541,2.08998,3.57165,
3.89780,1.92775,2.12398,2.25013,2.31659,2.13081,2.39677,2.13081,1.20262,2.17088,1.14797,
2.20366,2.33437,4.33057,3.04157,2.73395,3.93295,2.31104,2.08004,3.00230,1.99933,1.33117,
2.16363,2.09515,2.00692,2.39677,1.66716,2.04886,2.36236,2.90260,2.58664,2.17816,2.41541,
2.09419,1.14004,1.32121,2.83810,3.04438,1.20144,1.93044,3.03009,2.17695,1.89413,2.63968)
x=1:66
plot(x,y,type = 'b', lwd=4, pch = 16, axes = TRUE, xlim = c(0,66), ylim = c(0,5.2),
cex.axis=1.7,cex.lab=1.7,cex.main=1.7,main="Phase I R chart",xlab="Sample
number",ylab="Sample Range",font.lab=2, font.axis=2)
abline(h = c(0.73390, 2.25816, 4.50503), lty = 1, lwd=4)
text(-0.3,0.88,'LCL',cex=1.3)
text(-0.25,2.40, 'CL',cex=1.3)
text(-0.3,4.65,'UCL',cex=1.3)
legend('top',legend=c("Sample Range"),lty=c(4),lwd=4,cex=1.3)


y=c(2.01853,2.91920,4.45021,2.95736,1.51506,2.81029,4.93736,2.37804,1.77614,3.02742,
2.57546,2.75977,2.79944,2.80652,3.42199,1.84617,3.40668,2.56580,4.36928,2.31233,2.25909,
2.96867,3.26754,2.47950,3.07547,2.22639,3.16200,1.95783,3.04362,2.08667,5.01360,4.39698,
3.45749,2.74148,2.23044,2.50751,2.74355,3.05065,3.07448,1.79586,4.69931,3.42567,1.91733,
4.56313,2.56539,2.73652,3.49720,3.04362,4.57635,3.82346,4.44667,2.87577,2.55697,2.47826,
2.04839,2.55445,4.71983,4.90245,2.54594,2.84231,5.03199,4.47194,3.15656,1.96238,1.66278,
3.12534)
x=1:66
plot(x,y,type = 'b', lwd=4, pch = 16, axes = TRUE, xlim = c(0,66), ylim = c(1.50,5.00),
cex.axis=1.7,cex.lab=1.7,cex.main=1.7,main="Phase I Xbar chart",xlab="Sample
number",ylab="Sample Mean",font.lab=2, font.axis=2)
abline(h = c(2.27346, 3.05185, 3.83024), lty = 1, lwd=4)
text(-0.5,2.42,'LCL',cex=1.3)
text(-0.45,3.20, 'CL',cex=1.3)
text(-0.5,3.98,'UCL',cex=1.3)
legend('top',legend=c("Sample Mean"),lty=c(4),lwd=4,cex=1.3)
```

Code for Table 5.3 :   Calculation of c, v and l

```
n=10
m=38
d2=function(n){
pt=function(w){1-ptukey(w,n,Inf)}
integrate(pt,lower=0,upper=Inf)[[1]]}
d2=d2(n)
EW2=function(n){
ptt=function(a){(1-ptukey(sqrt(a),n,Inf))}
integrate(ptt,lower=0,upper=Inf)[[1]]}
d3=function(n){
sqrt(EW2(n)-d2^2)}
d3=d3(n)
M=function(m){
d3^2/(m*d2^2)}
r=function(m){
(-2+2*sqrt(1+2*M(m)))^-1}
t=function(m){
M(m)+1/(16*r(m)^3)}
v=function(m){
(-2+2*sqrt(1+2*t(m)))^-1}
cc=function(m){
1+(1/(4*v(m)))+(1/(32*v(m)^2))-(5/(128*v(m)^3))}
v(m)
cc(m)
l=qt(1-(1-(1-0.05)^(1/m))/2,v(m))
(l/cc(m))*(sqrt((m-1)/m))
l
```

Code for Figure 5.6

```
y=c(2.76205,3.44207,0.95097,2.99700,3.27504,2.76165,1.56524,1.82951,1.49734,1.34360,
2.79736,2.39696,2.36541,3.57165,3.89780,1.92775,2.12398,2.31659,2.39677,1.14797,2.20366,
4.33057,3.04157,2.73395,3.93295,3.00230,2.16363,2.09515,2.00692,2.39677,2.04886,2.90260,
2.58664,2.17816,2.09419,2.83810,3.04438,3.03009,2.63968)
x=1:39
plot(x,y,type = 'b', lwd=4, pch = 16, axes = TRUE, xlim = c(0,39), ylim = c(0,5.8),
cex.axis=1.7,cex.lab=1.7,cex.main=1.7,main="Phase I R chart",xlab="Sample
number",ylab="Sample Range",font.lab=2, font.axis=2)
abline(h = c(0.88014, 2.52915, 4.88632), lty = 1, lwd=4)
text(-0.3,1.03,'LCL',cex=1.3)
text(-0.25,2.68, 'CL',cex=1.3)
text(-0.3,5.03,'UCL',cex=1.3)
legend('top',legend=c("Sample Range"),lty=c(4),lwd=4,cex=1.3)


y=c(2.91920,2.95736,2.81029,2.37804,3.02742,2.57546,2.75977,2.79944,2.80652,3.42199,
3.40668,2.56580,2.31233,2.96867,3.26754,2.47950,3.07547,3.16200,3.04362,3.45749,2.74148,
2.50751,2.74355,3.05065,3.07448,3.42567,2.56539,2.73652,3.49720,3.04362,3.82346,2.87577,
2.55697,2.47826,2.55445,2.54594,2.84231,3.15656,3.12534)
x=1:39
plot(x,y,type = 'b', lwd=4, pch = 16, axes = TRUE, xlim = c(0,39), ylim = c(1.50,5.00),
cex.axis=1.7,cex.lab=1.7,cex.main=1.7,main="Phase I Xbar chart",xlab="Sample
number",ylab="Sample Mean",font.lab=2, font.axis=2)
abline(h = c(2.07972, 2.91128, 3.74284), lty = 1, lwd=4)
text(-0.5,2.23,'LCL',cex=1.3)
text(-0.45,3.06, 'CL',cex=1.3)
text(-0.5,3.89,'UCL',cex=1.3)
legend('top',legend=c("Sample Mean"),lty=c(4),lwd=4,cex=1.3)
```

108

Code for Figure 5.7

```
y=c(2.76205,3.44207,0.95097,2.99700,3.27504,2.76165,1.56524,1.82951,1.49734,1.34360,
2.79736,2.39696,2.36541,3.57165,3.89780,1.92775,2.12398,2.31659,2.39677,1.14797,
2.20366,4.33057,3.04157,2.73395,3.93295,3.00230,2.16363,2.09515,2.00692,2.39677,
2.90260,2.58664,2.17816,2.09419,2.83810,3.04438,
3.03009,2.63968)
x=1:38
plot(x,y,type = 'b', lwd=4, pch = 16, axes = TRUE, xlim = c(0,39), ylim = c(0,6.5),
cex.axis=1.7,cex.lab=1.7,cex.main=1.7,main="Phase I R chart",xlab="Sample
number",ylab="Sample Range",font.lab=2, font.axis=2)
abline(h = c(0.88454, 2.54179, 4.91074), lty = 1, lwd=4)
text(-0.3,1.03,'LCL',cex=1.3)
text(-0.25,2.69, 'CL',cex=1.3)
text(-0.3,5.06,'UCL',cex=1.3)
legend('top',legend=c("Sample Range"),lty=c(4),lwd=4,cex=1.3)


y=c(2.91920,2.95736,2.81029,2.37804,3.02742,2.57546,2.75977,2.79944,2.80652,3.42199,
3.40668,2.56580,2.31233,2.96867,3.26754,2.47950,3.07547,3.16200,3.04362,3.45749,
2.74148,2.50751,2.74355,3.05065,3.07448,3.42567,2.56539,2.73652,3.49720,3.04362,
2.87577,2.55697,2.47826,2.55445,2.54594,2.84231,3.15656,3.12534)
x=1:38
plot(x,y,type = 'b', lwd=4, pch = 16, axes = TRUE, xlim = c(0,39), ylim = c(1.50,5.00),
cex.axis=1.7,cex.lab=1.7,cex.main=1.7,main="Phase I Xbar chart",xlab="Sample
number",ylab="Sample Mean",font.lab=2, font.axis=2)
abline(h = c(2.05363, 2.88727, 3.72091), lty = 1, lwd=4)
text(-0.5,2.20,'LCL',cex=1.3)
text(-0.45,3.04, 'CL',cex=1.3)
text(-0.5,3.87,'UCL',cex=1.3)
legend('top',legend=c("Sample Mean"),lty=c(4),lwd=4,cex=1.3)
```

Code for Figure 5.8

```
y=c(2.84461,2.30022,4.90008,1.70379,3.60782,2.51310,4.14968,2.39677,2.84461,2.30022,
4.90008,1.70379,3.60782,2.51310,4.14968)
x=1:15
plot(x,y,type = 'b', lwd=4, pch = 16, axes = TRUE, xlim = c(0,15), ylim = c(0,6.5),
cex.axis=1.7,cex.lab=1.7,cex.main=1.7,main="Phase II R chart",xlab="Time",ylab="Sample
Range",font.lab=2, font.axis=2)
abline(h = c(0.84414, 2.54179, 5.06075), lty = 1, lwd=4)
text(-0.3,0.99,'LCL',cex=1.3)
text(-0.25,2.70, 'CL',cex=1.3)
text(-0.3,5.21,'UCL',cex=1.3)
legend('top',legend=c("Sample Range"),lty=c(4),lwd=4,cex=1.3)


y=c(2.69522,3.10191,2.60799,2.66396,2.77041,2.86722,3.12495,3.04362,
2.69522,3.10191,2.60799,2.66396,2.77041,2.86722,3.12495)
x=1:15
plot(x,y,type = 'b', lwd=4, pch = 16, axes = TRUE, xlim = c(0,15), ylim = c(1.30,4.50),
cex.axis=1.7,cex.lab=1.7,cex.main=1.7,main="Phase II Xbar chart",xlab="Time",ylab="Sample
Mean",font.lab=2, font.axis=2)
abline(h = c(2.04384, 2.88727, 3.73070), lty = 1, lwd=4)
text(-0.3,2.19,'LCL',cex=1.3)
text(-0.25,3.04, 'CL',cex=1.3)
text(-0.3,3.88,'UCL',cex=1.3)
legend('top',legend=c("Sample Mean"),lty=c(4),lwd=4,cex=1.3)
```

110

R code for the Phase II charting constants that were used in to construct Figure 5.8

```r
n=10
m=38
aa=seq(from=0.001241,to=0.001244,length.out=3)
d2=function(n){
pt=function(w){1-ptukey(w,n,Inf)}
integrate(pt,lower=0,upper=Inf)[[1]]}
d2=d2(n)
EW2=function(n){
ptt=function(a){(1-ptukey(sqrt(a),n,Inf))}
integrate(ptt,lower=0,upper=Inf)[[1]]}
d3=function(n){
sqrt(EW2(n)-d2^2)}
d3=d3(n)


library(cubature)
ICARL=function(m,a){
M=function(m){
d3^2/(m*d2^2)}
r=function(m){
(-2+2*sqrt(1+2*M(m)))^-1}
t=function(m){
M(m)+1/(16*r(m)^3)}
v=function(m){
(-2+2*sqrt(1+2*t(m)))^-1}
cc=function(m){
1+(1/(4*v(m)))+(1/(32*v(m)^2))-(5/(128*v(m)^3))}
uclxbar=function(x){x[1]/sqrt(m)+qnorm(1-a/2,0,1)*cc(m)*sqrt(x[2])/sqrt(v(m))}
lclxbar=function(x){x[1]/sqrt(m)-qnorm(1-a/2,0,1)*cc(m)*sqrt(x[2])/sqrt(v(m))}
PNSxbar=function(x){pnorm(uclxbar(x),0,1)-pnorm(lclxbar(x),0,1)}
uclrchart=function(x){qtukey(1-a/2,n,Inf)*cc(m)*sqrt(x[2])/sqrt(v(m))}
lclrchart=function(x){qtukey(a/2,n,Inf)*cc(m)*sqrt(x[2])/sqrt(v(m))}
PNSrchart=function(x){ptukey(uclrchart(x),n,Inf)-ptukey(lclrchart(x),n,Inf)}
AFAR=function(x){1-PNSxbar(x)*PNSrchart(x)}
CFAR=function(x){ AFAR(x)^-1*dnorm(x[1],0,1)*dchisq(x[2],v(m))}
b=qchisq(0.99999,v(m))
adaptIntegrate(CFAR,c(-100,0),c(100,b),tol=1e-10)[[1]]}



ICARLxbar_rchart=numeric(length(aa))
Const=matrix(nrow=length(aa),ncol=3)
for (j in 1:length(aa)){
Const[j,]=c(qnorm(1-aa[j]/2),qtukey(aa[j]/2,n,Inf),qtukey(1-aa[j]/2,n,Inf))
ICARLxbar_rchart[j]=ICARL(m,aa[j])}
ICARL370=ICARLxbar_rchart-370
Results1=cbind(ICARL370,rep(m,length(aa)),aa,Const)
colnames(Results1)=c("ICARL370","m","p","Xbar","SprL","SprU")
Results1
write.table(Results1, "clipboard",sep="\t",col.names=NA)
```

Chapter 6

Concluding Remarks: Summary and Recommendations for Future Research

In this final section, we give a brief summary of the research conducted in this dissertation and offer concluding remarks concerning unanswered questions and future research opportunities. We also list the research outputs associated with this dissertation.

1.   Summary

Statistical process control (SPC) is a collection of statistical procedures and problem solving tools that are used to control, monitor and improve the quality of the output of a process. In this dissertation, we focused on a variety of aspects related to a powerful statistical tool often used in quality improvement efforts within the realm of SPC, namely, the control chart. More specifically, we focused the joint monitoring of the mean and standard deviation of a normally distributed process using the $(\overline{X}, R)$ charting scheme. We showed that the standard or conventional use of the $(\overline{X}, R)$ scheme is not correct, because it results in inflated false alarm rate (*FAR*). The *FAR* inflation is caused by multiple testing, parameter estimation and the standard use of the 3-sigma limits. Thus, we provided a technique for obtaining the correct control limits, which accounts for the effects of these three issues. We also provided tables of the correct charting constants to aid practitioners in implementing the $(\overline{X}, R)$ charting scheme. Using our new tables of new charting constants together with some data transformation and data reduction techniques, we applied the $(\overline{X}, R)$ charting scheme to student evaluation of teaching (SET) survey data. Our application proved that, contrary to popular belief, SPC charts can be and are used outside the traditional manufacturing domain. Furthermore as a prelude to our case study we reviewed non-standard applications of SPC charts reported in literature from 2000 to 2012. Our review identified six non-standard application domains. These were healthcare, environment, general service sector, statistics, animal production and in personal everyday situations. Further, we pointed out the benefits and problems associated with such applications (i.e. non-standard applications of SPC charts).

112

2.   Recommendations for future research

2.1   Joint monitoring of the mean and standard deviation of a normal process

i. While, a lot of work has been done in monitoring the mean and the standard deviation of a normally distributed process using Shewhart or Shewhart-type charts, few studies have considered the performance of these charts as they are applied in tandem, as a combination of two charts. Multiple charts used in this manner are often called combination charting schemes (or combo schemes). From a practical standpoint, these combo scheme procedures must be made more accessible to practitioners and, to this end, the ease of implementation is vital. Computer programs, add-ons to popular software packages such as Minitab® SAS®, and R® and / or websites would greatly help in this effort.

ii. There is a major shortcoming regarding the application of combo schemes in industry. This could be due to a number of contributing factors, such as the fact that these methods are not well-known, since they are only typically touched on in undergraduate and / or postgraduate courses in most programs. Also, in a search of standard SPC books on the market, very little on combo schemes were found. For example, in the well-known SPC book by Montgomery (2013) the combo scheme is not mentioned at all.

iii. Our work can be extended to other types of two chart joint charting schemes for the mean and variance of the normal distribution in Phase II. For example the $\left(\overline{X},S\right)$, (Median, Range) scheme and the $\left(X,MR\right)$.charting schemes.

iv. As expressed by McCracken and Chakraborti (2013) *"Research in the area of parametric joint monitoring has largely overlooked cases in which processes are known to be non-normal. This is an important area for further research, since few non-normal parametric joint monitoring schemes are currently available in literature."*

v. Only a handful of nonparametric joint monitoring charts are currently available in the literature and they are all one-chart schemes (see McCracken and Chakraborti (2013)). Thus there is a great opportunity to make significant contributions in this area.

113

vi. As mentioned in Section 5.3.3 of Chapter 5, control charts for joint monitoring in Phase I are absent from the literature. The major difficulty in Phase I is designing the scheme so that it has a specified overall *FAP*. Further research is needed to address this difficult issue.

2.2   Non-standard applications of SPC charts

There are a lot of problems that need to be resolved surrounding the non-standard applications of SPC charts. They include

i. The nature of data obtained from non-standard application domains may not be normally distributed. Furthermore auto-correlation and cross-correlation potentially complicates the problem.

ii. Sample sizes may be very large and variable. Recall that common control chart tables in literature were not created for very large samples.

iii. Event frequency may be long, particularly in surveys, and common control charts are not well suited in analyzing infrequent events. Thus, identification of special causes may be more difficult.

iv. Cause and effect relationships may not be obvious.

v. The combined use of mean and variance charts   (i.e. the joint monitoring question) in relation to non-standard applications still needs investigation.

All of these above issues raise important questions for further research.

3.   Research outputs

Next we list the research outputs associated with this dissertation.

3.1   National conferences and departmental seminars (presentations)

i. Diko, M.D., Chakraborti, S. and Graham, M.A. (2013). "New limits for the Xbar-R chart scheme." The 55th annual conference of the South African Statistical Association (SASA), Polokwane, Limpopo Province, 4 – 8 November 2013.

ii. Diko, M.D., Chakraborti, S. and Graham, M.A. (2013). "New limits for the Xbar-R chart scheme." Departmental Seminar, University of Pretoria, Pretoria, South Africa, Nov 2013.

iii. Diko, M.D., Chakraborti, S. and Graham, M.A. (2012). "A review of non-standard applications of Statistical Process Control (SPC) charts." The 54th annual conference of the South African Statistical Association (SASA), Nelson Mandela Metropolitan University (NMMU), Port Elizabeth, 5 – 9 November 2012.

iv. Diko, M.D., Chakraborti, S. and Graham, M.A. (2012). "A review of non-standard applications of Statistical Process Control (SPC) charts." Departmental Seminar, University of Pretoria, Pretoria, South Africa, Nov 2012.

3.2   Papers in progress

i. Diko, M.D., Chakraborti, S. and Graham, M.A. (2014). "Monitoring the process mean: an old problem revisited"

ii. Diko, M.D., Chakraborti, S. and Graham, M.A. (2014). "New control limits for the $\left(\overline{X}, R\right)$ charting scheme in Case U."

The end.

115

References

Alwan, L.C. and Roberts, H.V. (1988). "Time series modelling for statistical process control." *Journal of Business and Economic Statistics*, **6**, 86–95.

Barbosa, E.P., Gneri, A., Meneguetti, A. "Range Control Charts Revisited: Simpler Tippett-like Formulae, It's Practical Implementations and the Study of False Alarm." Technical Report, Department of Statistics, Imecc/UNICAMP, Cidade Universitaria Zeferino Vaz Distrito de Barao Geraldo, Brazil.

Barnard, G.A. (1959). "Control charts and stochastic processes." *Journal of the Royal Statistical Society*, B, **21** (2), 239-271.

Bateman, P., Ho, A.T.S. and Woodward, A. (2009). "Camera identification using statistical process control techniques for anomaly detection." *7th International Conference on Information, Communications, and Signal Processing, ICICS*, Macau.

Bateman, P., Ho, A.T.S. and Woodward, A. (2010). "Accurate detection of out-of-control variations from digital camera devices." 978-1-4244-5309-2, *IEEE*, 3056-3059.

Baum, D.H., Ward, S., Baum, C.L, Lee, N., Polson, D.D., Harris, D.L. and Nielsen, B. (2005). "Statistical process control methods used to evaluate the serologic responses of pigs infected with three Salmonella serovars." *Journal of Swine Health and Production*, **13** (6), 304–313.

Bersimis, S., Psarakis, S. and Panaretos, J. (2007). "Multivariate statistical control charts: An overview." *Quality and Reliability Engineering International*, **23** (5), 517-543.

Borror, C.M., Montgomery, D.C. and Runger, G.C. (1999). "Robustness of the EWMA control chart to non-normality." *Journal of Quality Technology*, **31** (3), 309-316.

Cadden, D., Driscoll, V. and Thompson, M. (2008). "Improving teaching effectiveness through the application of SPC methodology." *College Teaching Methods & Styles Journal*, **4** (11), 33-46.

Canel, C., Mahar, S., Rosen, D. and Taylor, J. (2010). "Quality control methods at a hospital." *International Journal of Health Care Quality Assurance*, **23** (1), 59 – 71.

116

Cassady, C., Bowden, R., Liew, L. and Pohl, E.A. (2000) "Combining preventive maintenance and statistical process control: a preliminary investigation." *IIE Transactions*, **32** (6), 471–478.

Chakraborti, S. (2000). "Run length, average run length and false alarm rate of Shewhart $\overline{X}$ chart: exact derivations by conditioning." *Communications in Statistics: Simulation and Computation*, **29** (1), 61-81.

Chakraborti, S. (2006). "Parameter estimation and design considerations in prospective applications of the $\overline{X}$ chart." *Journal of Applied Statistics*, **33** (4), 439-459.

Chakraborti, S. and Graham, M.A. (2007). "Nonparametric control charts." *Encyclopedia of Statistics in Quality and Reliability*, **1**, 415 – 429, John Wiley, New York.

Chakraborti, S., Human, S.W. and Graham, M.A. (2009). "Phase I statistical process control charts: An overview and some results." *Quality Engineering*, **21** (1), 52-62.

Chakraborti, S., Human, S.W. and Graham, M.A. (2011). "Nonparametric (distribution-free) quality control charts." In *Handbook of Methods and Applications of Statistics: Engineering, Quality Control, and Physical Sciences*. N. Balakrishnan, Ed., 298-329, John Wiley & Sons, New York.

Chakraborti, S., Van der Laan, P. and Bakir, S.T. (2001). "Nonparametric control charts: An overview and some results." *Journal of Quality Technology*, **33** (3), 304-315.

Champ, C.W. and Jones, L.A. (2004). "Designing Phase I $\overline{X}$ Charts with Small Sample Sizes." *Quality and Reliability Engineering International*, **20**, 497-510.

Chao, M.T. and Cheng, S.W. (1996). "Semicircle control chart for variables data." *Quality Engineering*, **8**, 441-446.

Chen, G. (1997). "The mean and standard deviation of the run-length distribution of $\overline{X}$ charts when control limits are estimated." *Statistica Sinica*, **7**, 789-798.

117

Chen, G. (1998). "The run length distributions of the R, s and $s2$ control charts when σ is estimated." *The Canadian Journal of Statistics*, **26** (2), 311-322.

Chen, H. and Huang, C. (2014). "The CUSUM residual chart for respiratory syndromic surveillance data." *IIE Transactions*, **46** (8), 790-797.

Chowdhury, S., Mukherjee, A. and Chakraborti, S. (2013). "A new distribution-free control chart for joint monitoring of unknown location and scale parameters of continuous distributions." *Quality and Reliability Engineering International*, **30** (2), 191-204.

Corbett, C. and Pan, J.N. (2002). "Evaluating environmental performance using statistical process control techniques." *European Journal of Operational Research*, **139** (1), 68-83.

Cornou, C., Vinther, J. and Kristensen, A.R. (2008). "Automatic detection of oestrus and health disorders using data from electronic sow feeders." *Livestock Science*, **118**, 262-271.

Correia, F. and Oliveira, P. (2010). "Monitoring chronic respiratory patients by control charts with variable limits." *Semana de Engenharia 2010 Guimarães*.

Correia, F., Nêveda, R. Oliveira, P. (2011). "Chronic respiratory patient control by multivariate charts." *International Journal of Health Care Quality Assurance*, **24** (8), 621 – 643.

Costa, A.F.B. and Rahim, M.A. (2004). "Monitoring process mean and variability with one non-central chi-square chart." *Journal of Applied Statistics*, **31** (10), 1171-1183.

Cox, T.F. and Dunn, R.T. (2002). "An analysis of decathlon data." *Journal of the Royal Statistical Society, Series D (The Statistician)*, **51** (2), 179-187.

Curran, E., Harper, P., Loveday, H., Gilmour, H., Jones, S., Benneyan, J., Hood, J. and Pratt, R. (2008). "Results of a multicentre randomised control trial of statistical control charts and structured diagnostic tools to reduce ward acquired meticillin-resistant Staphylococcus aureus: the CHART Project." *Journal of Hospital Infection*, **70**, 127-135.

Davis, M.E., Parrott, T., Brown, D.C., De Rodas, B.Z., Johnson, Z.B., Maxwell, C.V. and Rehberger, T. (2008). "Effect of Bacillus-based direct-fed microbial feed supplement on growth

performance and pen cleaning characteristics of growing-finishing pigs." *Journal of Animal Science*, **86** (6), 1459-1467.

Del Castillo, E. (2002). Statistical Process Adjustment for Quality Control (Wiley Series in Probability and Statistics). John Wiley & Sons, Inc. New York, page 357.

De Vries, A. and Conlin, B.J. (2003). "Design and performance of statistical process control charts applied to estrous detection efficiency." *Journal of Dairy Science*, **86** (6), 1970–1984.

De Vries, A. and Reneau, J.K. (2010). "Application of statistical process control charts to monitor changes in animal production systems." *Journal of Animal Science*, **88** (13), E11-E24.

Ding, X., Wardell, D. and Verma, R. (2006). "An assessment of statistical process control-based approaches for charting student evaluation scores." *Decision Sciences Journal of Innovative Education*, **4** (2), 259-272.

DiStefano, C., Zhu, M. and Mindrila, D. (2009). "Understanding and Using Factor Scores: Considerations for the Applied Researcher." Practical Assessment, Research & Evaluation, **14** (20), 1-11.

Duclos, A. and Voirin, N. (2010). "The p-control chart: a tool for care improvement." *International Journal for Quality in Health Care*, **22** (5), 402–407.

Dzik, W.S., Beckman, N., Selleng, K., Heddle, N., Szczepiorkowski, Z., Wendel, S. and Murphy, M. (2008). "Errors in patient specimen collection: application of statistical process control." *Transfusion*, **48**, 2143-2151.

Fraile, L.J., Crisci, E., Weenberg, J., Armadans, M., Mendoza, L., Ruiz, L., Bernaus, S. and Montoya, M. (2009). "Effect of treatment with phytosterols in three herds with porcine respiratory disease complex." *Journal of Swine Health and Production*, **17** (1), 32-41.

Fuhrman, T.J. (2002). "Quality milk starts with quality management." *Proceedings of the 43rd Annual Meeting of the National Mastitis Council*, 131-139.

Gan, F.F. (1997). "Joint monitoring of process mean and variance." Nonlinear Analysis, *Proceedings of the 2nd World Congress of Nonlinear Analysis*, USA, **30** (7), 4017-4024.

Gorsuch, R. (1983). "Factor analysis". Hillsdale, NJ: L. Erlbaum Associates.

Grennstam, N. (2005). "On predicting milk yield and detection of ill cows." Stockholm, Sweden: k^{th} *Royal Institute of Technology*.

Hawkins, D.M. (1987). "Self-starting CUSUM charts for location and scale." *The Statistician*, **36** (4), 299-316.

Hawkins, D.M. and Deng, Q. (2009). "Combined charts for mean and variance information." Journal of Quality Technology, **41** (4), 415-425.

Human, S.W., Graham, M. A. (2007). "Average run lengths and operating characteristic curves". *Encyclopedia of Statistics in Quality and Reliability*, **1**, 159-168, John Wiley.

Human, S.W., Chakraborti, S., Smit, C.F. (2010). "Shewhart-type Control charts for Variation in Phase I Data Analysis." *Computational Statistics and Data Analysis*, **54**(4), 863-874.

Human, S.W., Kritzinger, P. and Chakraborti, S. (2011). "Robustness of the EWMA control chart for individual observations". *Journal of Applied Statistics*, **38** (10), 2071-2087.

Jensen, J.B. and Markland, E. (1996). "Improving the application of quality conformance tools in service firms." *The Journal of Services Marketing*, **10** (1), 35-55.

Jensen, W.A., Jones-Farmer, L.A., Champ, C.W. and Woodall, W.H. (2006). "Effects of parameter estimation on control chart properties: A literature review." *Journal of Quality Technology*, **38** (4), 349-364.

Khoo, M.B.C., Wong, V.H., Wu, Z. and Castagliola, P. (2011). "Optimal designs of the multivariate synthetic chart for monitoring the process mean vector based on median run length." *Quality and Reliability Engineering International*, **27** (8), 981-997.

Kottner, J. and Halfens, R. (2010). "Using statistical process control for monitoring the prevalence of hospital-acquired pressure ulcers." *Ostomy Wound Management*, **56** (5), 54-59.

Krieter, J., Engler, J., Tölle, K.-H., Timm, H.H. and Hohls, E. (2008). "Control charts applied to simulated sow herd datasets." *Livestock Science*, **121** (2), 281-287.

Lotze, T.H. and Shmueli, G. (2009). "How does improved forecasting benefit detection? An application to biosurveillance." *International Journal of Forecasting*, **25**, 467–483.

Lukas, J.M., Hawkins, D.M., Kinsel, M.L. and Reneau, J.K. (2005). "Bulk tank somatic cell counts analyzed by statistical process control tools to identify and monitor subclinical mastitis incidence." *Journal of Dairy Science*, **88** (11), 3944–3952.

Lukas, J.M., Reneau, J.K., Wallace, R., Hawkins, D. and Munoz-Zanzi, C. (2009). "A novel method of analyzing daily milk production and electrical conductivity to predict disease onset." *Journal of Dairy Science*, **92** (12), 5964-5976.

MacCarthy, B.L. and Wasusri, T. (2001). "Statistical process control for monitoring scheduling performance - addressing the problem of correlated data." *Journal of the Operational Research Society*, **52** (7), 810-820.

MacCarthy, B.L. and Wasusri, T. (2002). "A review of non-standard applications of statistical process control (SPC) charts." *International Journal of Quality & Reliability Management*, **19** (3), 295-320.

Madsen, T.M. and Kristensen, A.R. (2005). "A model for monitoring the condition of young pigs by their drinking behaviour." *Computers and Electronics in Agriculture*, **48** (2), 138–154.

Maguad, B.A. (2005). "Monitoring Teacher's Performance using Statistical Process Control Charts." *International Journal of Quality and Productivity Management,* **5** (1), (III) 1-10.

Maguad, B.A. (2006). "Using SPC to assess performance in a graduate course of business." *ASBBS eJournal*, **2**, (1).

Maguad, B.A. (2007). "Using process variation analysis to monitor teachers' performance." *The

121

Journal of Adventist Education, **69** (4), 26-32.

Marks, N.B. and O'Connell, R.T. (2003). "Using statistical control charts to analyze data from student evaluations of teaching." *Decision Sciences Journal of Innovative Education*, **1** (2), 259-272.

Masson, P., De Raemaker, F. and Bon, F. (2005). "Quality control procedures for chloride and nitrate ions analysis in plant samples by ion chromatography." *Accreditation and Quality Assurance*, **10** (8), 439-443.

Masson, P. (2007). "Quality control techniques for routine analysis with liquid chromatography in laboratories." *Journal of Chromatography A*, **1158** (1-2), 168–173.

McCracken, A.K. and Chakraborti, S. (2013a). "Control Charts for Joint Monitoring of Mean and Variance: An Overview." *Quality Technology & Quantitative Management*, **10** (1), 17-36.

McCracken, A.K., Chakraborti, S. and Mukherjee, A. (2013b). "Control Charts for Simultaneous Monitoring of Unknown Mean and Variance of Normally Distributed Processes." *Journal of Quality Technology*, **45**(4), 360-375.

Mertens, K., Decuypere, E., De Baerdemaeker, J. and De Ketelaere, B. (2011). "Statistical control charts as a support tool for the management of livestock production." *Journal of Agricultural Science*, **149** (3), 369 – 384.

Mertens, K., De Ketelaere, B., Vaesen, I., Löffel, J., Ostyn, B., Kemps, B., Kamers, B., Bamelis, F., Zoons, J., Darius, P., Decuypere, E. and De Baerdemaeker, J. (2008). "Data-based design of an intelligent quality control chart for the daily monitoring of the average egg weight." *Computers and Electronics in Agriculture*, **61** (2), 222-232.

Mertens, K., Vaesen, I., Löffel, J., Kemps, B., Kamers, B., Zoons, J. and De Ketelaere, B. (2009). "An intelligent control chart for monitoring of autocorrelated egg production process data based on a synergistic control strategy." *Computers and Electronics in Agriculture*, **69** (1), 100-111.

Montgomery, D.C. (2013). Statistical Quality Control: A Modern Introduction, 7th ed., John Wiley & Sons, Singapore Pte. Ltd.

122

Morgan, C. and Dewhurst, A. (2007). "Using SPC to measure a national supermarket chain's suppliers' performance." *International Journal of Operations and Production Management*, **27** (8), 874-900.

Nakahati, Y.W., Leão, B.P. and Galvão, K.H. (2010). "Health monitoring of aircraft horizontal stabilizer systems using SPC techniques." *XVIII Congresso Brasileiro de Automatica, Bonito-MS*.

Nelson, L.S. (2003). "When should the limits on a Shewhart control chart be other than a center line of $\pm$ 3-sigma?" *Journal of Quality Technology*, **35** (4), 424-425.

Page, E.S. (1954). "Continuous inspection schemes." *Biometrika*, **41** (1), 100-115.

Pastell, M. and Madsen, H. (2008). "Application of CUSUM charts to detect lameness in a milking robot." *Expert Systems with Applications*, **35** (4), 2032–2040.

Pazhayamadom, D.G., Kelly, C.J., Rogan, E. and Codling, E.A. (2013). "Self-starting CUSUM approach for monitoring data poor fisheries." *Fisheries Research*, **145**, 114-127.

Perla, R.J., Provost, L.P. and Murray, S.K. (2011). "The run chart: a simple analytical tool for learning from variation in healthcare processes." *BMJ Quality & Safety*, **20**, 46-51.

Pettersson, M. (2004). "SPC with applications to churn management." *Quality and Reliability Engineering International*, **20** (5), 397-406.

Psarakis, S. and Papaleonida, G.E.A. (2007). "SPC procedures for monitoring autocorrelated processes." *Quality Technology & Quantitative Management*, **4** (4), 501–540.

Pujar, S., Calvert, S., Cortina-Borja, M., Chin, R.F.M, Smith, R.A., Cross, J.H., Das, K., Pitt, M. and Scott, R.C. (2010). "Statistical Process Control (SPC) - A simple objective method for monitoring seizure frequency and evaluating effectiveness of drug interventions in refractory childhood epilepsy." *Epilepsy Research*, **91**, 205-213.

Qiu, P. (2014). Introduction to Statistical Process Control, CRC Press, Taylor and Francis Group, Florida.

123

Quesenberry, C.P. (1993). "The effect of sample size on estimated limits for the $\overline{X}$ and X control charts." *Journal of Quality Technology*, **25**, 237–247.

Quimby, W.F., Sowell, B.F., Bowman, J.G. P., Branine, M. E., Hubbert, M. E. and Sherwood, H.W. (2001). "Application of feeding behaviour to predict morbidity of newly received calves in a commercial feedlot." *Canadian Journal of Animal Science*, **81** (3), 315-320.

Reneau, J.K. (2000). "Process control: Timely feedback for quality milk production at the farm." *Proceedings of the 41st Annual Meeting of the National Mastitis Council*, 140-148.

Reneau, J.K. and Kinsel, M.L. (2001). "Record systems and herd monitoring in production-oriented health and management programs in food producing animals." In *Herd Health: Food Animal Production Medicine*, 3rd Edition (Ed. M. O. Radostits), pp. 107–146. Philadelphia, PA: W.D. Saunders Company.

Roberts, S.W. (1959). "Control chart tests based on geometric moving averages." *Technometrics*, **1** (3), 239-250.

Ryan, T. P. (2000). Statistical Methods for Quality Improvement: Second Edition, John Wiley & Sons.

Shehab, R.L. and Schlegel, R.E. (2000). "Applying quality control charts to the analysis of single-subject data sequences." *Human Factors*, **42** (4), 604-616.

Shewhart, W.A. (1926). "Quality control charts." *Bell Systems Technical Journal*, 593-603.

Stapenhurst, T. (2005). Mastering statistical process control: A handbook for performance improvement using cases. Oxford : Butterworth-Heinemann.

St-Pierre, N.R. and Cobanov, B. (2007a). "A model to determine the optimal sampling schedule of diet components." *Journal of Dairy Science*, **90** (12), 5383–5394.

St-Pierre, N.R. and Cobanov, B. (2007b). "Optimal sampling schedule of diet components: Model robustness to departure from assumptions." *Journal of Dairy Science*, **90** (12), 5395-5404.

124

Tasdemir, A. (2012). "Effect of autocorrelation on the process control charts in monitoring of a coal washing plant." *Physicochemical Problems of Mineral Processing*, **48** (2), 495–512.

Thor, J., Lundberg, J., Ask, J., Olsson, J., Carli, C., Harenstam, K.P. and Brommels, M. (2007). "Application of statistical process control in healthcare improvement: systematic review." *Qual Saf Health Care*, 16, 387-399.

Trevanich, A. and Bourke, P. (1993). "EWMA control charts using attributes data." *Journal of the Royal Statistical Society, Series D: The Statistician*, **42** (3), 215-215.

Wallace, R.L. (2009). "Milking management systems: Your computer can tell you about more than just reproduction*." Four-state dairy nutrition and management conference*, Dubuque, Iowa, 121-125.

Wardell, D.G. and Candia, M.R. (1996). "Statistical Process Monitoring of Customer Satisfaction Survey Data." *Quality Management Journal*, **3** (4), 36-50.

Wasusri, T. and MacCarthy, B.L. (2001). "Using SPC chart techniques in production planning and scheduling: Two case studies." *Proceedings of the Twelfth Annual Conference of the Production and Operations Management Society,* POM-2001, March 30-April 2, 2001, Orlando Fl.

Weib, C.H. and Atzmüller, M. (2010). "EWMA control charts for monitoring binary processes with applications to medical diagnosis data." *Quality and Reliability Engineering International*, **26**, 795-805.

Western Electronic Company. (1956). Statistical Quality Control Handbook, Western Electric Corporation, Indianapolis, IN.

Wirtschafter, D.D., Pettit, J., Kurtin, P., Dalsey, M., Chance, K., Morrow, H.W., Seid, M., Byczkowski, T.L., Huber, T.P., Milstein, J.M., Bowles, S.M., Fichera, S. and Kloman, S. (2010). "A statewide quality improvement collaborative to reduce neonatal central line-associated blood stream infections." *Journal of Perinatology*, **30**, 170-181.

Woodall, W.H. and Montgomery, D.C. (1993). "Research issues and ideas in statistical process control." Journal of Quality Technology, **31**(4), 376-386.

Yang, S.-F, Cheng, T.-C., Hung, Y.-C., Cheng, S.W. (2012). "A new chart for monitoring service process mean." *Quality and Reliability Engineering International*, **28** (4), 377-386.

Yi, G., Coleman, S. and Ren, Q. (2006). "CUSUM method in predicting regime shifts and its performance in different stock markets allowing for transaction fees." *Journal of Applied Statistics*, **33** (7), 647-661.